Universitetet i Stavanger

FACULTY OF SCIENCE AND TECHNOLOGY

MASTER'S THESIS

Study programme/specialization: Petroleum Geosciences Engineering	Spring semester, 2017 Open
Author: Javeria Qamar	…… (signature of author)
Faculty Supervisor: Nestor Fernando Cardozo External Supervisors: Bing Wang (iRes-Geo Technology) & Lothar Schulte (Schlumberger SIS)	
Title of master's thesis: **Dry well analysis of well 6407/10-5 at 793 area, Norwegian Sea.**	
Credits (ECTS): 30	
Keywords: *Dry Well Analysis* *Norwegian Sea* *Exploration* *Seismic Interpretation* *Basin Modelling* *2D Reconstruction* *Seismic Attribute Analysis* *Top 6 fault Seal Analysis*	Number of pages: 76 + supplemental material/other: CD/ flash drive Stavanger, 15th June 2017

Dry well Analysis of well 6407/10-5 at 793 area, Norwegian Sea

By

Javeria Qamar

MSc Thesis

Presented to the Faculty of Science and Technology

University of Stavanger

University of Stavanger

2017

ACKNOWLEDGEMENTS

This Master thesis is the final requirement for the completion of the Master's degree in Petroleum Geosciences Engineering at The University of Stavanger, Norway.

I would like to express my gratitude to my supervisors Bing Wang, Lothar Schulte and Nestor Cardozo for their guidance and continuous supervision throughout this Master's thesis.

Also, I would like to thank Petrobank for providing the dataset for this project and The University of Stavanger for providing an excellent environment of study.

Lastly, I would like to show my appreciation for the support I received from my friends, family and especially my mother, Nighat Qamar and my husband, Shahzeb Haider, who were there for me during my emotional breakdowns and my stressful phases.

Dry well Analysis of well 6407/10-5 at 793 area, Norwegian Sea

ABSTRACT

The region of investigation is located in the Norwegian Sea, which is an area of high hydrocarbon activity. Many reservoirs have been successfully identified, drilled, and now they are producing in large oil & gas fields. However, the Norwegian Sea has a complex geology as it resulted from Permian to Late Jurassic crustal extension, which created rift basins and several horst and graben structures. Most of the important hydrocarbon reservoirs in the Norwegian Sea are Jurassic. Because of the complex geology, identifying these reservoirs and successfully positioning wells is challenging.

The research for this project is conducted on a dry well, 6407/10-5 in area 793 that was drilled along the western fault bounded Frøya High in the Norwegian Sea. The Frøya High is a Triassic paleo-uplift: a NNE-SSW trending horst bounded by the Vingleia and Klakk fault complexes on the eastern side and a major fault on the western side, which separates it from the Froan Basin. A Jurassic rollover anticline developed along the western margin of the Frøya High where the well is located. Since 2015, many fields such as Pil, Bue and Snilehorn, have been discovered in the same geological trend. However, in the study area, the two wells 6407/10-1 and 6407/10-2, drilled in the 1980s, only contain hydrocarbon shows, and the newly drilled well 6407/10-5 is dry. This study focuses on identifying the failure reason of the dry well 6407/10-5.

Newly acquired 3D seismic data covering the study area, well reports, log data and geochemical reports of the wells 6407/10-1 and 6407/10-2 are used for the project. This research provides an understanding of the geological elements of the petroleum system of the study area i.e., seal, reservoir, source and trap, which lead to debate the reasons for failure of the well. A set of methodologies are defined to test each element. Here, local source is not functional and top seal of the reservoir is heavily faulted. Trap failure is the main reason for dry well as fault besides the trap has high potential of leaking.

Contents

List of Figures

List of Tables

1. Introduction

1.1 Technical Challenges in finding oil prospects

Exploring oil and gas reservoirs is a long and complicated process. It comprises years of research and survey work and still two out of three exploration wells are unsuccessful in fulfilling their original objectives, primarily because of the unexpected geology (Schlumberger, 2017). The process of exploration comprises continuous experimentation and new learnings because uncertainties and unexpected developments always drape over (Rønnevik, 2000) so new researches are conducted constantly.

Multiple factors work and function together to generate a potential reservoir discovery. These factors include the presence of a trap, top seal, hydrocarbon charge and its migration, good quality reservoir sands, sealing of the trap and a mature source rock. These aspects should never be treated in isolation. Rather their relation with each other should be the main focus. Data and analogues used for subsurface modelling and its understanding are never fully accurate as they predict the events but not the actual circumstances (Rønnevik, 2000).

An analysis conducted by the Norwegian Continental Shelf Exploration states that 33% of dry wells were drilled just because of a perceived Direct Hydrocarbon Indicator (geo365, 2017). A case study of exploration well failures for the Moray Firth and Central North Sea consisting of 97 wells, drilled in a span of 10 years, shows that 81 of these wells were declared dry. A pie chart of the failure reasons is presented in Figure 1. This figure shows that the absence of a target reservoir and the failure of top seal were the most common reasons for failure (Mathieu, 2015).

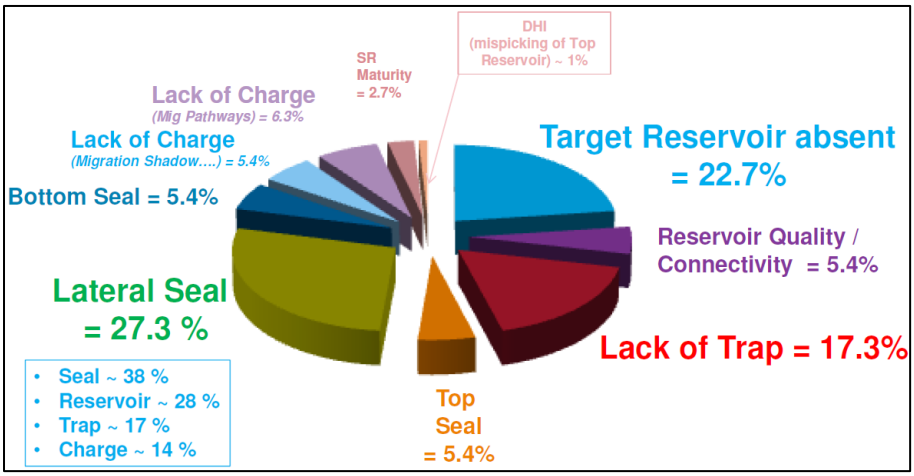

Figure 1: Pie chart showing failure reasons (from Mathieu, 2015)

1.2 Norwegian Continental Shelf (NCS) Wildcat Wells Evaluation

For the evaluation of the Norwegian wildcat wells, a project was conducted in the year 2000. Its focus was to check how well the risks were understood before drilling and then to compare those risks to the reasons for encountering a dry well. Before drilling, three main factors were held responsible for a dry well: charge, trap and reservoir. These factors are further divided into sub-factors. For example, failure of the trap is divided into absence of closure, absence of top seal, and absence of lateral seal. Table 1 shows an evaluation of seven anonymous dry wells from the NCS. Each factor has three possible answers: ok, fail or not relevant (nr).

Table 1. Evaluation of dry prospects with their reasons (from Ofstad et al., 2000)

Dry prospect form, showing example answers

Prospect name	Reason for dry prospect — ok, fail, nr (= not relevant)										
	charge				trap				reservoir		
	charge	presence of source	maturity of source	migration of HC	trap	presence of closure	presence of top seal	presence of lateral seal	reservoir	presence of reservoir	quality of reservoir
A	ok	ok	ok	ok	ok	ok	ok	ok	fail	fail	nr
B	fail	ok	ok	fail	ok	ok	ok	ok	fail	fail	nr
C	fail	ok	ok	fail	ok	ok	ok	ok	ok	ok	ok
D	ok	ok	ok	ok	fail	fail	ok	fail	ok	ok	ok
E	ok	ok	ok	ok	fail	ok	ok	fail	ok	ok	ok
F	ok	ok	ok	ok	fail	ok	fail	fail	ok	ok	ok
G	ok	ok	ok	ok	fail	ok	ok	fail	ok	ok	ok

The result, which is summarized in Figure 2, indicates that sometimes too pessimistic predictions are made. For example, the risk for ‘trap failure’ was 46% but post-drilling analysis defined the risk to be only 26%. Also, sometimes only one reason is given for a dry well, which is not true in all cases. Failure from a main factor is either the result of one of the sub factors or a combination of two or more of them.

Additionally, sometimes it is hard to pinpoint the factor responsible for well failure. On average, lack of trap, reservoir and charge are regarded equally as reasons for dry prospects. Within each of these categories, lack of lateral seal, absence of reservoir and lack of migration are reported as main reasons (from Ofstad et al., 2000).

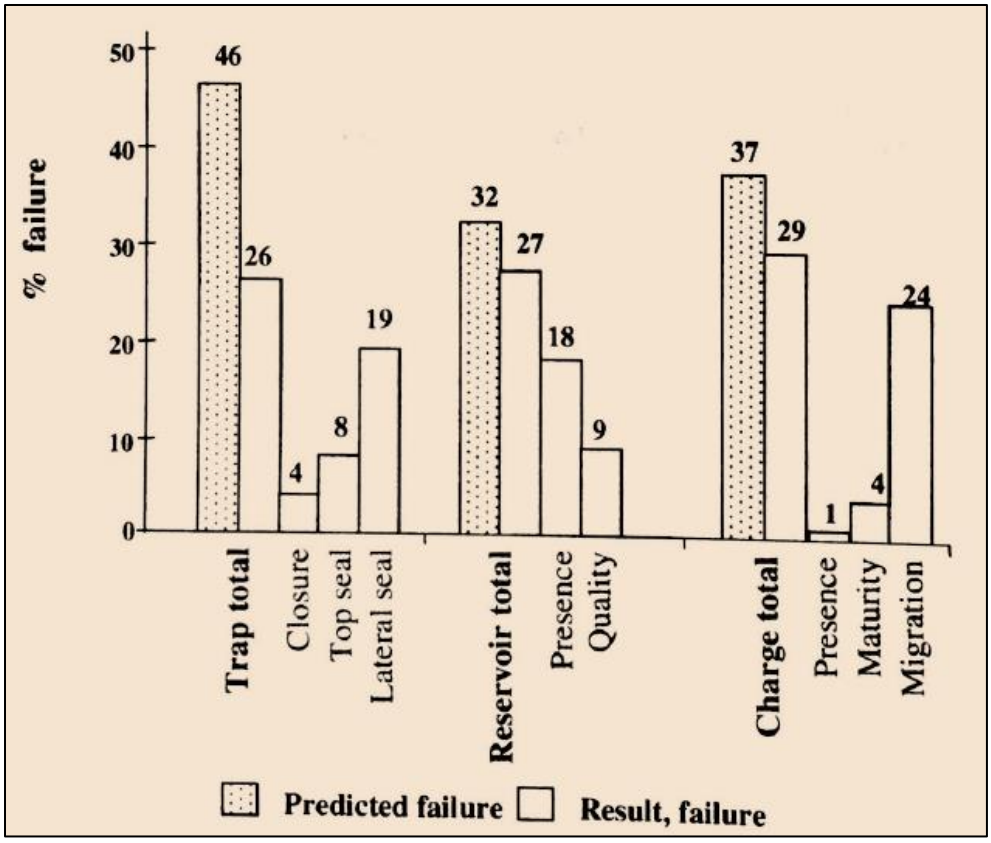

Figure 2: Comparison of pre-drill Risk assessment with post-drill critical factors (from Ofstad et al., 2000)

1.3 Norwegian Sea Petroleum Pitfalls

The Norwegian Sea lies between 62°N and 69°30' N in the Norwegian continental shelf (NCS). This part of the NCS is called Mid-Norwegian Shelf and it is known as a rifted continental margin (Bukovics and Ziegler, 1985). The margin experienced two major tectonic episodes: the Caledonian orogeny from Late Silurian to Early Devonian, and the North Atlantic continental breakup from Late Devonian to Eocene (Blystad et al., 1995). Major hydrocarbon reservoirs in the Norwegian Sea were deposited during the second tectonic episode. The North Atlantic continental breakup comprised four stages from continental rifting to oceanic drift. These stages played a significant role in the formation of structures, the deposition and quality of lithological facies, and the formation of functional hydrocarbon traps (Lien, 1990).

1.3.1 Structure

The structural geology and deposition of the reservoir formations have a direct influence on the interpretation pitfalls and success of the exploration approach. The area is divided into several structural elements with different individual styles.

- Salt tectonics spread over the area forming lateral discontinuity in Triassic intervals. Several salt diapirs have risen above and into the Jurassic and Cretaceous sequence, resulting in weak reflections on seismic data, hence inaccurate interpretations.

- Rotational fault movements in the area caused extensive erosion. The tilting of fault blocks and erosion of sedimentary packages sometimes cause correlation problems. Therefore, potential reservoir sands are overlooked.

- Tectonic inversion also prevailed in the area. This sometimes led to misinterpreted structures (Gowers, 2005).

1.3.2 Stratigraphy

Production from the Mid-Norwegian shelf is mainly taking place from heterolithic siliciclastic successions. Sandstones in the area are also altered diagenetically. Heterolithic sedimentary packages consist of layers of shales and siltstones interbedded with thin sandstones. Hydrocarbon traps in the area were formed during rifting by faulted and rotated blocks. The fluid flow is deeply affected by faulting in these heterolithic facies. However, the 3D fault geometry and juxtapositions are difficult to determine (Martinius et al., 2005).

1.3.3 Traps

The trap is also a critical factor resulting in the failure of wells. The most common play models in the NCS are Jurassic rotated fault blocks, comprised mainly of Jurassic and Triassic reservoirs. These reservoirs are charged by the Late Jurassic, oil-prone source rocks (Koch and Heum, 1995). Many play models have been tested in those reservoirs, but they have failed. Paleo-hydrocarbon columns were encountered so integrity of the traps was challenged. Leakage in those traps could occur either because of the reactivation of the adjacent faults or breaching of the top seal due to fracturing. These features are not evident on seismic data as no clear faulting is indicated on the apex of any structure.

1.3.4 Different kinds of seals

The limitations of stratigraphic seals also contribute to the lack of success because trap failures may also occur due to inadequate top, bottom or lateral seal. Thick reservoir packages are drilled based on the studies conducted from wireline logs and cores as paleo-oil columns are detected in these areas. Here, the viability of seal is questioned if the paleo-oil columns are found yet there is no hydrocarbon present.

1.3.5 Migration Paths and Oil Generation

Migration paths and wrong timings of the oil generation are also observed. A well was drilled in a Cretaceous submarine fan assumed to be charged from the oil prone source rock of Jurassic age beneath it, with a separation of only 10 meters. Some gas traces were recorded, but the well was dry. The source rock's percentage of extracted organic matter of hydrocarbons exceeded 60%

and hydrocarbon concentration indicated oil presence. However, the oil expelled from the source rock did not migrate into the reservoir directly above it. The 10-meter siltstone between source rock and reservoir prevented the vertical migration. Thus, the relationship between trap formation, hydrocarbon charge and generation is very important in evaluating the reliability of traps (Knutsen et al., 2000).

1.4 Exploration Trends in the Norwegian Sea

The exploration in the Norwegian Sea started in 1980. Six blocks were given the license to be explored. The main concerns, at that time were related to reservoir presence and reservoir quality**.** Also, only gas was predicted because the Upper Jurassic source rocks were deeply buried. However, reservoir facies of good porosity along with locally immature Upper Jurassic source rocks invalidated these risk factors. The Midgard gas discovery in 1987 led to the realization of Lower Jurassic coals as the active source rocks for gas.

Two major oil discoveries, Draugen and Norne, were made in Jurassic and Cretaceous sandstones respectively by using 2D seismic data of good quality. Before drilling, the reserves were estimated to be one fourth of the actual estimation because the reservoir facies and quality were underestimated.

In a block of the Norwegian Sea, Middle Jurassic tilted fault blocks were regarded as high-risk targets although leads and prospects were defined. This block was covered by 3D seismic data and subsequent operation proved the previously identified prospects and the planned drilling campaign.

By the mid-nineties, the Trøndelag Platform and the Halten Terrace were considered as ‘dry belts’ by most oil companies. However, the estimated reservoir quality and existing exploration models were challenged and the Lavrans gas and Kristin oil discoveries were subsequently made. Along with those, a total of 10 discoveries have been made.

The hydrocarbon potential of the Norwegian Sea makes it interesting for exploration, but the geological complexity results in a major challenge in finding hydrocarbon. For instance, several dry wells have been drilled, and several exploration wells found hydrocarbons shows but no commercial reservoirs. The Norwegian Petroleum Directorate (NPD) states that most of the dry prospects drilled in the Norwegian Sea are due to the absence of reservoirs in Cretaceous-Jurassic plays.

1.5 Objectives and Motivation:

The research for this project is conducted on a dry well, 6407/10-5 that was drilled in the Norwegian Sea. Three wells with hydrocarbon shows and two discoveries are present in the surrounding areas of this dry well. Discoveries in the Norwegian Sea are producing hydrocarbons from reservoir rocks of Jurassic age. Three exploration wells with hydrocarbon

shows, 6407/10-1, 6407/10-2 and 6407/10-3 were drilled in the study area. These wells were unable to meet their objectives. All of them were drilled primarily to test the hydrocarbon potential of the reservoir rocks of the area. In each case, either a couple of important reservoir rocks were missing or the whole Jurassic package was not encountered. The rocks present did not show any hydrocarbon potential (NPD, 2017).

This study focuses on conducting research on the petroleum system's elements and processes involved in making a hydrocarbon accumulation successful and hence developing suitable reasons that propose the failure of the well. The main and primary objective of this project is to perform a dry well analysis for well 6407/10-5 and provide a better understanding of the petroleum system for the area.

1.6 Study Area

Major rifting episodes of the Norwegian Sea resulted in large extensional basins and block-faulted areas. One such area is the Trøndelag Platform, which was formed by Middle Jurassic-Early Cretaceous rifting. The study area is located at the Frøya High paleo-uplift, which is a N-S trending horst, forming the southernmost part of the Trøndelag Platform. The Frøya High is bounded by normal faults at the eastern and western sides. Faulting started on the eastern boundary fault during the Late Permian-Triassic creating the Froan basin (figure 3). In the west, Middle Jurassic-Early Cretaceous rifting produced the Klakk and Vingleia fault complexes (Blystad et al., 1995). A Jurassic rollover anticline developed in the hanging wall of the Klakk fault along the western margin of the Frøya High, this is our area of interest (Figure 4).

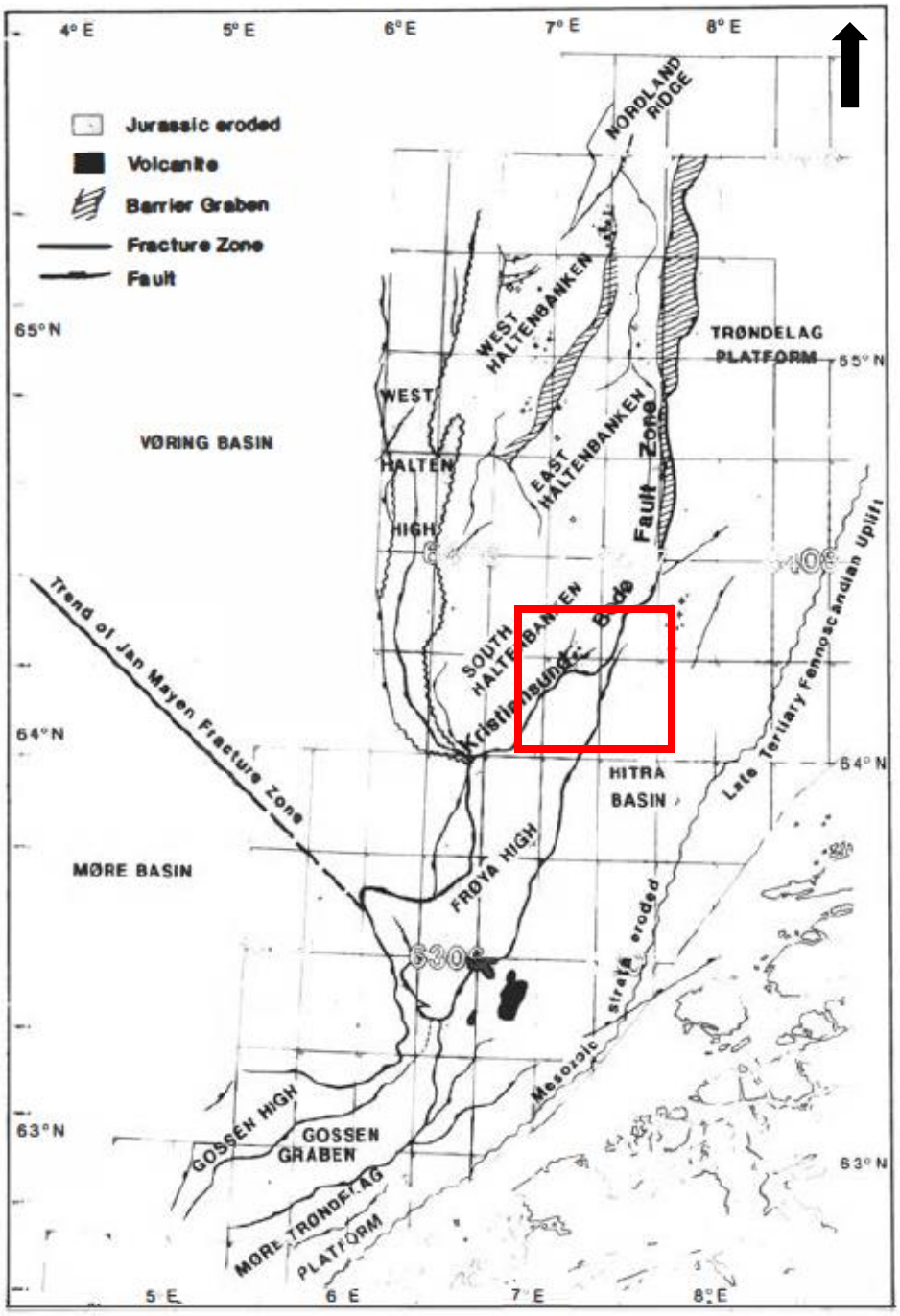

Figure 3: Detailed structural elements of Norwegian Sea. Red rectangle indicates location of Figure 4 (from Fagerland, 1990). Red rectangle is the area of study.

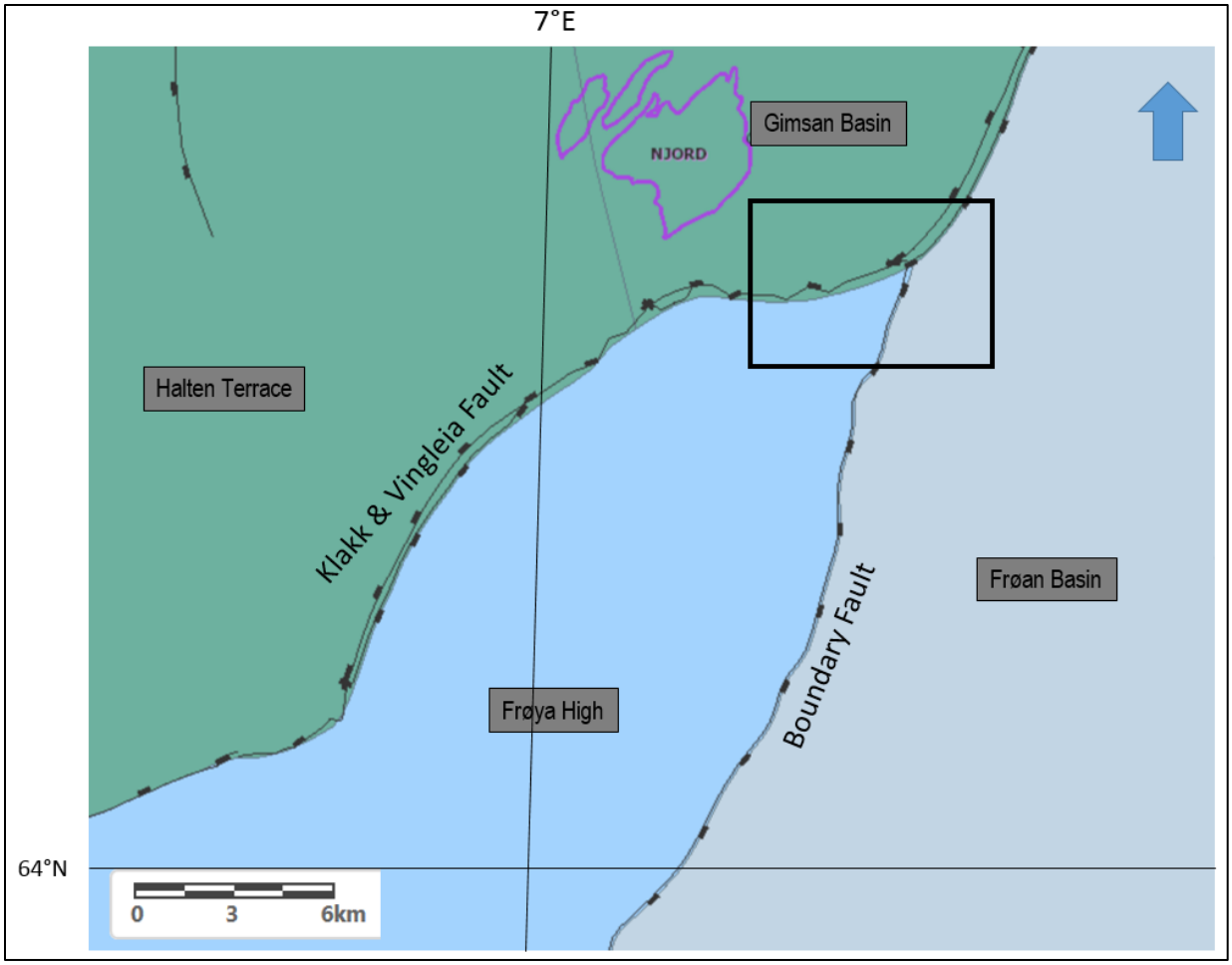

Figure 4: Geological setting of study area. Main faults and basins are shown. Black rectangle indicates location of the study area (NPD factpages, 2017).

1.7 Previous Work

The study area is located in Block 6407/10 of the Norwegian Sea. In the northwest, this area is adjacent to the Njord field. The dry well of the project is present amidst the discoveries of the neighboring block, which makes the study very interesting.

The Snilehorn oil discovery was made**,** northeast of the dry well 6407/10-5. The Pil and Bue discoveries were made southwest of the dry well. Three wells, 6407/10-1, 6407/10-2 and 6407/10-3 have been drilled in block 6407/10 since late 1980s, and they have hydrocarbon shows (Figure 5). A/S Norske Shell drilled well 6407/10-5 in 2015 to prove petroleum in Upper Jurassic rocks. Good quality reservoir sands were encountered but the well was declared dry.

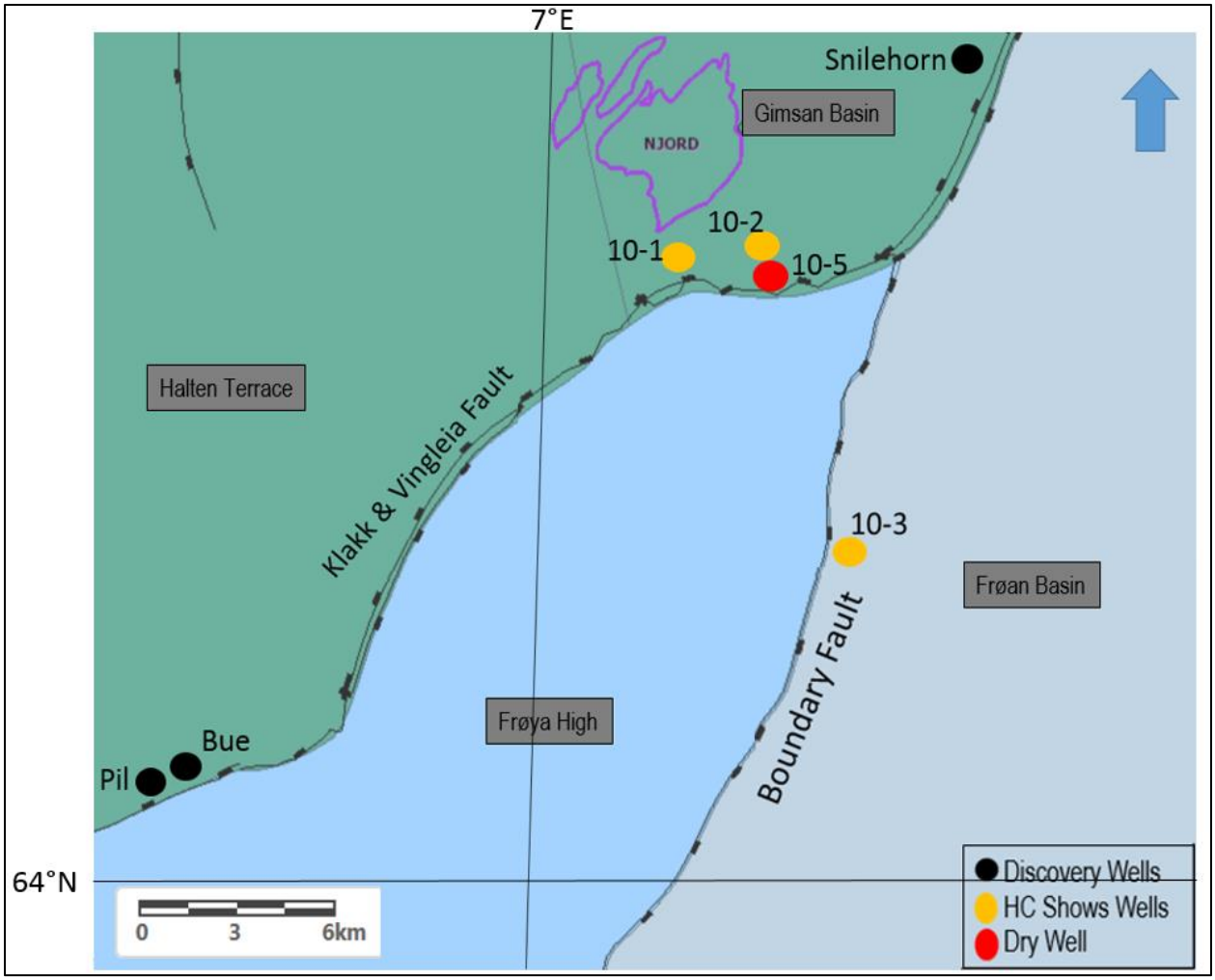

Figure 5: A map showing locations of the important wells of the area: discovery wells, wells with hydrocarbon shows and the dry well (modified from NPD factpages, 2017).

2. Geological Setting

2.1 Tectonics

Two plate tectonic episodes, the Caledonian Orogeny and the break-up of the North Atlantic influenced the development of the rifted passive continental margin of the Norwegian Continental Shelf (NCS), which is also known as the Mid Norwegian Shelf or Norwegian Sea.

2.1.1 Silurian to Devonian:

Continental collision began during Silurian because of the closing of the Iapetus Ocean. Ireland, Scandinavia, Greenland, Svalbard and the Northern Appalachians were influenced by these orogenic events (Mckerrow et. al., 2000). These lithospheric plates experienced compression until Late Devonian. During Middle to Late Devonian, the orogen collapsed forming intramontane extensional basins. Regional strike slip faulting also occurred (Figure 6; From Scotese, 2017).

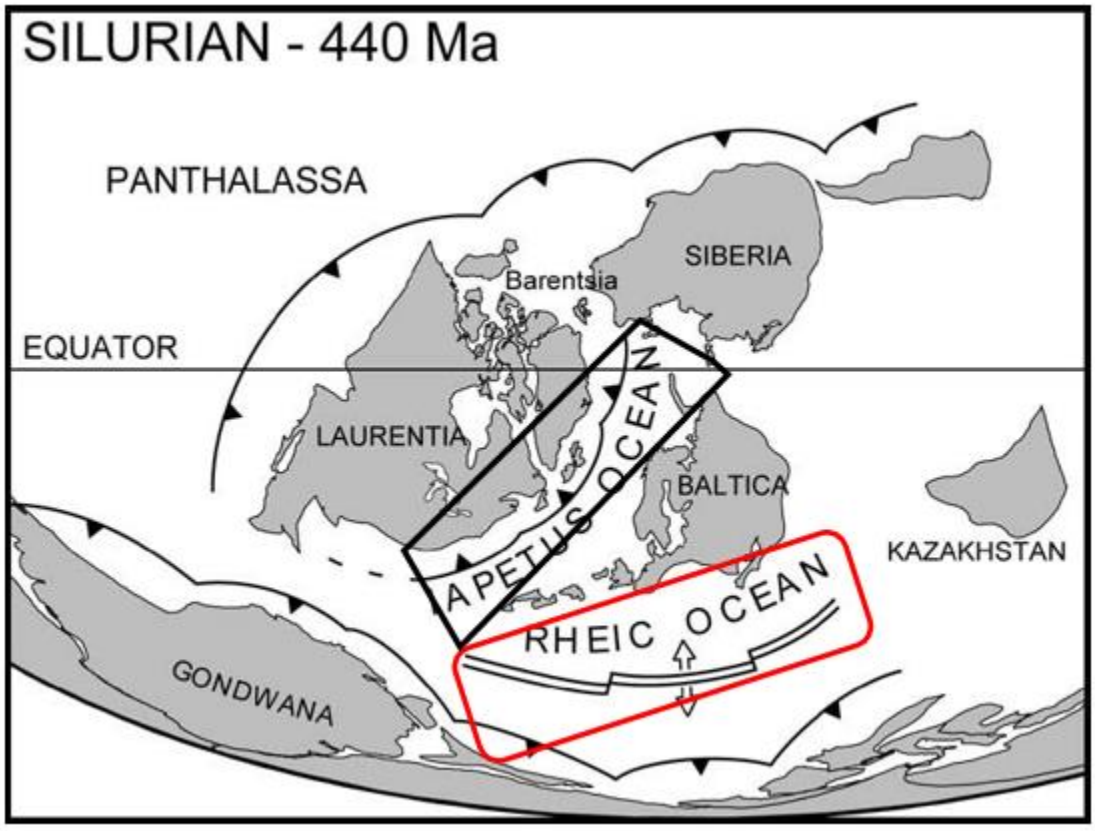

Figure 6: Black rectangle shows closing of Iapetus ocean that resulted in the formation of caledonides. Red rectangle shows rifting (From Scotese, 2017).

2.1.2 Carboniferous to Paleocene

Three main rifting events occurred from the Carboniferous to the Paleocene. These events characterize the evolution of the Mid Norwegian Shelf (Figure 7; Gomez et al., 2003). Rifting extended the continental crust of Norway and normal faulting created a series of extensional basins. The NCS was subdivided into several segments from SW to NE: the Møre margin, the Vøring margin together with the Trøndelag Platform, the Lofoten margin, and the Barents Sea - Svalbard margin (Figure 8; Mosar et al., 2002). These margins evolved during these three rifting events.

2.1.3 Eocene

During early Eocene, extension changed to compression with the onset of active sea floor spreading. Large anticlines were formed because of reactivation and inversion of major faults.

2.1.4 Neogene

Mainland Norway was tilted differentially and uplifted asymmetrically from Miocene to Pliocene. The sedimentary cover and basement rocks of Scandinavia were eroded and a 1500 m thick Plio-Pleistocene succession was deposited on the shelf (Blystad et al., 1995).

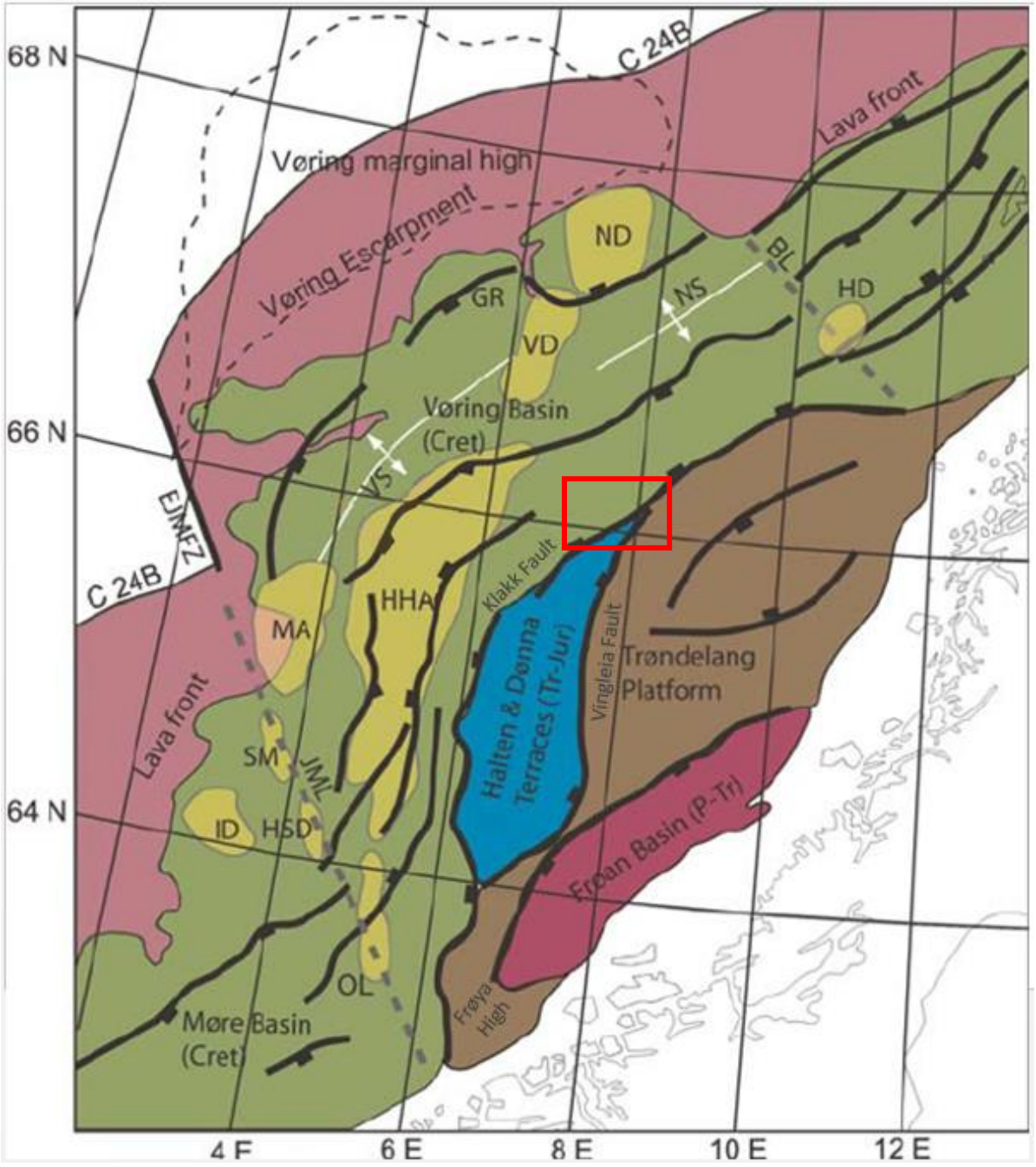

Figure 7: Simplified structural map of the Norwegian Sea illustrating the main structural provinces and structures. Abbreviations: BL, Bivrost Lineament; EJMFZ, East Jan Mayen Fracture Zone; GR, Gjallar Ridge; HD, Hedda Dome; HHA, Helland Hansen Arch; HSD, Havsule Dome; ID, Isak Dome; JML, Jan Mayen Lineament; MA, Modgunn Arch; ND, Naglfar Dome; NS, Na˚grind Syncline; OL, Ormen Lange Dome; SM, Souther Modgunn Arch; VD, Vema Dome; VS, Vigrid Syncline. Red rectangle indicates study area (From Dore et al., 2013). Red rectangle is the area of study.

2.2 Structural Styles

Three structural styles are present in the Norwegian Sea:

i. Normal faults are the most prominent features. Normal faults comprise both deep and shallow faults. Deep faults involve basement, and shallow faults detach in the Triassic evaporites.
ii. Strike-slip faults, mainly on the Halten Terrace.
iii. Salt tectonics in the Triassic evaporites. These are beds of halite and anhydrite that also act as detachment for the shallow normal faults (Blystad et al., 1995).

2.3 Structural Elements of the Study Area

The study area mainly comprises the Frøya High and the Halten Terrace. The Frøya High is bounded by the Froan Basin on the east and the Halten Terrace to the west. Major basin boundary faults separate these elements (Figure 8). A cross section is shown in Figure 9.

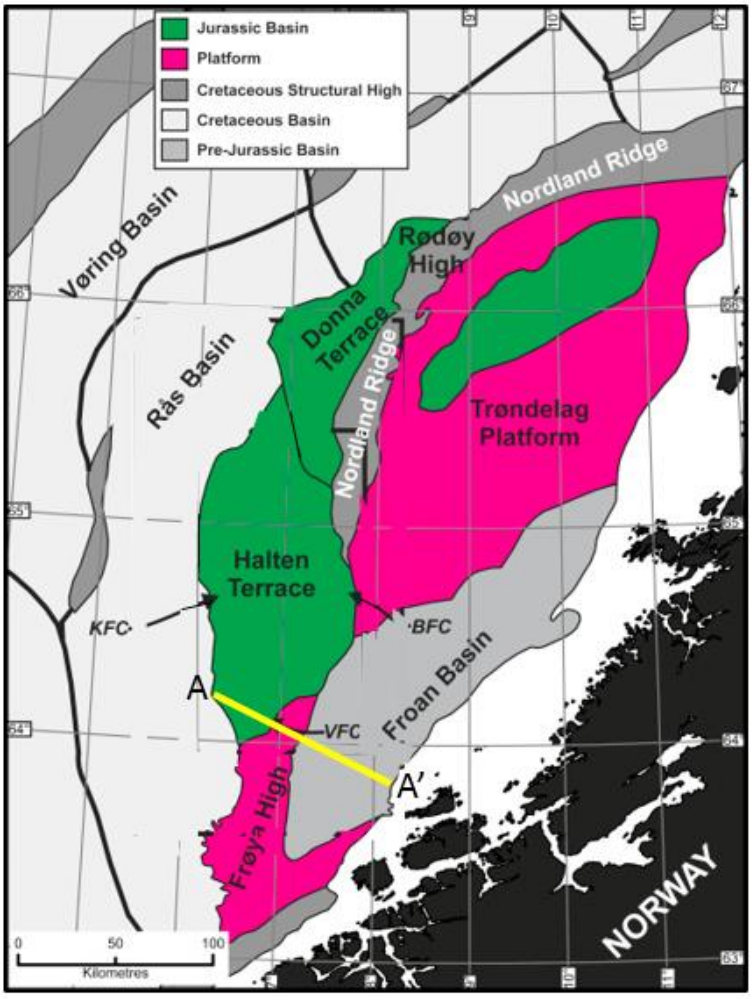

Figure 8: Structural elements of Norwegian sea. Yellow line shows the cross section in Figure 10 (Modified from Wilson et al., 2015).

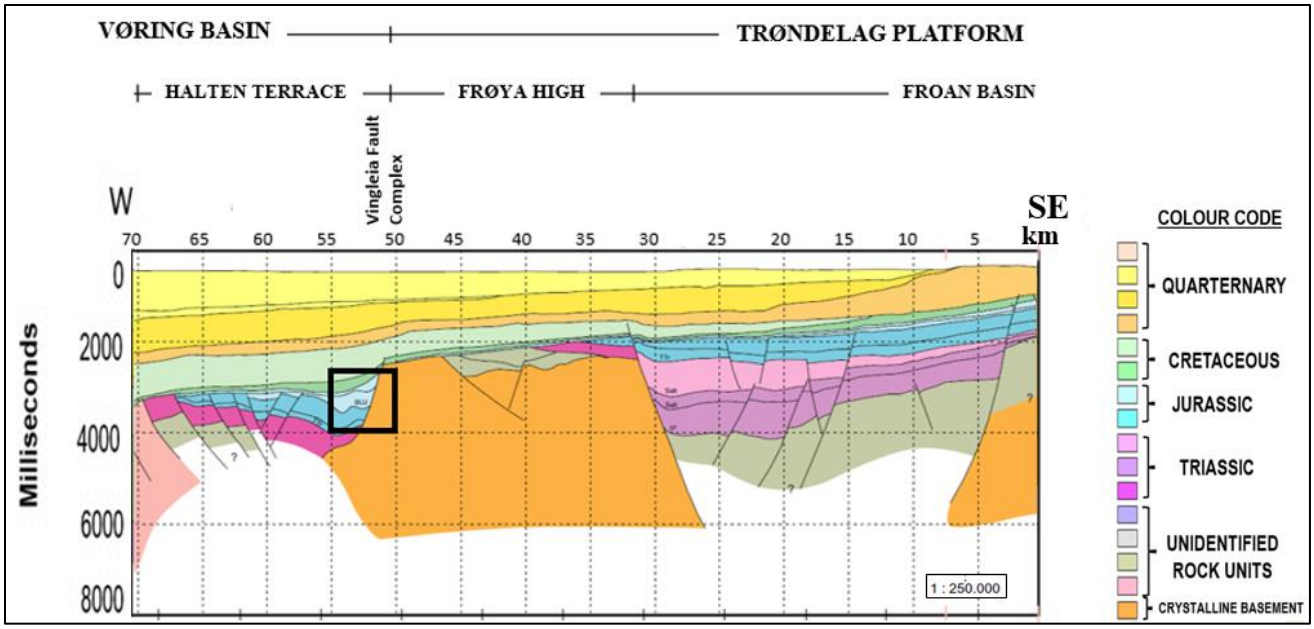

Figure 9: Cross section showing the stratigraphic succession and structures of the study area. Black rectangle indicates the study area (From Blystad et al., 1995).

i. Froan Basin

The Basin is a NNE trending, 250km long basin that is widest to the north. This basin is recognized as the southernmost basin of the eastern part of the Trøndelag platform. The Froan basin was formed during Permo-Triassic extension. Located at the eastern part of the Trøndelag Platform, the Froan Basin is the southernmost of poorly defined extensional basins. It is a set of half grabens with alternating polarity along strike, bounded by the Frøya High towards the west.

The basement of the basin was formed during early to late Permian and it is block faulted. During Cretaceous and Late Jurassic, tectonic activity in the Froan basin was moderate hence only minor Jurassic faults can be observed in this basin.

ii. Frøya High

The Frøya High is a N-S trending horst, which is on the southwestern part of the Trøndelag Platform. Vingleia and Klakk Fault complexes bound Frøya High on the western side, and the boundary fault of the Froan Basin makes the eastern boundary of the Frøya High.

The summit of the Frøya high is a flat smooth and prominent angular unconformity. This unconformity is of Late Jurassic-Early Cretaceous age, which indicates that this area was uplifted during the rifting episode of Jurassic to Cretaceous.

The Frøya high was faulted during the Early Permian rifting episode. Tectonically, this High is divided into an eastern and western part. The eastern part was more active during Late Permian and Triassic, whereas major tectonic activity in the west took place during the rifting episode of Middle Jurassic to Early Cretaceous. Both parts were active during Late Jurassic and Early Cretaceous but more displacement took place in the Late Jurassic. The western part was heavily faulted before the deposition of the Upper Jurassic Spekk Formation. This formation was eroded during the Early Cretaceous rifting phase (Blystad et al., 1995).

iii. Halten Terrace

The Halten Terrace is located between the Trøndelag Platform in the east and the Rås Basin in the west. The Bremstein fault complex is the boundary between the Trøndelag Platform and the Halten Terrace. The Vingleia fault complex separates the Halten Terrace from the Frøya High, and the Klakk Fault complex in the west acts as a boundary between the Rås Basin and the Halten Terrace.

The Halten Terrace is a result of Middle Jurassic to Early Cretaceous rifting. During the early stages of this rifting, major movement took place along the Klakk fault complex, whereas in later stages, the movement took place along the Bremstein Fault Complex. Jurassic faulting dominates the terrace. These Jurassic growth faults were reactivated in the northwestern part during the Early Cretaceous (Blystad et al., 1995).

Focus of Study Area

The western structures are the focus of this study. A rollover anticline developed along the western margin of the Frøya High during the Jurassic rifting, this is the area of interest. The large displacements of Jurassic sediments are clear as almost all the Jurassic succession is missing on the footwall of the fault. Only the last Jurassic formation i.e. the Åre Formation is observed in the footwall. This formation is against the potential reservoir of the studied dry well (Figure 10).

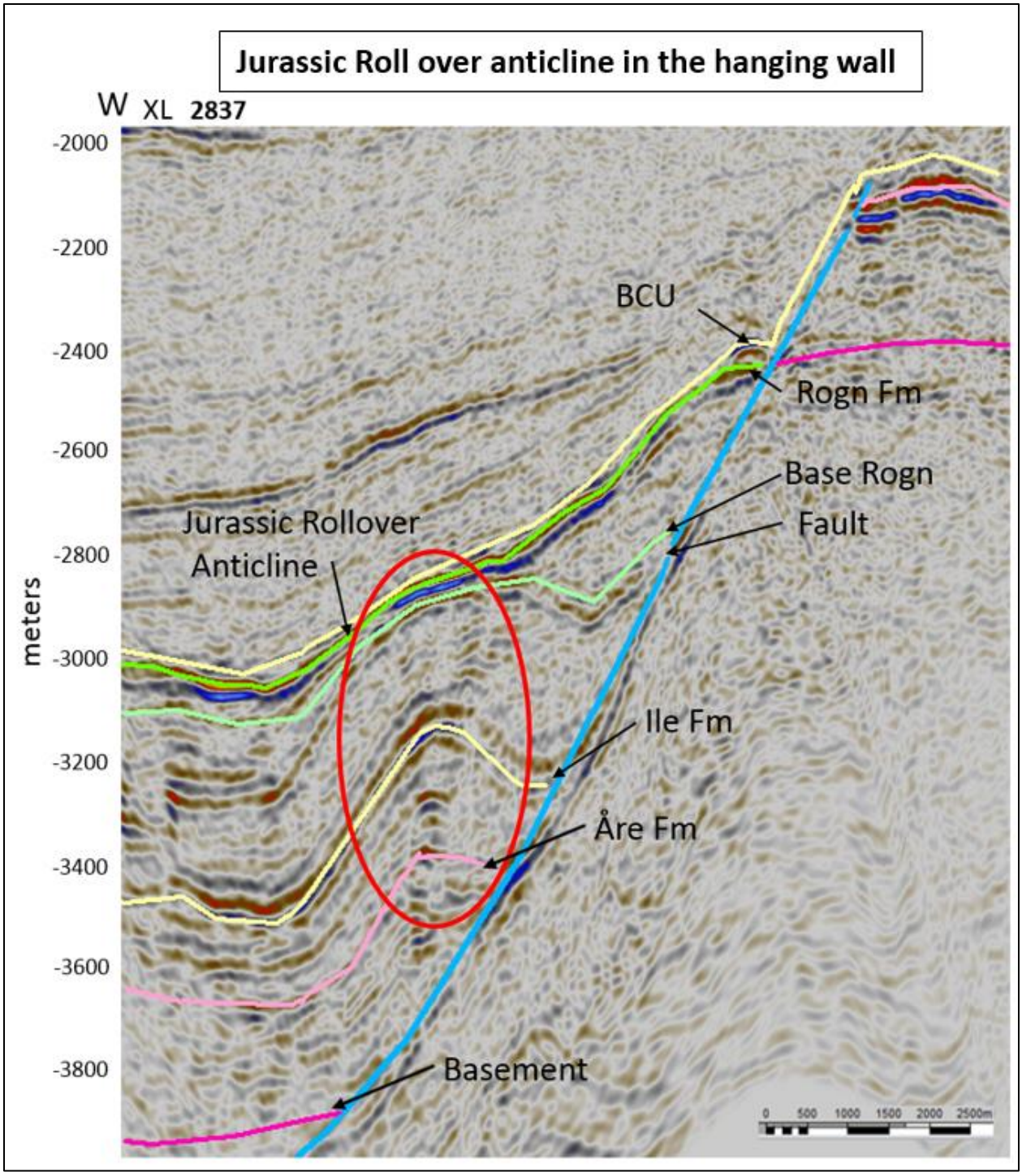

Figure 10: Seismic section showing the Jurassic rollover anticline, BCU, the main fault and reservoir formations in the area.

2.4 Stratigraphic Units

i. Triassic Sediments

In the Norwegian Sea, the Triassic succession is several thousand meters thick. During the Triassic, the climate was warm and it was more humid during the Late Triassic. Land areas were strongly oxidized and chemically weathered during the Early Triassic, depositing red-colored sediments along the coasts and on land. Mudstones and evaporites also predominated. Marine transgression took place during the Late Triassic, depositing 1000 m of evaporites and mudstones. Continental sedimentation followed, this younger continental sequence is known as the grey beds.

ii. The Båt Group

Deltaic to shallow marine sediments were deposited during the Early Jurassic.

a) **Åre Formation**

Deposition of the Åre Formation started in the Late Triassic in the form of coarse-grained sediments along the coast and on the continental shelf (Bøe et al., 2010). Delta plain deposits from swamps and channels during the Early Jurassic resulted in thick coal beds (NPD, 2017**).**

b) **Tilje Formation**

Strong tidal currents developed deposited sandy sediments of the Tilje formation during the Early Jurassic (Bøe et al., 2010).

c) **Ror Formation**

Mainland Norway experienced distinct erosion due to a wet climate (Bøe et al., 2010). This event is observed in the Ror Formation, which is an abrupt transition from sandstones to mudstones (NPD, 2017**).**

iii. The Fangst Group

Shallow marine to coastal/deltaic environment prevailed during Middle Jurassic in the Norwegian Sea.

a) Ile Formation

The Ile Formation deposited in a tidal-shoreline environment with a coarsening upward sequence from siltstone to sandstone.

b) Not Formation

The Not Formation was deposited in lagoons and sheltered bays. It is a mudstone-dominated formation, which coarsens upwards into bioturbated fine-grained sandstone.

c) Garn Formation

The Garn Formation was deposited in braided delta lobes under a wave-dominated shore facies system. This formation mainly consists of sandstone, but mudstone sediments dominate towards the north and south of the Halten Terrace and Trøndelag Platform.

iv. The Viking Group

Extensive organic-rich mud was deposited in isolated fault basins, which mainly comprises the Formations of the Viking Group**.**

a) The Melke Formation

The mudstones of the Melke Formation were deposited in an open marine environment with sandstones developed locally in the Dønna Terrace.

b) The Rogn Formation

The Rogn Formation consists of sandstone that is present within the mudstones of the Spekk Formation. The Rogn Formation is a shallow marine bar deposit and is the reservoir rock of this project.

c) The Spekk Formation

The mudstones of the Spekk Formation have a high organic content as they were deposited under anoxic marine conditions. This mudstone is the major source rock of the area.

v. The Cromer Knoll and Shetland Groups

These groups made the Cretaceous group of sediments, which developed in submarine fans in a deep-water environment. Mudstones and siltstones dominate the lithology, forming good seals while sandstones have good reservoir properties.

vi. The Rogaland Group

This group forms the Late Cretaceous package in the Norwegian Sea. Fine-grain sediments dominate but a high-quality reservoir sand is also present (NPD, 2017).

Figure 11 shows an interpreted seismic section correlated with well tops and the stratigraphic succession of the study area.

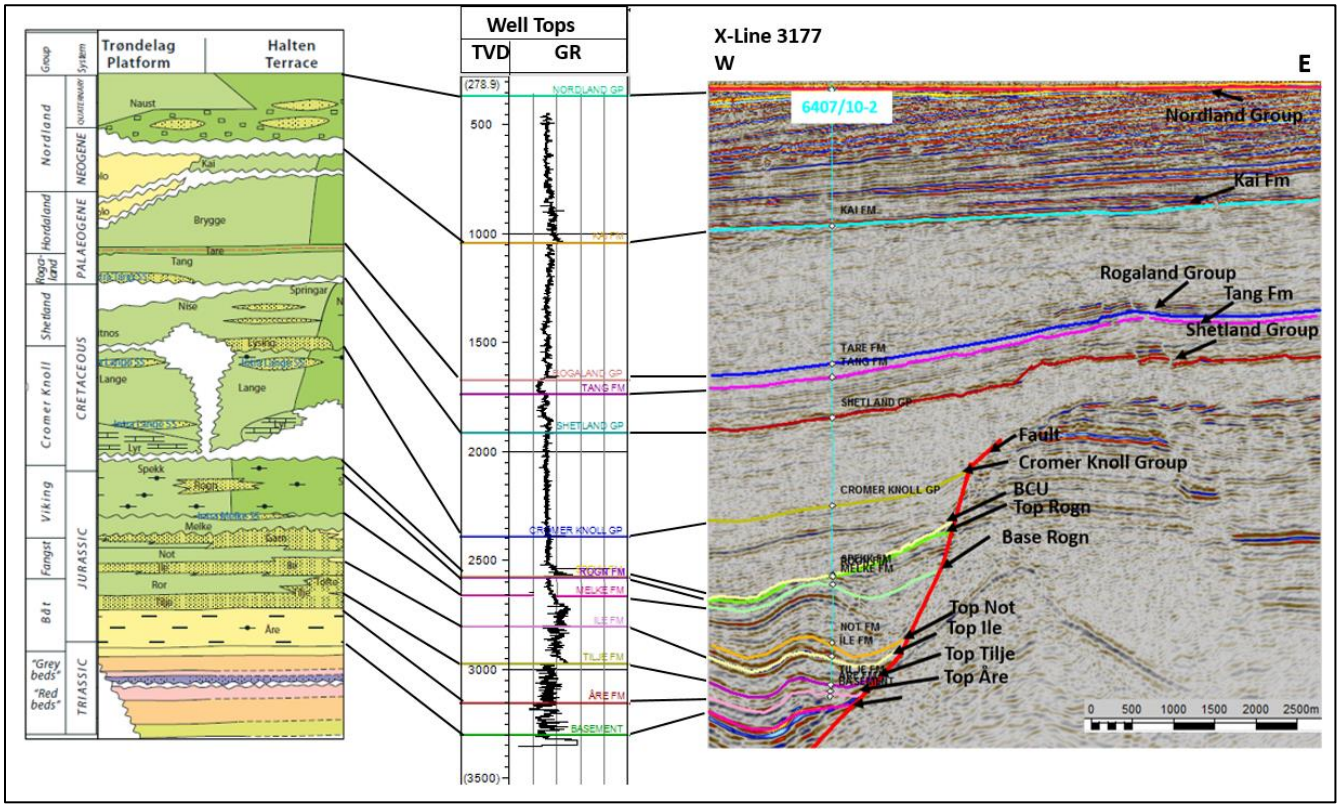

Figure 11: Stratigraphic column (from NPD, 2017) correlated with well tops and GR log of well 10-2 and interpreted seismic section.

3. Dataset and Methodology

3.1 Dataset

The due release date for the data published for the dry well 6407/10-5 is September 2017. This project uses the following available data, provided by Petrobank:

- 3D PSTM seismic dataset covering the PL793 license area
- Well 6407/10-1
- Well 6407/10-2 (Figure 12).

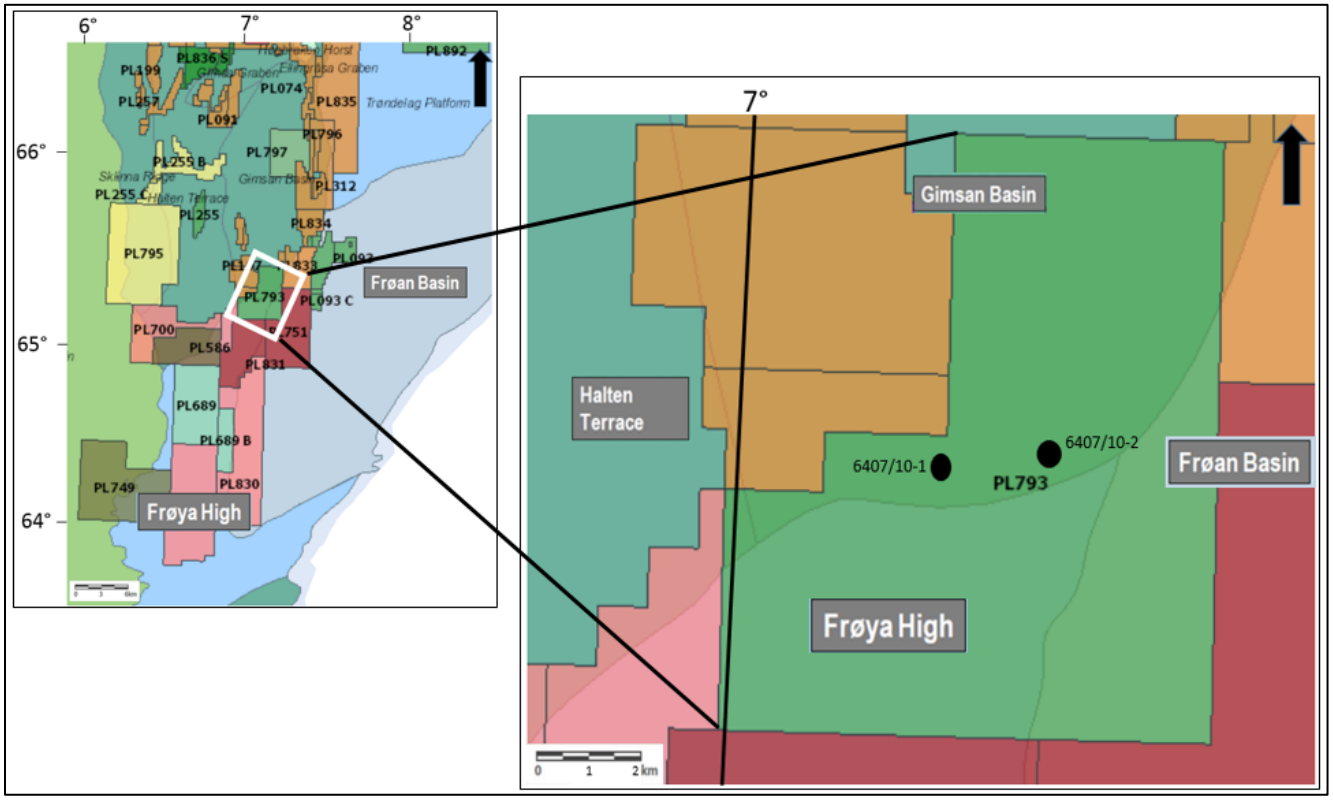

Figure 12: (A) Dataset location in Norwegian Sea. (B) License area is shown together with major among structural elements of the Study Area (modified from npd.no).

3.1.1 3D seismic dataset

The 3D seismic survey for the project has E-W crosslines of 17 km and N-S inlines of 26 km. The maximum two-way travel time is 5200 ms. Other parameters of the 3D cube are shown in the table below (Table 2).

Table 2. Parameters of the 3D cube of the project.

Seismic Survey	**DN0902DNR12**
Type of seismic survey	3D
Number of traces	5000
Number of samples per trace	1251
Sample interval	4
Number of cells total	3504231144
Number of inlines	1348
Number of crosslines	2078
Inline interval	12.50
Crossline interval	12.50
Storage type	ZGY Seismic format
Polarity	Normal
Quality of data	Good
Comments	Clear image, easy for seismic interpretation

3.1.2 Well 6407/10-1

Well 6407/10-1 is one of the two wildcats drilled in the Vingleia-Klakk fault complex, which marks the western boundary of the Froan Basin. It is located at inline 2116, crossline 3333 of the 3D seismic dataset covering the PL793 license area. The total depth of the well is 3347 m, reaching the basement at 3301 m. The well is water bearing and there are no hydrocarbon bearing intervals encountered. Only poor gas shows were reported in the Jurassic succession, in the upper part of the Tilje Formation and in the Ile Formation. All formations do not show economic volumes of producible hydrocarbons. Log data including Caliper, Density, Gamma Ray, Sonic and Neutron is also provided together with detailed well reports (Modified from npd.no).

3.1.3 Well 6407/10-2

Well 6407/10-2 is the second of the two wildcats drilled in the Vingleia-Klakk fault complex. It is in the same seismic 3D survey outline, at inline 2136, crossline 3177. The well was drilled down to a depth of 3825 m, till the Early Jurassic Tilje Formation. Weak to very weak shows were detected in the Jurassic sandstones. There was no shallow gas encountered and no hydrocarbons were present in the Ile and Tilje Formation. Similar log data as for well 6407/10-1 are provided (NPD, 2017).

4. Methodology

The study for this project is carried out by using three software packages: Petrel, Move and Genesis. The methodology is divided into six following methods, which are used to analyze the reasons of the failure for the dry well:

- Seismic Well Tie & Seismic Interpretation
- 2D Restoration
- Basin Modelling
- Top Seal Analysis
- Fault Seal Analysis

4.1 Seismic Interpretation

Seismic Well Tie

To tie the well to the seismic data, synthetic seismograms were generated for wells; 6407/10-1 and 6407/10-2. This was performed in two steps: 1) The sonic log was calibrated with check shots for each well; 2) Synthetic seismograms were generated by using a wavelet that has been deterministically derived from the log reflectivity and a seismic trace in the vicinity of the well. The wavelet has an amplitude and phase spectrum similar to the seismic.

Sonic log calibration for seismic well tie comes with a couple of challenges. Check shot calibration is necessary because the check shots show a very large sampling (maybe 100m or more). The sonic log is densely sampled, however typically it starts measuring the instantaneous velocity well below the seismic reference datum (SRD). Consequently, it delivers a too high average velocity between the first sonic sample and the SRD. The check shot calibration is solving the problem through adjusting the integrated sonic log with the check shot times. The time depth curve derived from the calibrated sonic log delivers a more accurate time depth relationship than the check shot survey. Secondly, dispersion occurs due to the difference in the frequency range of the sonic log and the seismic waves. The check shot calibration addresses the velocity changes coming from the different frequency range used by the sonic log measurement.

The main objective of generating a synthetic seismogram is to tie seismic data to borehole geology. The seismic reflectors are correlated with subsurface geology via the synthetic trace.
Synthetic seismograms of both wells were generated accordingly and tied with the seismic (Figure 13).

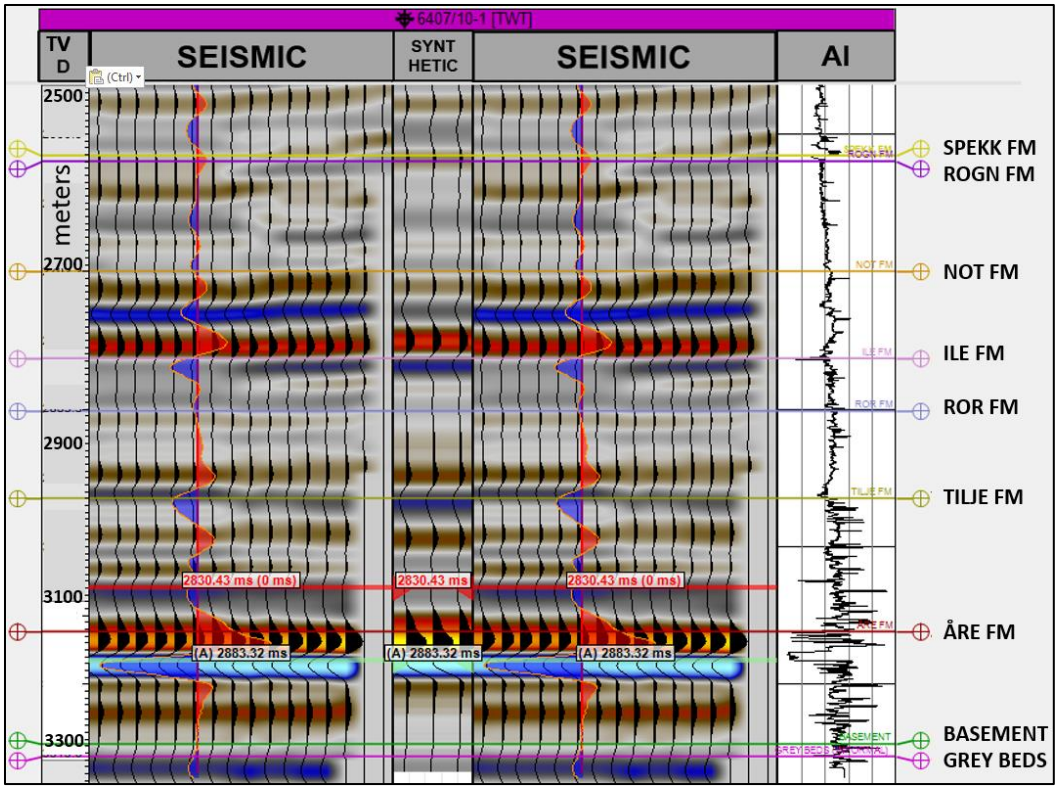

Figure 13 (A): Seismic well tie (Well 6407/10-1).

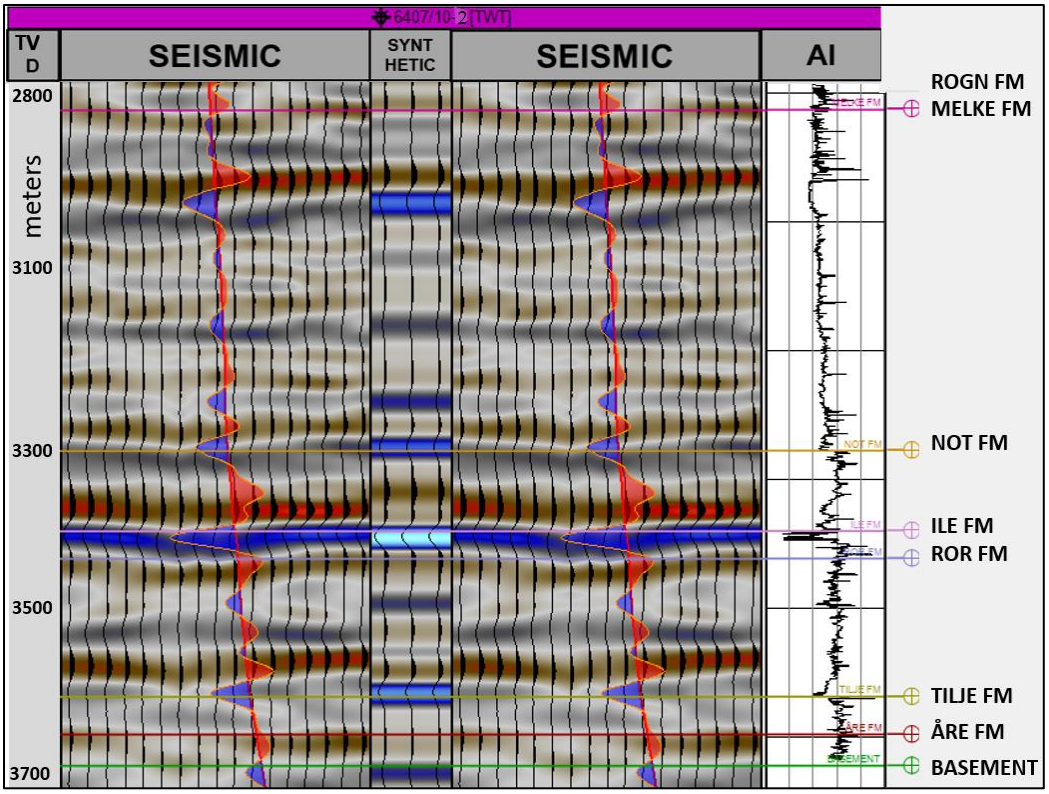

Figure 13 (B): Seismic well tie (Well 6407/10-2).

Seismic Interpretation

The 3D seismic data provided for the project is of good quality with clear reflectors. The main stratigraphic focus for interpretation is the Jurassic interval. A polygon was made defining the area of interest. Within this polygon, the seismic interpretation was performed on crosslines and in-lines. The Base Cretaceous unconformity (BCU) horizon interpretation is shown in Figure 14 as an example. Both wells available for the project and the Jurassic rollover anticline where the dry well is drilled are a part of the polygon area.

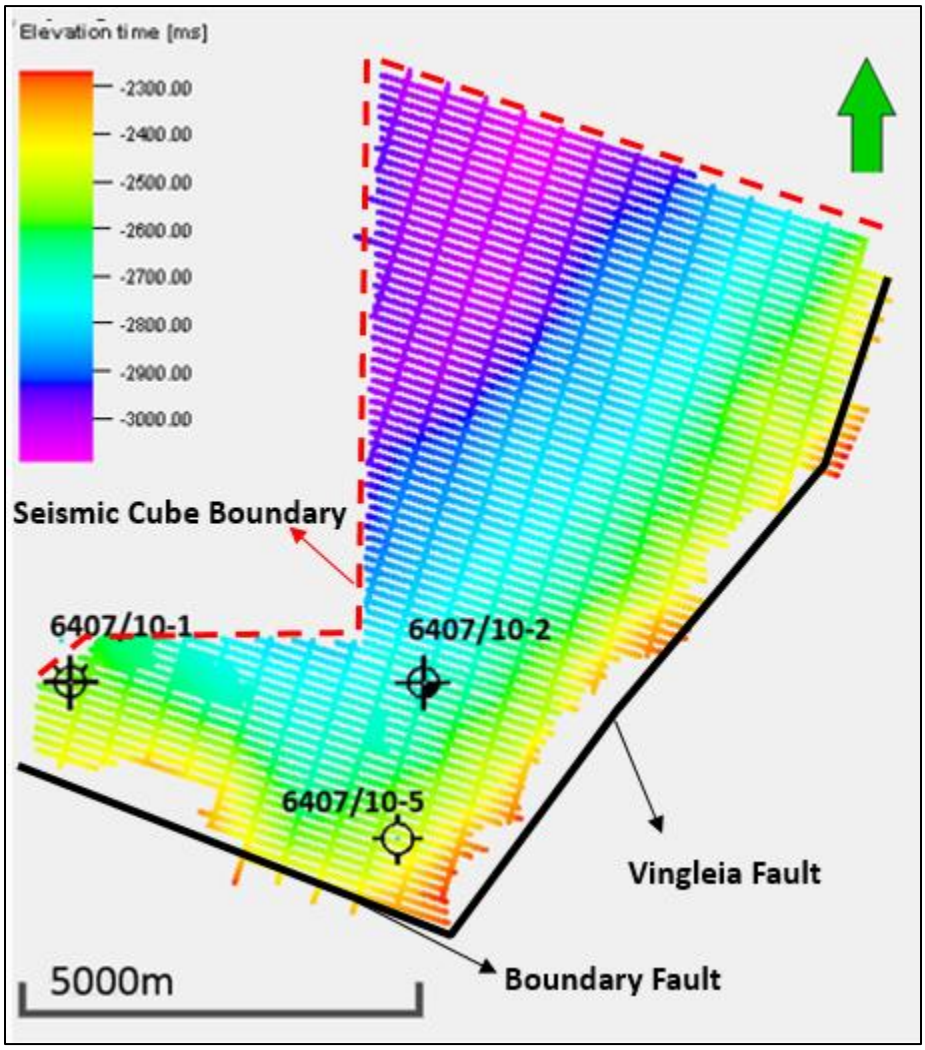

Figure 14: Extent of project's area showing the interpreted seismic lines and location of the three wells together with the interpreted BCU horizon.

The major objective of the interpretation was to map the Jurassic rollover anticline with all the potential Jurassic reservoirs. Several horizons and the major fault were interpreted on the seismic lines inside the polygon. The anticline is present in the hanging wall of the fault. The footwall

shows no clear reflectors of the Jurassic sandstones. On some seismic lines, the Åre coal is interpreted lying over the basement in the footwall. Well 6407/10-3 was drilled in the footwall and it encounters the Spekk Formation lying over Triassic sediments, which supports this interpretation.

Six key horizons were identified along with the major fault. These horizons were interpreted based on the seismic well tie of the two wells of the project. These horizons are:

1. BCU that is the top of Spekk Formation
2. Top of Rogn Formation
3. Base of Rogn Formation
4. Top of Ile Formation
5. Top of Tilje Formation
6. Top of Åre Formation

BCU is the unconformity that acts as the base of the Spekk Formation. The Spekk Formation is the primary source rock of the area. The secondary source rock is the Åre Formation. Sandstones of the Rogn Formation were the target reservoirs for well 6407/10-5. The top and base of the Rogn Formation is interpreted in order to obtain knowledge of its thickness variations. The Ile and Tilje Formations are also considered as reservoir rocks in the Norwegian Sea. Hence, these horizons were interpreted as well (Figure 15).

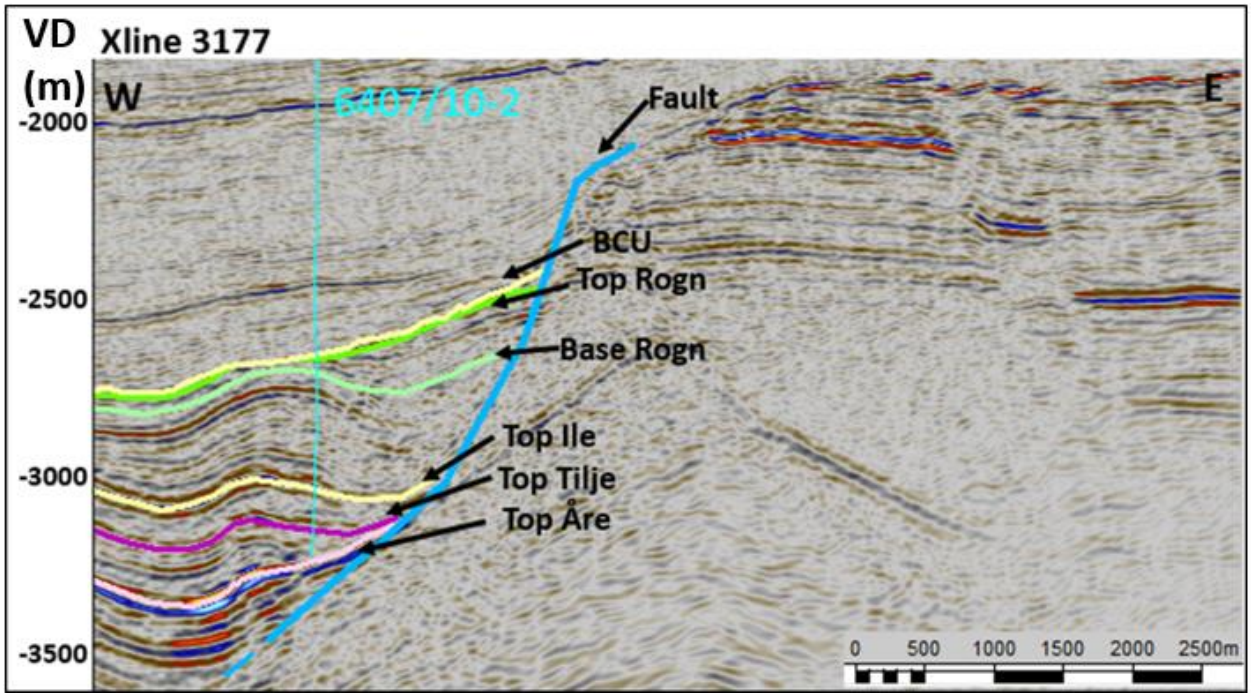

Figure 15: Seismic cross section with interpreted horizons.

4.2 2D Restoration

Phenomenon

Restoration is a technique that allows reconstructing through time a sequence of profiles in a sedimentary basin margin. The restored profiles give information on the total extension or shortening experienced by the basin (Lingrey and Vidal-Royo, 2015).

Cross-sections are restored for two main reasons: 1) Balancing of a cross section provides confirmation that the cross section can be restored by following a reasonable kinematic pathway to their undeformed state, 2) The restored section gives information on how the structural deformation was developed. This is crucial to know in exploration as migration of hydrocarbons, development of traps, reservoir distribution and hydrocarbon generation are all influenced by structural development.

The section balancing and restoration techniques are generally based on the assumption that the volume of the hanging wall is preserved during deformation. This is an approximation, because growth sedimentation and compaction affect the hanging wall. A balanced cross section gives information about the gain and loss of sediments in sedimentary layers and also the amount of extension or shortening. This tells us about the compaction of sediments and its influence on the porosity.

The dry well of this project is drilled on a rollover anticline. The rollover anticline is a common phenomenon in extensional regimes where listric normal faults results in the bending of hanging-wall strata. A 2D modeling technique is used to produce balanced structural cross sections that illustrate curved faults as a product of a large number of small straight fault fragments (Xiao et al., 1992).

Case Study

Structural restoration is divided into three components of a deformed rock body: 1) beds displaced by faults, 2) rotation that may occur on limbs of the folds or displacement along curved faults, 3) distortion causing shear in rocks. These three components are demonstrated by three different cases. Figure 16 shows a normal fault with 375m offset in its restored state and the following Figures demonstrate the three cases.

Case A shows a 375-m net slip movement along the dip of the normal fault. In case B, 375 m of fault translation occurred along with 4.4° of rotation. Whereas case C depicts all the three components discussed above: fault translation of 375 m, 8.7° of tilt rotation and flexural alteration in both hanging wall and footwall. To restore these cross sections in 2D, un-faulting is required in case A in order to rejoin the hanging wall with the footwall. In case B, layers need to be untilted and case C requires an unfolding distortion (Lingrey and Vidal-Royo, 2015).

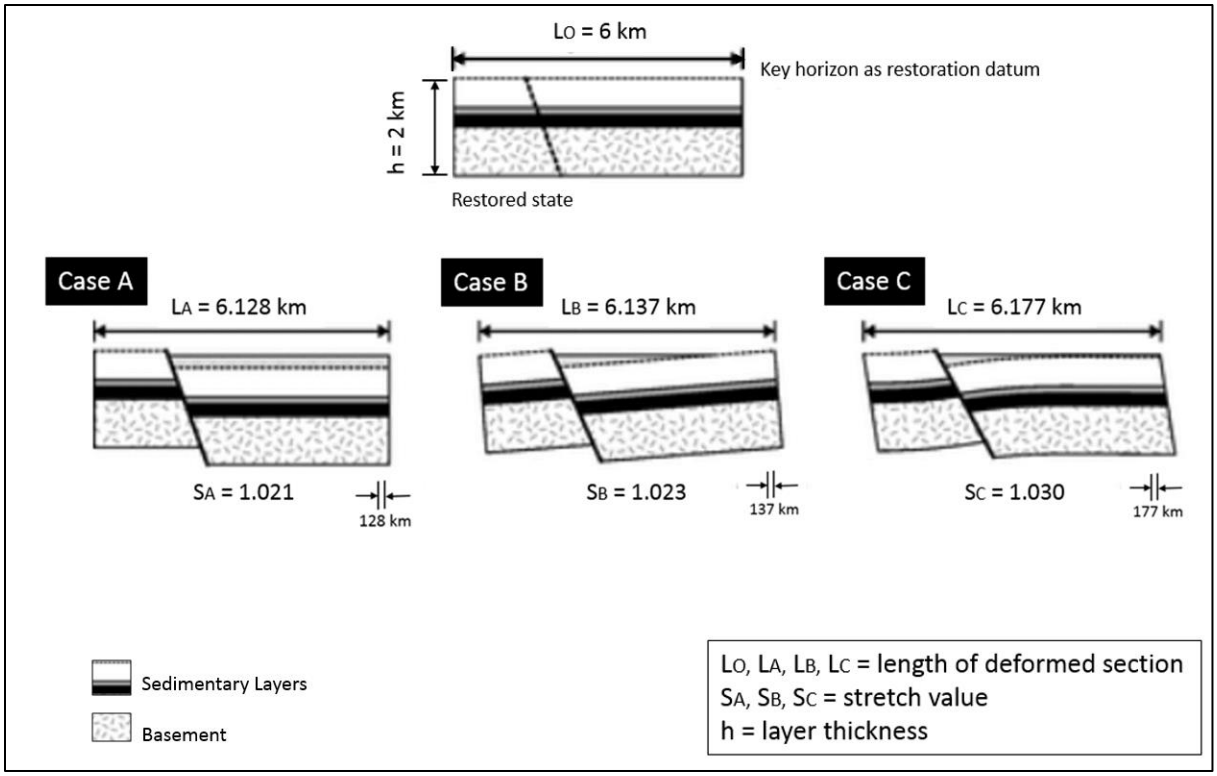

Figure 16: Three components for a faulted structural profile with area constant in 2D (from Lingrey and Vidal-Royo, 2015).

Principle of Decompaction

A seismic section of crossline 3177 was selected to perform 2D restoration and decompaction for which the Move software was used. Move is a structural modelling software that offers a complete range of tools to construct models and perform kinematic analysis in 2D and 3D.

Decompaction is mainly affected by the lithology. Therefore, a stratigraphic chart of all the lithological percentages and the rock properties of each sedimentary layer were generated into a database (Table 3 & 4). The decompaction process is based on the following equation (Sclater and Christie, 1980)

$$\boldsymbol{f = f0 * (e^{-cy})}$$

where ***f*** is the present-day porosity;

f0 **is** the porosity at the surface;

c is porosity-depth coefficient and

y **is** the depth in meters.

The equation describes a decrease of the porosity with depth as a consequence of compaction. When the layers are decompacted, they thicken and there is a gain in the area of a certain sedimentary layer. Note that the effect of decompaction on shales is larger compared to sandstones.

Procedure

The whole section is interpreted. This is done in the time domain whereas 2D restoration is performed in the depth domain. A simple time depth conversion was applied to a small cube that covers the seismic section used for 2D restoration. The underlying velocity model is based in interval velocities extracted from the calibrated sonic log of the well 6407/10-2. The velocities are calibrated with the well tops of both wells. The seismic volume cube is converted into the depth domain and a depth section was interpreted. The result is transferred from Petrel to Move. Once done, all the sedimentary layers interpreted on the seismic section are turned into separate polygons. These polygons are then used in the restoration process.

To restore a section with multiple layers, stratigraphic key horizons are identified. The youngest horizon is picked and typically converts to a flat, horizontal datum, which defines the geological time of its original position. When there is faulting and folding present in the section, then first the sedimentary layers are un-faulted (Lingrey and Vidal-Royo, 2015). In this way, the fault offset is removed. Then any folding of the layers is removed. For decompaction, isostatic correction is applied. For this project, airy isostasy was used**.** Vertical Simple shear module was applied for un-faulting the footwall and hanging wall. This method when applied to un-faulting tends to maintain the initial length of the rock body and points on the curved rock body are linearly translated hence there might be a loss in thickness and 2D move shows this loss of thickness as a function of area.

A sequence of restored stratigraphic layers is generated which gives information about the gain and loss of sediments within each sedimentary layer and also the amount of extension.

The procedure described above is performed on the 2D seismic section (Figure 17).

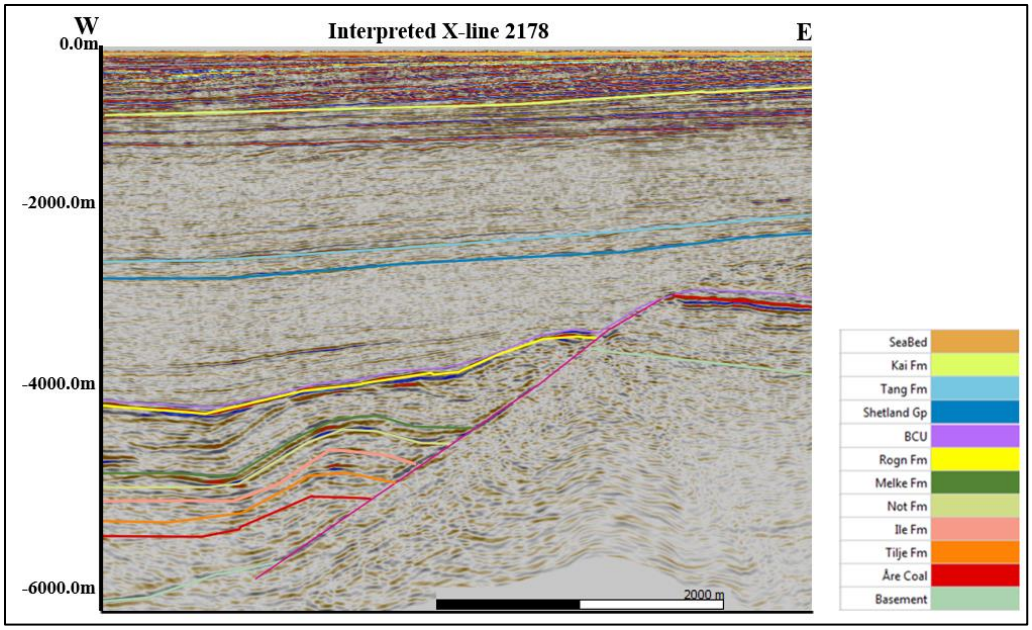

Figure 17: Interpreted seismic section (crossline 2178) used for 2D restoration.

Table 3. Stratigraphy of all the layers used in 2D restoration, taken from well 6407/10-2. Abbreviations: Fm= formation, Gp= Group.

Stratigraphy | Rock Properties | Strat. Column | Compaction Curves

	Horizon	Colour	Rock Type	Age	Height	Thickness	Active
1	SeaBed		Nordland	7.0 Ma		649.0 m	☑
2	Kai Fm		Kai Fm	33.0 Ma		96.0 m	☑
3	Hordland Gp		Hordland Gp	56.0 Ma		522.0 m	☑
4	Rogaland Gp		Rogaland Gp	61.0 Ma		62.0 m	☑
5	Tang Fm		Tang Fm	66.0 Ma		188.0 m	☑
6	Shetland Gp		Shetland Gp	84.0 Ma		501.0 m	☑
7	Cromer Knoll ...		Cromer Knoll ...	93.0 Ma		443.0 m	☑
8	BCU		BCU	145.0 Ma		9.0 m	☑
9	Rogn Fm		BCU	157.0 Ma		605.0 m	☑
10	Melke Fm		Shale	162.5 Ma		200.0 m	☑
11	Not Fm		Default	165.2 Ma		200.0 m	☑
12	Ile Fm		Ile Fm	168.0 Ma		246.0 m	☑
13	Tilje Fm		Tilje Fm	185.0 Ma		58.0 m	☑
14	Åre Coal		Åre coal	195.0 Ma		56.0 m	☑
15	Basement		Basement	252.0 Ma		525.0 m	☑

Table 4. Rock Properties of all sedimentary layers. These properties were used for decompaction of the sediments.

Stratigraphy | Rock Properties | Strat. Column | Compaction Curves

	1: Rock Type	2: Rock Group	3: Background_colour	4: pattern	5: Sandstone(%)	6: Shale(%)	7: Limestone(%)	8: Porosity
	Sandstone	Sand			100	0	0	0.49
	Shale	Shale			0	100	0	0.63
	Limestone	Limestone			0	0	100	0.41
Unit					%	%	%	
1	Default	Sand						0.56
2	ShalySand	Silt						0.56
3	Salt	Salt						0.00
4	Chalk	Limestone						0.70
5	Nordland	Shale			20	80	0	0.60
6	Kai Fm	Shale			10	90	0	0.62
7	Hordland Gp	Shale			4	88	8	0.61
8	Rogaland Gp	Silt			35	60	5	0.57
9	Tang Fm	Shale			0	90	10	0.61
10	Shetland Gp	Shale			5	85	10	0.60
11	Cromer Knoll ...	Shale			30	70	0	0.59
12	BCU	Shale				100		0.63
13	Rogn Fm	Sand			60	30	10	0.52
14	Ile Fm	Sand			80	10	10	0.50
15	Tilje Fm	Sand			90	10	0	0.50
16	Basement	Basement						
17	Åre coal	Shale				100		0.63

4.3 Basin Modelling

Phenomenon

Basin modelling is a process in which the burial history for the formations present in the study area is generated. Age, thickness and lithologies of these formations are used as input data. Those data are usually obtained from well reports, outcrops and seismic. A basin model gives information about the depositional and thermal histories when a rock's physical data is combined with geochemical or thermal data.

Geochemical data is obtained from final well reports and geochemical analyses performed on well cuttings and cores of well 6407/10-1 and 6407/10-2. Temperature data of different formations of the wells are calibrated with other thermal parameters and then temperature is assigned to all depths for modelling the maturity of the hydrocarbons. All these values are used to reconstruct the timing of the kerogen transformation, hydrocarbon generation and expulsion.

Procedure

Basin modelling is a part of this project to determine the hydrocarbon's presence, maturity of source rock, kerogen transformation and all other parameters related to hydrocarbon charge. They are critical in determining the validity of a reservoir. The software 'Genesis version 4.92' was used to perform 1D basin modelling for the dry well. Two source rocks: Spekk Formation and Åre Formation are present in the area.

- The Spekk Formation was deposited in marine anoxic bottom water conditions. The dark claystones of this formation show high organic content and they are the main functional source rock in the Norwegian Sea. Type II kerogen is present in the Spekk Formation with a Total Organic Content (TOC) value around 4%. This is the primary source rock.
- The Åre Formation was deposited in coastal to delta plain environments along-with swamps. Coal beds are up to 8 m thick at some places. It is considered immature in the vicinity of the Trøndelag Platform. The Åre Formation is considered as a secondary source rock with TOC value around 3% and type III kerogen.

Data of these source rocks from the geochemical and final well reports of the two wells 6407/10-1 and 6407/10-2 are used as geochemical & physical parameters of the basin model. Their kerogen types, TOC, borehole temperature and Hydrogen Index (HI) have also been added. These values are shown in Tables 5 and 6 for Well 6407/10-1 and in Tables 7 and 8 for Well 6407/10-2. A geothermal gradient of 32 °C/km is used.

All these parameters are used in generating the burial history graph for both wells. Graphs for burial history, transformation ratio, oil and gas expulsion and generation are made for two source rocks in both wells. Their patterns are evaluated.

Well 6407/10-1

Table 5. Input data for burial history reconstruction.

FORMATION	Age in Million Years	Formation top	Thickness (meters)	Main Lithology	Remarks
NAUST FM	11.61	366	675	Shale	
KAI FM	33.9	1041	199	Shale	
BRYGGE FM	48.6	1240	431	Shale	
TARE FM	58.7	1671	64	Shale & Siltstone	
TANG FM	61.7	1735	178	Shale	
SHETLAND GP	83.5	1913	477	Shale	
CROMER KNOLL GP	89.3	2390	183	Shale	
SPEKK FM	150.8	2573	6	Shale	Source Rock
ROGN FM	161.2	2579	123	Sandstone	Reservoir Rock
NOT FM	167.7	2702	101	Shale	
ILE FM	175.6	2803	65	Sandstone	Reservoir Rock
ROR FM	183	2868	106	Sandstone	
TILJE FM	196.5	2974	181	Sandstone	Reservoir Rock
ÅRE FM	199.6	3155	164	Coal & Sandstone	Source Rock
GREY BEDS	237	3319	81	Sandstone	

Table 6. Input data for geochemical parameters.

LITHOLOGY	Depth	TOC	SI (mg/g)	S2 (mg/g)	HI (S2/TOC)	TPI	TMAX (deg C)	Kerogen Type
Spekk Formation	2572	0.68	0.07	0.38	56	0.1 6	439	Type II
	2575	2.76	0.36	6.32	229	0.05	430	
	2577	3.84	0. 6 9	11.35	296	0.06	425	
Åre Formation	3157	13.07	3.86	46.86	359	0.08	434	Type III
	3162	5.29	0.42	4.44	84	0.09	434	
	3170	3.24	0.26	2.57	79	0.09	433	
	3195	2.32	0.35	2.32	100	0.13	434	
	3210	4.81	0.38	2.99	62	0.11	438	
	3275	2.74	0.58	4.62	169	0.11	433	

Well 6407/10-2

Table 7. Input data for burial history reconstruction.

FORMATION	Age in Million Years	Formation top	Thickness (meters)	Main Lithology	Remarks
NAUST FM	11.61	359	650	Shale	
KAI FM	33.9	1009	96	Shale	
BRYGGE FM	48.6	1105	515	Shale	
TARE FM	58.7	1627	62	Shale & Siltstone	
TANG FM	61.7	1689	188	Shale	
SHETLAND GP	83.5	1877	501	Shale	
CROMER KNOLL GP	89.3	2378	392	Shale	
LYR FM	145.5	2770	51	Shale	
SPEKK FM	150.8	2821	9	Shale	Source Rock
ROGN FM	161.2	2830	74	Sandstone	Reservoir Rock
MELKE FM	164.7	2904	423	Shale	
NOT FM	167.7	3327	109	Shale	
ILE FM	175.6	3436	43	Sandstone	Reservoir Rock
ROR FM	183	3479	200	Sandstone	
TILJE FM	196.5	3679	58	Sandstone	Reservoir Rock
ÅRE FM	199.6	3737.14	56	Coal & Sandstone	Source Rock
GREY BEDS		3793.69		Sandstone	

Table 8. Input data for geochemical parameters.

LITHOLOGY	Depth	TOC	SI (mg/g)	S2 (mg/g)	HI (S2/TOC)	TPI	TMAX (deg C)	Kerogen Type
Spekk Formation	2820	0 . 8	0 . 0	0 . 4	44	0.08	433	Type II
	2822	1.8	0.2	3 . 0	165	0.05	433	
	2822	0.1	0	0.2	214	0	436	
	2823	4.9	1.1	20.3	414	0.05	421	
	2824	4.1	1 . 0	1 8 . 6	450	0.05	431	
	2825	2.4	0 . 4	7.1	297	0.06	432	
	2825	3.4	0 . 5	10.1	297	0.05	432	
	2827	1.6	0 . 3	4	250	0.06	433	
Åre Formation	3740	6.85	0.48	5.3	77	0.08	434	Type III
	3749	13.09	1.49	29.52	226	0.05	435	
	3758	2.65	0.35	3.42	129	0.09	431	
	3765	1.64	0.26	1.14	70	0.19	434	
	3777	2.21	0.38	2.3	104	0.14	432	
	3789	13.48	2.01	34.31	255	0.06	432	

4.4 Top Seal Analysis

Loss of top seal integrity based on faulting and fracturing could also be a reason for a dry well. Determining the presence and orientation of fractures from seismic data is extremely difficult as these fractures are below seismic resolution (Chopra and Marfurt, 2006). However, faults are easier to identify. Several seismic attributes have been developed which can be used as an aid in the interpretation of seismic data. They help in observing detailed structures and small-scale faults.

Seismic Attributes

Seismic attributes describe the features and characteristics of seismic data. A seismic attribute is defined as the rate of change in quantity with respect to time or space or both. They assist in qualitative interpretation and can describe the geometry related to structure and stratigraphy (Hart, 2008).

Basic seismic properties are used to derive seismic attributes such as frequency, amplitude etc. Seismic amplitudes are sometimes, unable to display minor features like small faults or thin lithological units. Here seismic attributes can be used to observe the desired features (Chopra and Marfurt, 2006).

Seismic attributes are classified as surface and volume attributes. Volume attributes are more useful for this project as these attributes define the major faults in 3D. Often, many attributes are combined to work together and produce desired results for enhancement of subsurface physical and geometric features (Chopra and Marfurt, 2006).

Evaluation of Top Seal

Petrel software is used to extract seismic attributes for evaluating the top seal. In order to observe the presence of faults and their patterns, the influence of the seismic noise on the seismic attributes has to be studied as seismic noise does not show any pattern whereas faults and fractures are visualized as a pattern. Therefore, two small cropped cubes have been generated. One cube covers a volume within the top seal. The other cube mainly comprised seismic noise, which is present at greater depths. Figure 18 shows a seismic section highlighting the seal and the noise area.

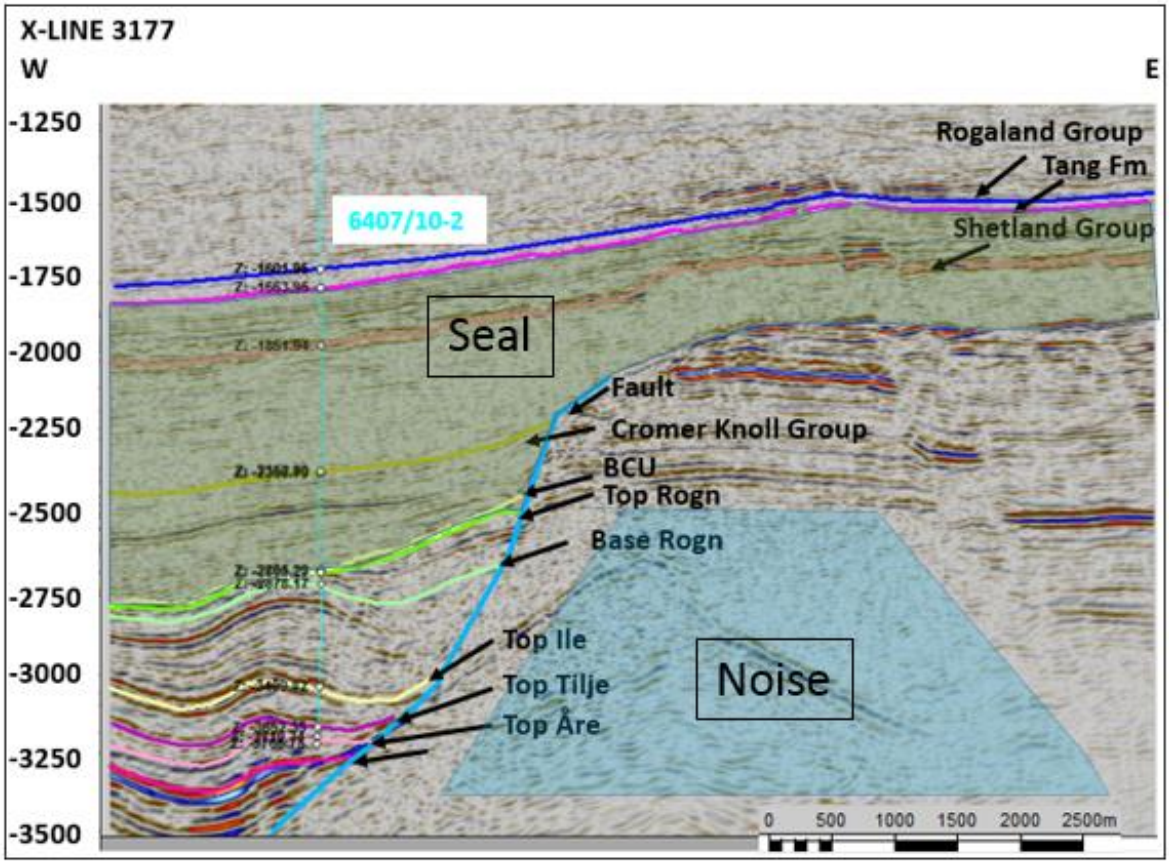

Figure 18: Seismic section showing the reservoir with top seal and area with low S/N.

A combination of attributes was run to extract the faults/fractures on both cropped cubes and their results were compared.

Workflow for Attribute Analysis

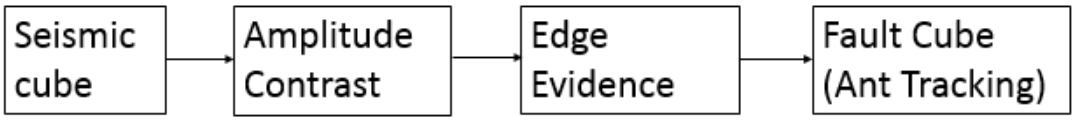

I. Amplitude Contrast

Amplitude contrast is an attribute that can be used to understand the distribution of fine details in the subsurface. The attribute functions in the three main directions, which are normalized and combined. Thus, enhancing the contrast of the seismic data's subtle features like small faults (Figure 19).

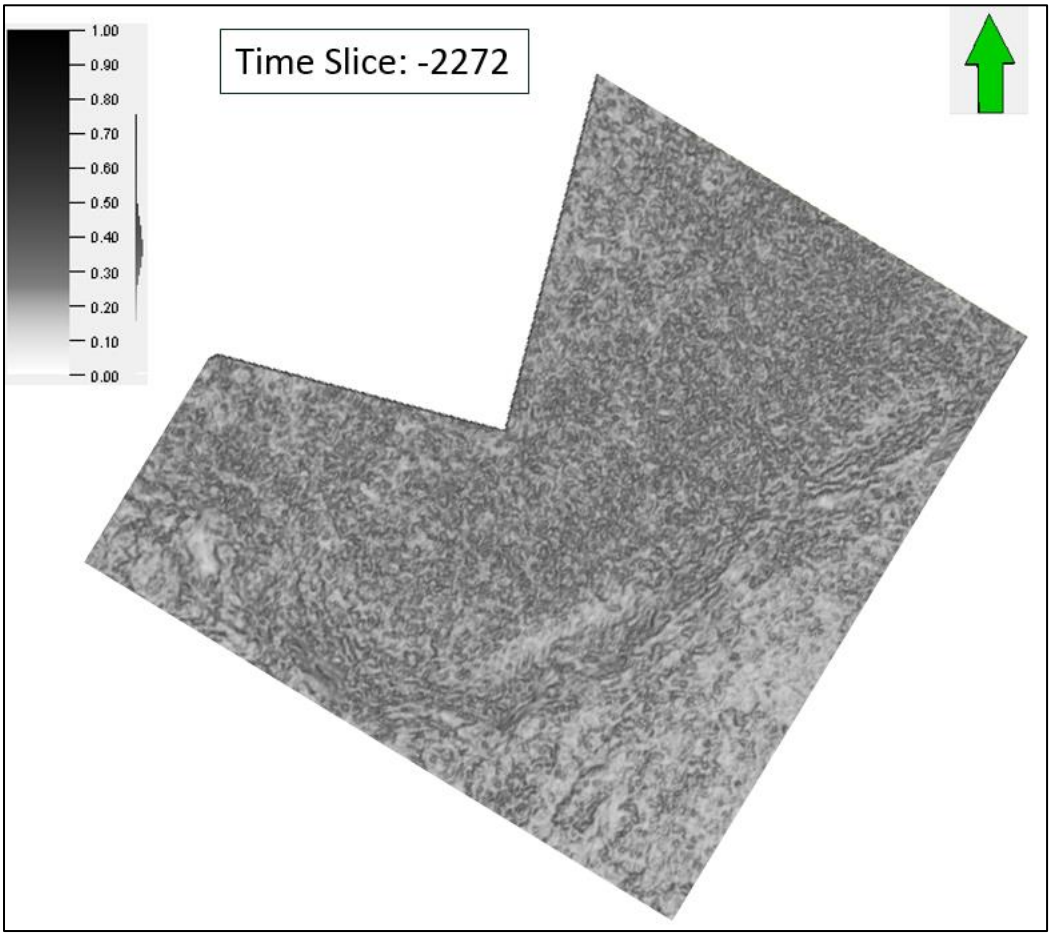

Figure 19: Amplitude contrast on a time slice of seismic cube.

II. Edge Evidence

To aid the fault identification, the amplitude contrast cube is used as input to the next attribute i.e. edge evidence. Edge evidence is a method used to enhance and delineate ridges and edges such as faults (Volcan et al., 2014). It can be adapted to different directions resulting in horizontal and vertical edge identification or edge identification along inline or crossline direction. Figure 20 shows the result of the edge evidence attribute applied to the amplitude contrast cube.

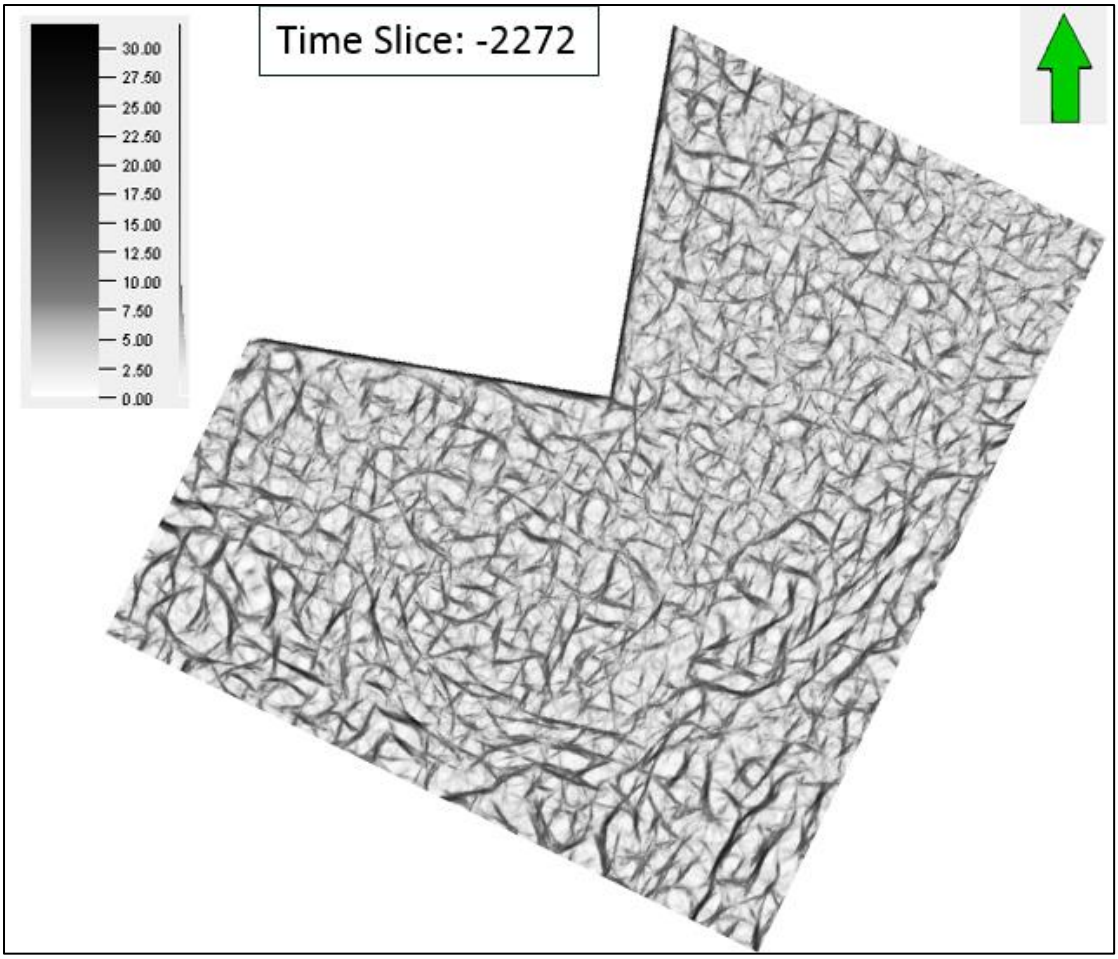

Figure 20: Same time slice as in Figure 19 showing enhancement of linear features after application of edge evidence attribute.

III. Ant Tracking

The Ant tracking attribute enhances discontinuities such as faults, based on the concept of swarm intelligence. The attribute cannot be applied directly to the seismic cube. The fault pattern needs to be enhanced using, for instance, the sequence of attributes amplitude contrast followed by edge evidence as described above. The benefit of ant tracking lies in its ability to efficiently suppress the remaining noise in the conditioned cube and enhancing the continuity of the fault pattern. The challenge is to identify and in some cases, reduce coherent noise that may show up together with the faults. Therefore, ant tracking offers powerful filtering tools that allow extracting the linear features of specific dip and azimuth ranges. Figure 21 shows the result of the ant tracking attribute applied to the edge evidence cube.

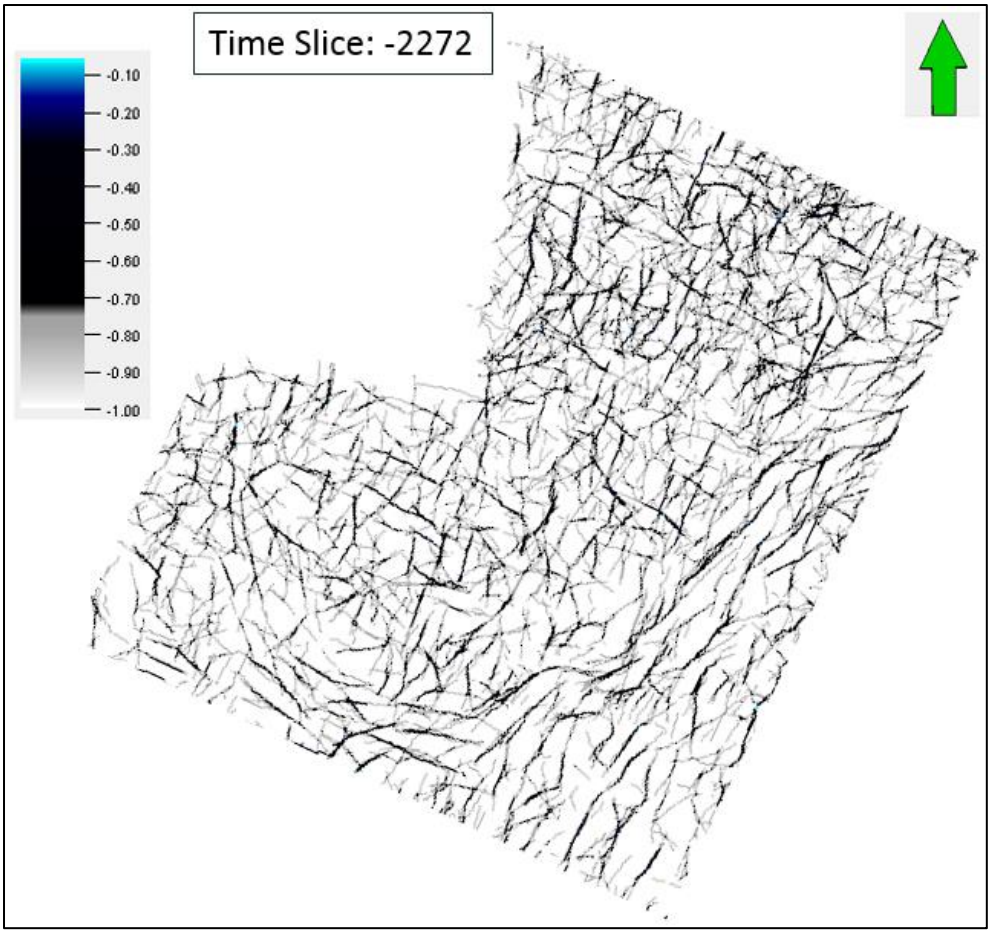

Figure 21: Time slice with much clearer linear patterns as a result of ant tracking. Back ground noise is largely removed.

4.5 Fault Seal Analysis

Faults can act as a barrier or a conduit for fluid flow. Many factors act together to enhance fault sealing such as fault zone architectures, difference of pressure across faults, fault rock properties etc (Cerveny et al., 2005). In order to check if the fault in the study area has sealing characteristics, the following analysis were performed:

- Fault Juxtaposition
- Shale Gouge Ratio

Fault Juxtaposition

The trap formed in the study area is a rollover anticline in the hanging wall of a normal fault. For such traps, formed in the hanging wall, neighboring fault compartments play a major role in sealing hydrocarbons.

For fault juxtaposition, three cases are shown in Figure 22. Figure 22a shows layers of sands in the hanging wall opposing shale on the other side of the fault. In this case, a fault is potentially sealing.

Figure 22b shows sandstone against sandstone but there is a seal membrane in the form of clay smear in the fault zone, which separates the two sandstones and act as a barrier. Depending on the thickness of the smear it may prevent fault leakage.

The last Figure 22c shows that sandstone in the hanging wall is juxtaposed against sandstone. The sand layers are separated by thin shale layers which are not sufficient to provide a significant shale smear inside the fault zone. The fault here is likely to be leaking.

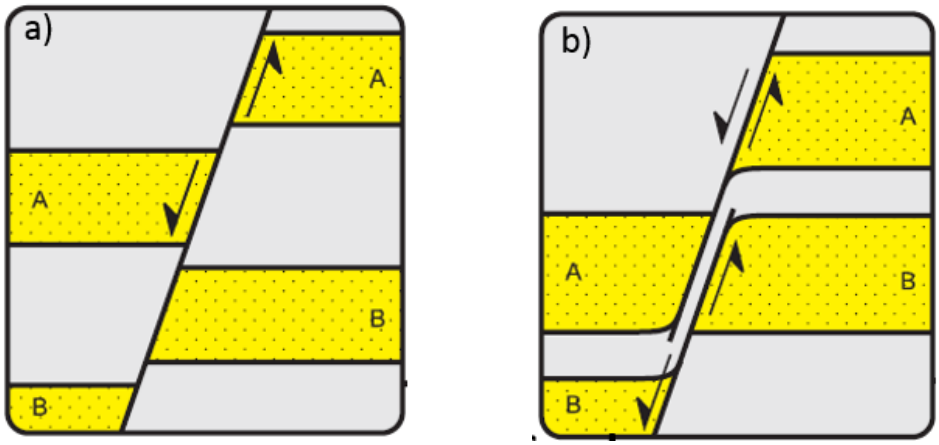

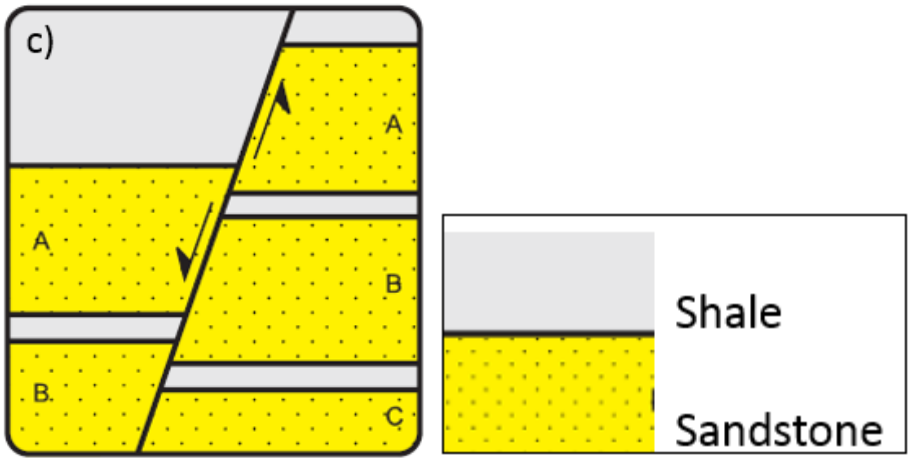

Figure 22: Fault Juxtaposition. a) Juxtaposition Seal. b) Clay Smear c) Sand-Sand Juxtaposition (from Færseth et al., 1999).

In extensional settings, there are two groups regarding reservoir juxtaposition. First is the self-separated reservoir in which the reservoir in the hanging wall is completely separated from the footwall. It might be juxtaposed to a shale or another sandstone unit. If the reservoir in the hanging wall faces a sandstone, a clay membrane must be present in between these two in order to prevent leakage (Figure 22b).

The second group is self-juxtaposed reservoir, in which the reservoir is partially juxtaposed with itself along the fault. Here also a seal membrane is required in order to make the fault sealing (Figure 22c; Færseth et al., 1999). From seismic interpretation and 2D restoration, it is clear that the Rogn Formation is juxtaposed against the Åre Formation. The Åre Formation consists of sandstone and coal. This indicates that fault juxtaposition in the study area is described by Figure 22b. However, the amount of shale within the fault zone needs to be determined.

Shale Gouge Ratio

The amount of shale within a fault zone is described by the Shale Gouge Ratio (SGR). SGR is a percentage of clay or shale in the slipped interval of the fault zone. The algorithm calculates the net amount of clay or shale from the host lithology that has been displaced and passed through the point of consideration of the fault. The sum of the shale layer thickness is multiplied by the clay percentage. This product is divided by the fault throw:

$$SGR = \frac{(\text{Shale layer thickness})\ x\ (\text{Clay percentage})}{\text{Fault throw}}$$

The SGR is an important parameter to define the sealing behavior of the fault. The fault seal analysis was done using Petrel software to generate the juxtaposition triangle diagrams for well

6407/10-1 based on the lithological layers. In addition, the SGR as a function of the fault throw was derived for this well.

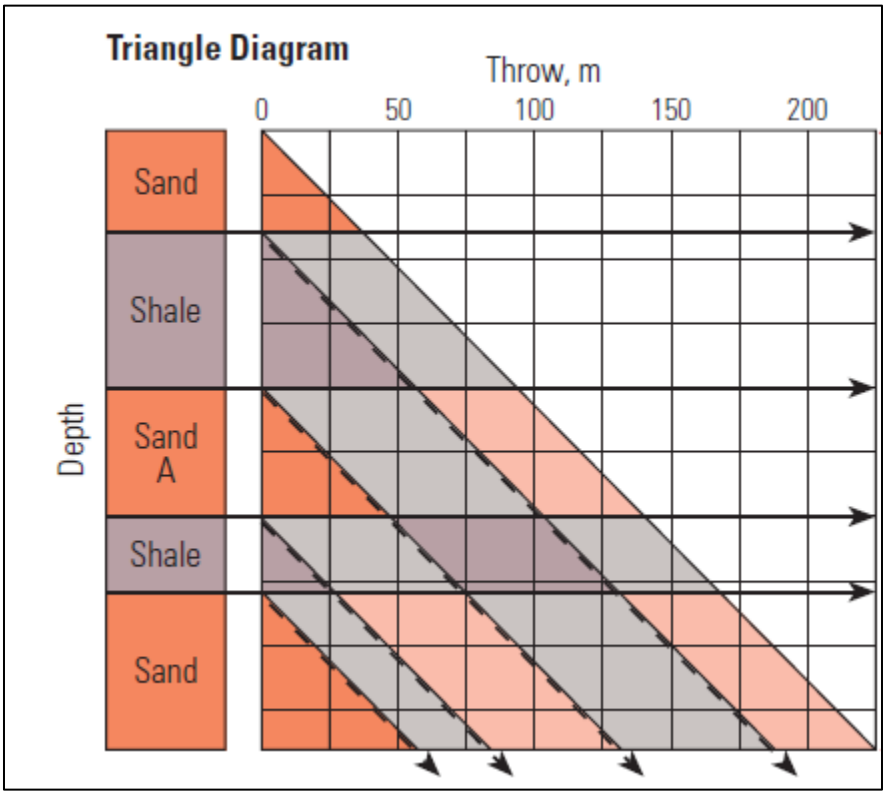

Figure 23: Triangle Diagram showing juxtaposition of sand and shale (modified from Cerveny et al., 2005).

Figure 23 shows the principle of the triangle diagram for a shale-sand layering. The column on the left side gives the stratigraphy. The horizontal axis describes the 'throw'. Simulating the movement of a normal fault the diagram shows the juxtaposition of any of the layers to the left as a function of the fault throw. The SGR can be calculated as a function of the throw for each point within the diagram, once the shale content for each layer has been defined. This allows estimating the sealing behavior of the fault for the reservoir layer, by following the layer in the diagram and reading the SGR value at the throw value of the fault.

5. Observations & Results

5.1 Seismic Interpretation

The seismic cross line 3177 passes through well 6407/10-2. The interpretation was performed for the seismic horizons identified in the well tops. The rollover anticline was mapped. The base and top of the Rogn Formation defining the target reservoir was also interpreted (Figure 24).

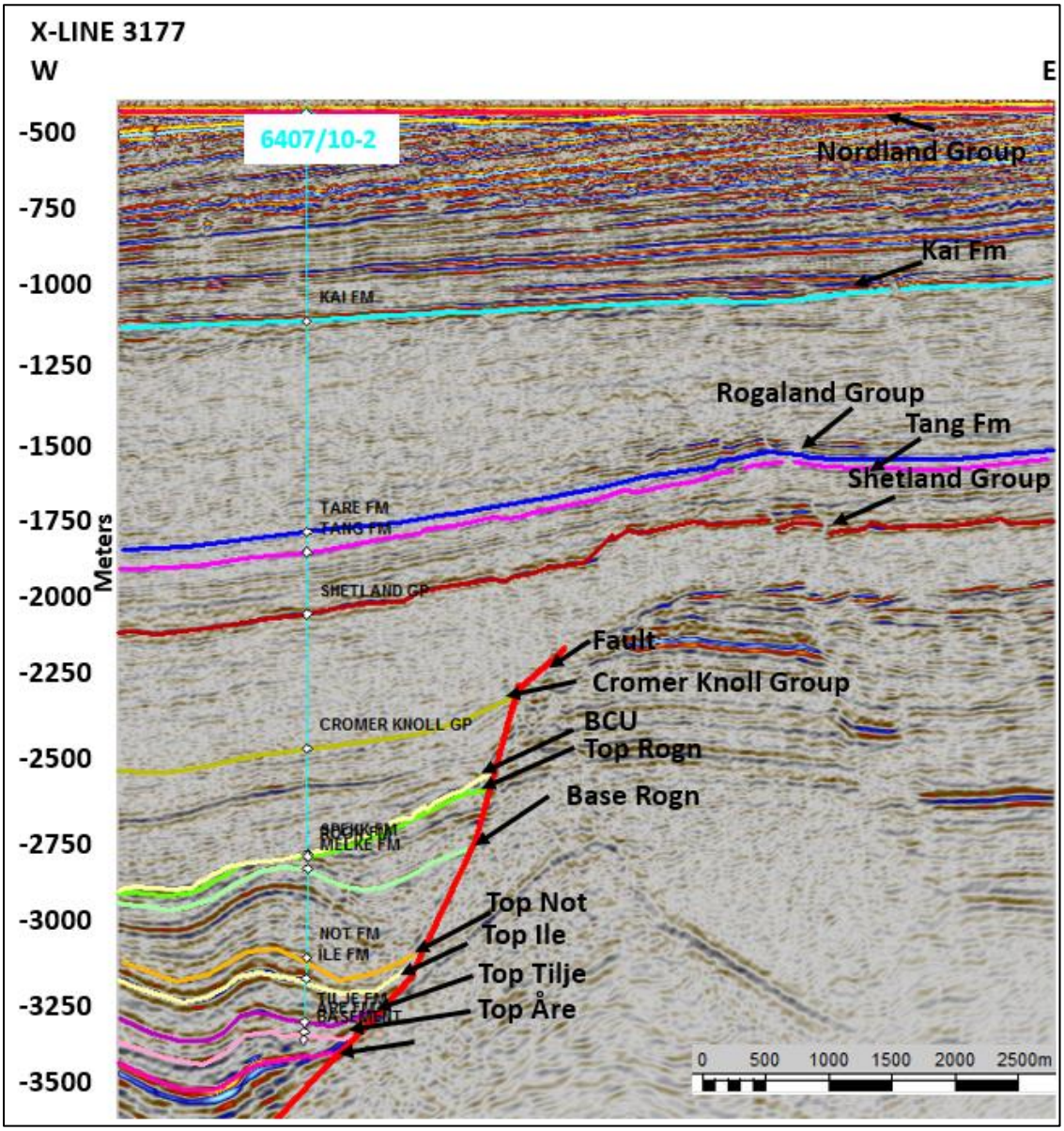

Figure 24: Seismic crossline 3177, passing through well 6407/10-2, with all the interpreted horizons and faults.

The top of the Rogn Formation is partly eroded by the BCU, just at the apex of anticline. The interpreted top of the Rogn Formation shows a fairly elongated pinch out next to well 6407/10-2. The following two Figures illustrate this pinchout (Figures 25 and 26).

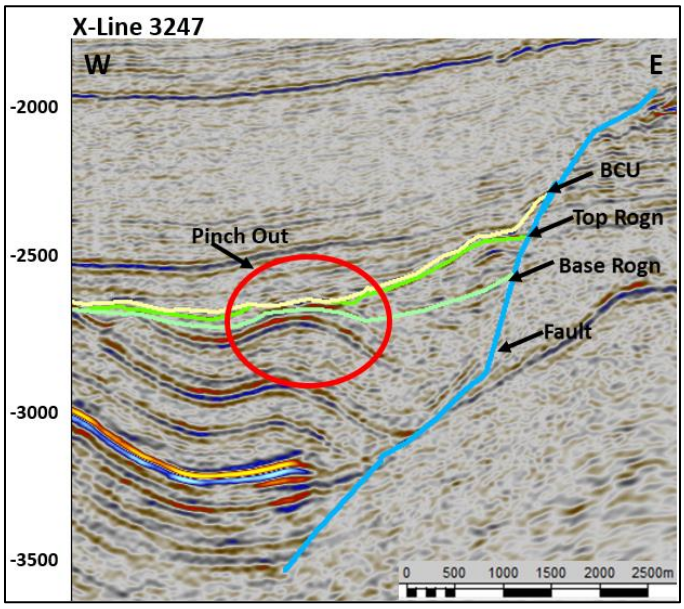

Figure 25: Seismic crossline 3247 showing top Rogn Formation pinching towards the BCU.

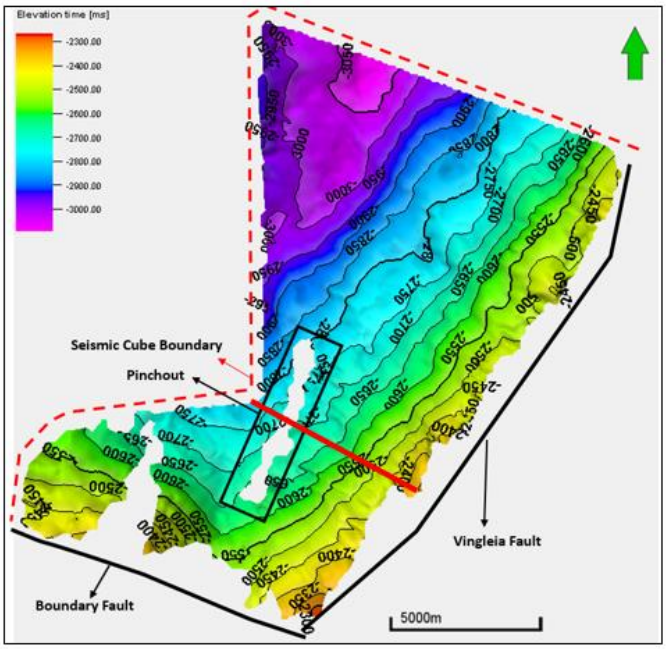

Figure 26: Surface map of the top Rogn Formation showing the pinchout. Red line shows the location of seismic line 3247.

Figures 27 and 28 shows the structural maps for the BCU and the base Rogn. Both surfaces are smooth and show no evidence of erosion. This shows that the BCU only affects the top of the Rogn Formation.

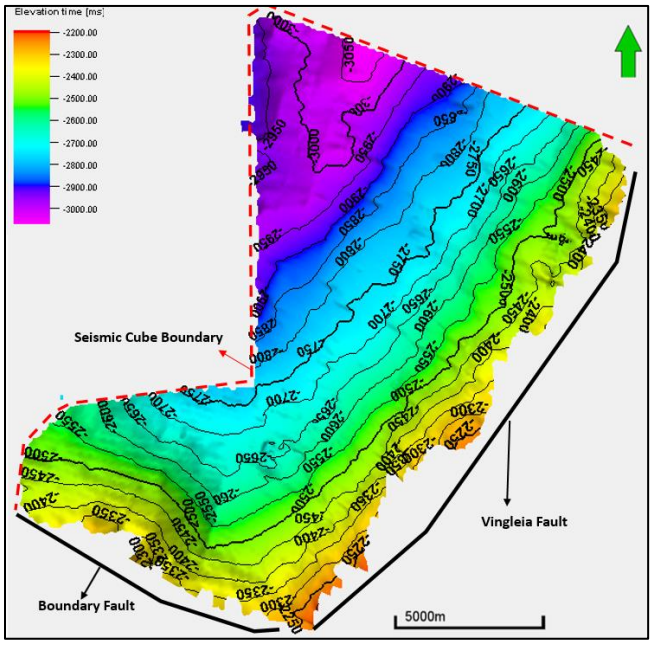

Figure 27: Surface map of Spekk Formation (BCU).

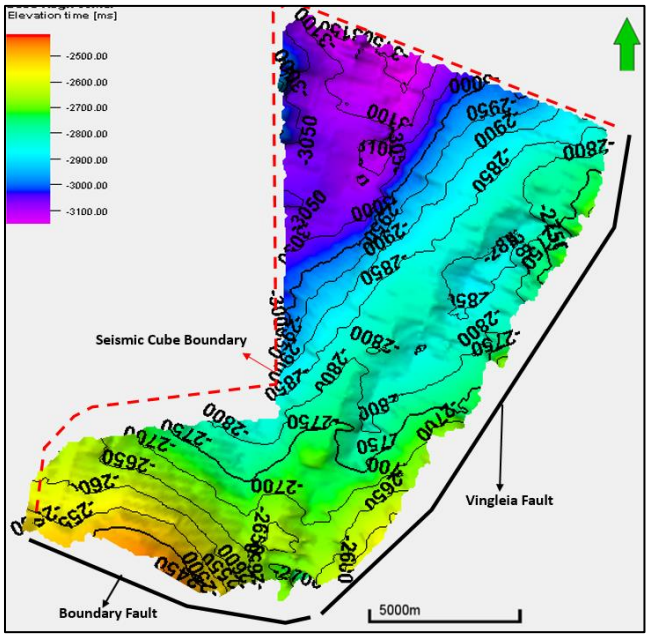

Figure 28: Surface map of base Rogn Formation.

5.2 2D Restoration & Decompaction

The seismic section of crossline 3177 (Figure 24) was restored and all the sedimentary layers were decompacted. The Move software measures the area of polygons representing each formation's compartment in the hanging wall and footwall of the fault. If there is a gain in thickness, the polygon after decompaction becomes larger, hence the software measures a larger area. If the thickness becomes lesser, the area of the polygon decreased.

There was a gain or loss observed in the present area of every layer as compared to the area of same layer when decompacted. As decompaction affects shale intervals more than sand intervals, this trend was clearly observed. When mudstones are decompacted, porosity increases largely as compared to other lithologies and hence resulting in a larger area. There is a gain in area for all shale intervals around BCU. Compaction of shales is faster than sands. The potential source rock, Spekk Fm, lying below BCU shows the largest gain. The area of this formation becomes twice after decompaction as BCU is a large unconformity and represents a lot of erosion. All the rocks were restored back, thus gaining more area. The compaction and loss in porosity is directly influenced by the stress produced by the overburden. Rate of compaction effects directly the subsidence history. This can be observed in burial history curve in Figures 36 and 37 that shale layers have steeper down going subsidence curve as compared to sandstone's gentler subsidence curve.

All the sandstones of the Jurassic age lying below BCU experienced minor losses in their areas except for the Not Formation as it is mud dominated and probably experienced a gain in porosity. There is a clear increase in the formation thicknesses after decompaction.

The Vingleia fault is of Jurassic age. There is a total extension of 2948.9 m from Jurassic to basement. When the Rogn Formation was removed and the Melke Formation was decompacted, the last extension of 1124.9 m was calculated. Within the next older layers, there is a gradual increase in the extension with two big jumps: one is 638 m for the Ile Formation to Tilje Formation, and the other is 683 m from the Åre Formation to basement.

This Jurassic extension produced deep and shallow water sediments that act as a collection of plays in the hanging walls or footwalls of extensional faults. The summits of the footwall blocks experienced massive erosion but the eroded strata never entered the hanging walls because of the structural dip and the resulting drainage (Larsen et al., 2013). This pattern was observed as unconformable Jurassic sequence is present in the hanging wall where only two Jurassic rocks were observed in the footwall.

Figures 29 and 30 show all the layers of the seismic section with their present-day thickness. The top formation i.e. the Nordland Group is at sea level so it is considered flat. Table 9 summarizes the area of each sedimentary layer before and after decompaction, including the amount of extension experienced by each layer.

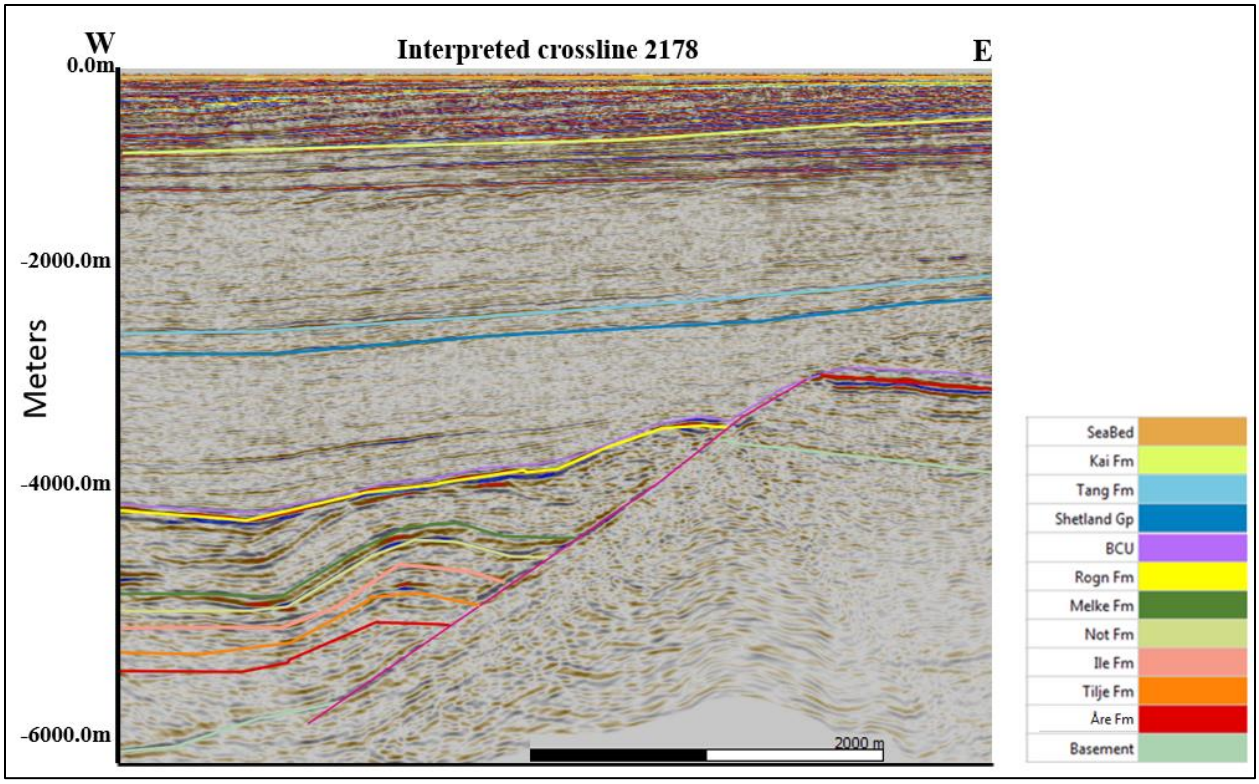

Figure 29: Interpreted seismic section.

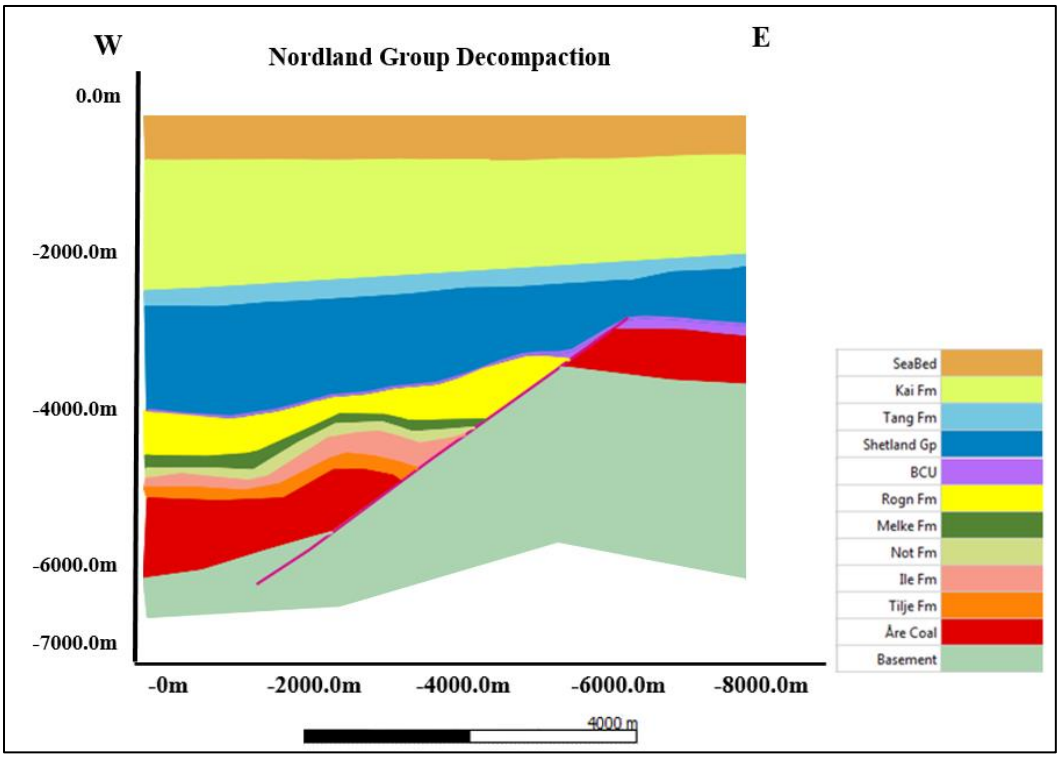

Figure 30: Decompaction of first sedimentary layer (Seabed).

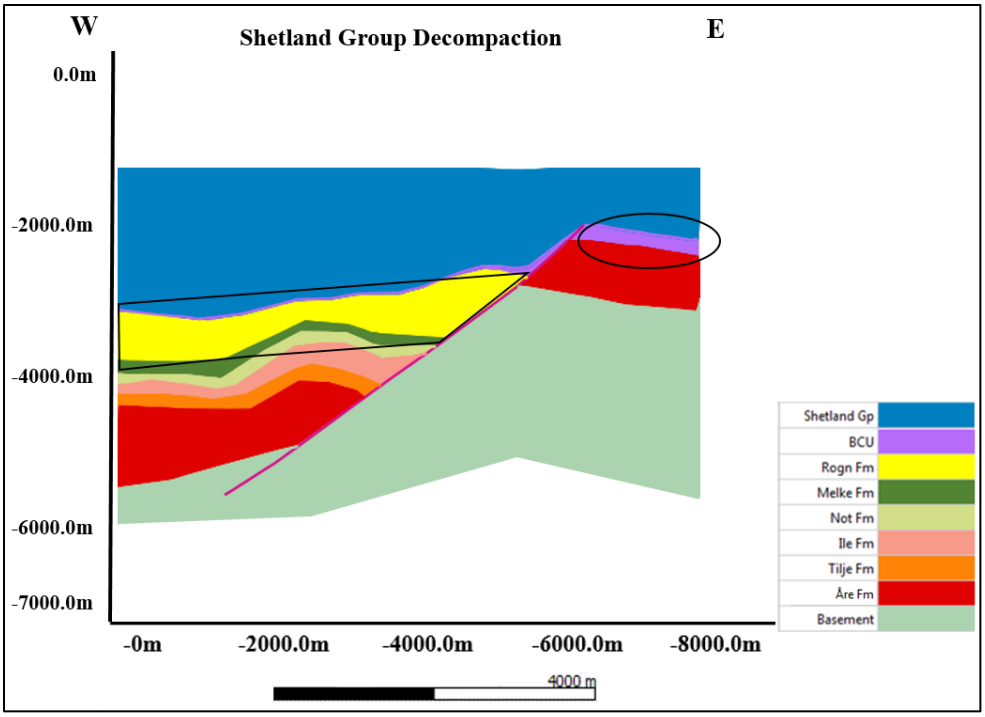

Figure 31: Decompaction of Shetland Group. Black polygon over Spekk Fm and Rogn Fm show pre-decompaction thicknesses of these layers.

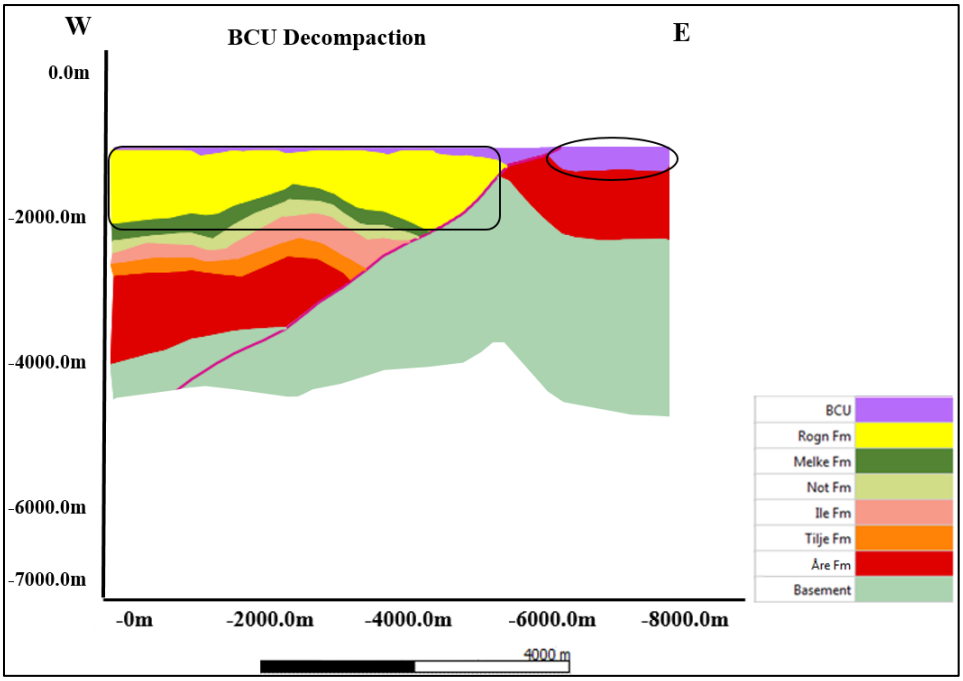

Figure 32: Decompaction of Spekk Fm. Black boundaries over Spekk Fm and Rogn Fm show post decompaction thicknesses of these layers.

Figures 31 and 32 show pre- and post- decompaction thicknesses of the source rock: Spekk Fm and the reservoir rock: Rogn Formation. A gain in thickness is observed in both formations.

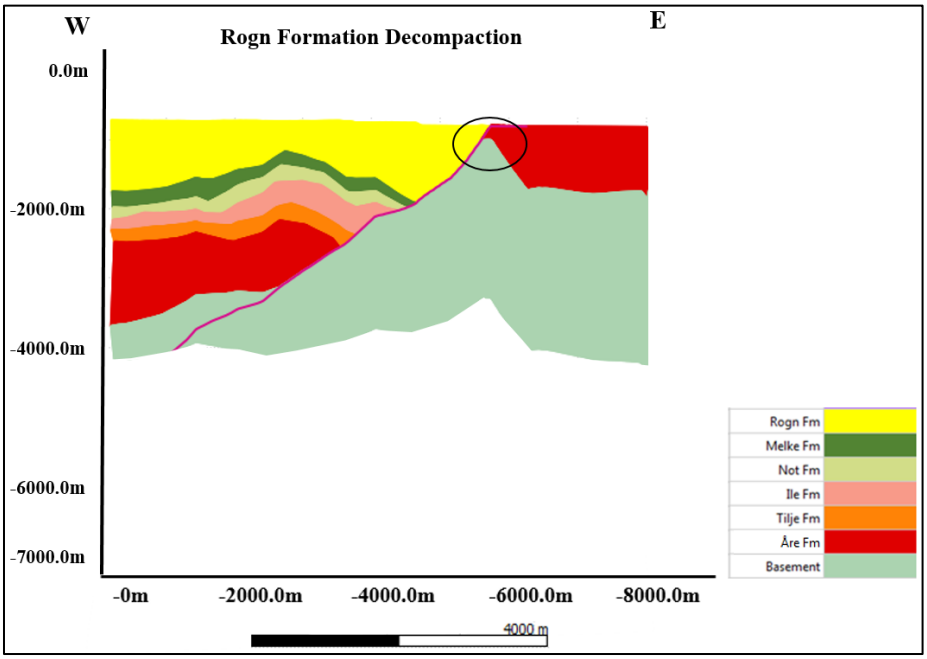

Figure 33: Decompaction of Rogn Fm. Black circle shows its juxtaposition with Åre Fm.

Figure 33 shows that the sandstone of the Rogn Formation is juxtaposed with the Åre Formation when it was deposited. The lithology of the Åre Formation consists of coal beds and sandstones. This observation is further discussed in paragraph 5.5.

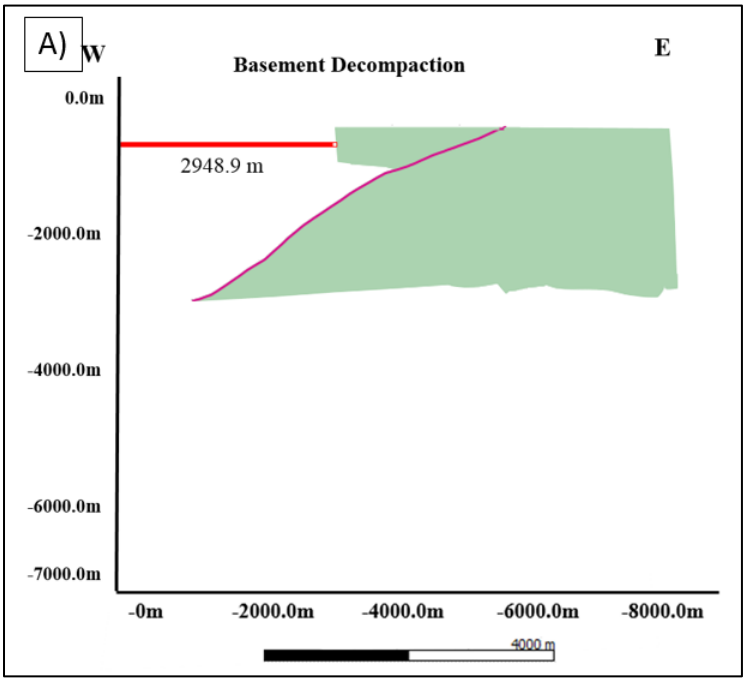

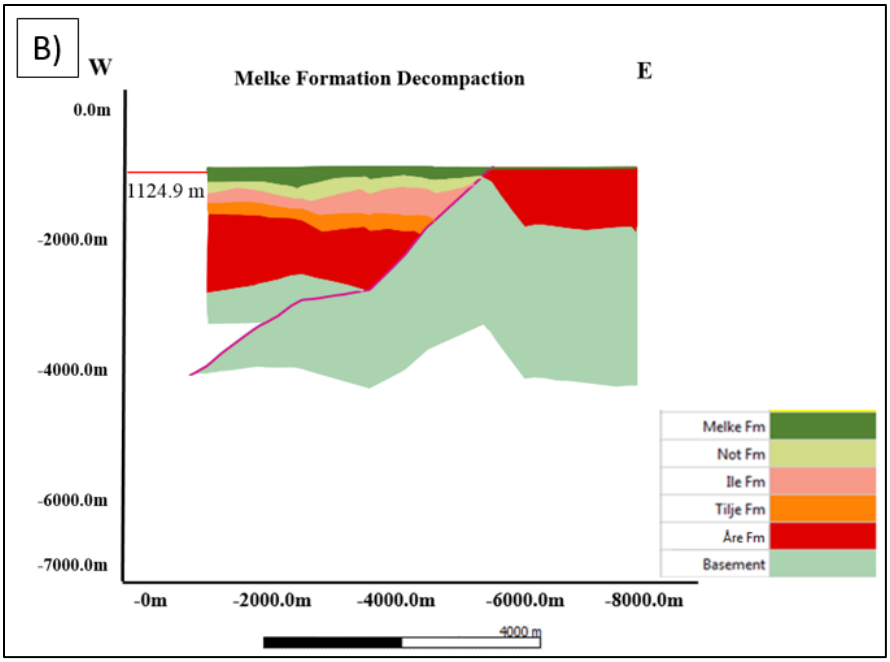

Figure 34: (A) Length of initial extension. (B) Length of final extension

Figure 34a shows that the first extension of 2948.9 m took place before Jurassic rocks were deposited. All the Jurassic rocks experienced extension till the Melke Fm. This is the final formation that experienced an extension of 1124.9 meters (Figure 34b).

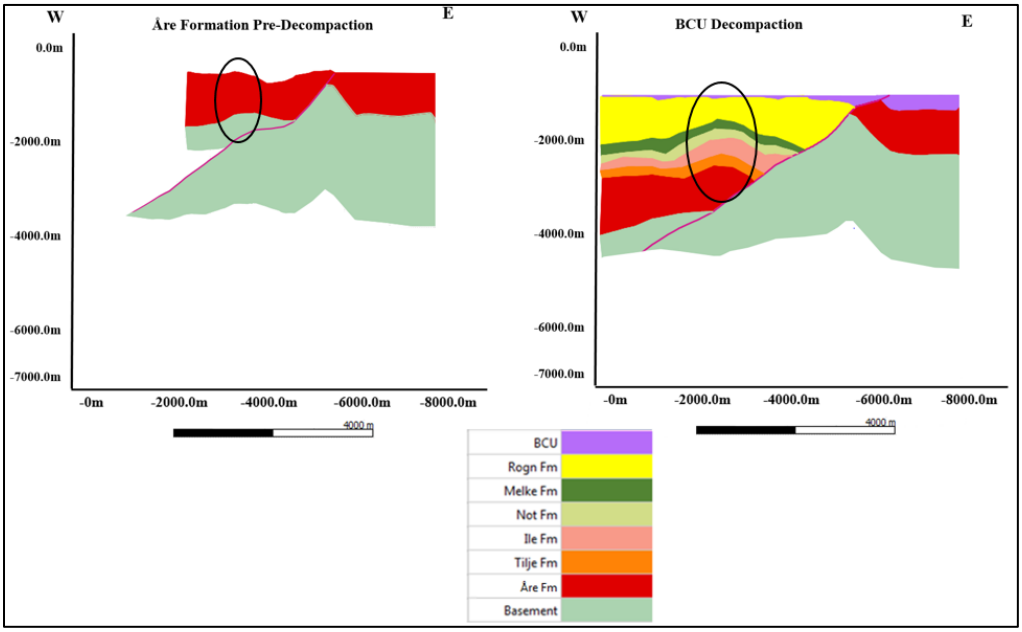

Figure 35: Åre formation pre- and post- decompaction. Black rings show rollover anticline.

Figure 35 shows that the trap i.e. the Jurassic rollover anticline started forming in Early Jurassic with the initiation of the faulting (left graph). The graph on the right shows the trap in its present form.

Table 9. Summary of gain and loss of areas of sedimentary layers. The last column represents extension lengths.

Formation	Present Area	Decompacted Area	Extension
Seabed	4408445 m²	4408445 m²	0 m
Kai Fm	11519838 m²	13213241 m² (Gain)	0 m
Tang Fm	1870015 m²	3119557 m² (Gain)	0 m
Shetland Group	10530829 m²	11674877 m² (Gain)	0 m
BCU (Spekk Fm)	378866 m²	630763 m² (Gain)	0 m
Rogn Fm	4293802 m²	4293763 m² (Loss)	0 m
Melke Fm	916668 m²	916478 m² (Loss)	1124.9 m
Not Fm	765215 m²	765340 m (Gain)	1282.3 m
Ile Fm	1084125 m²	1084022 m² (Loss)	1417.1 m
Tilje Fm	751973 m²	751929 m² (Loss)	2055.2 m
Åre Fm	2813129 m²	2813104 m² (Loss)	2265.0 m
Basement	950370 m²	950356 m² (Loss)	2948.9 m

5.3 Basin Modelling

The data of both wells, 6407/10-1 and 6407/10-2 were used to perform basin modelling to understand the petroleum system of the area. A series of graphs were generated and interpreted.

Burial History Graphs

Burial history graphs of the two wells are shown in Figures 36 and 37. Both wells are close to each other so they depict similar subsidence curves. There are four unconformities present in the area, which are illustrated by the up-going curve at ca. -140 M.Y (million years), -110 M.Y., -80 M.Y. and -20 M.Y. For burial history curve, an estimation of eroded thickness was made at the time of each unconformity by calculating the amount deposited in a certain period of time. From this relationship of thickness deposited with time, the relationship of thickness eroded was estimated. The upgoing curves highlight a decrease in temperature as there is an uplift and the strata is at shallower depth, hence lower temperature.

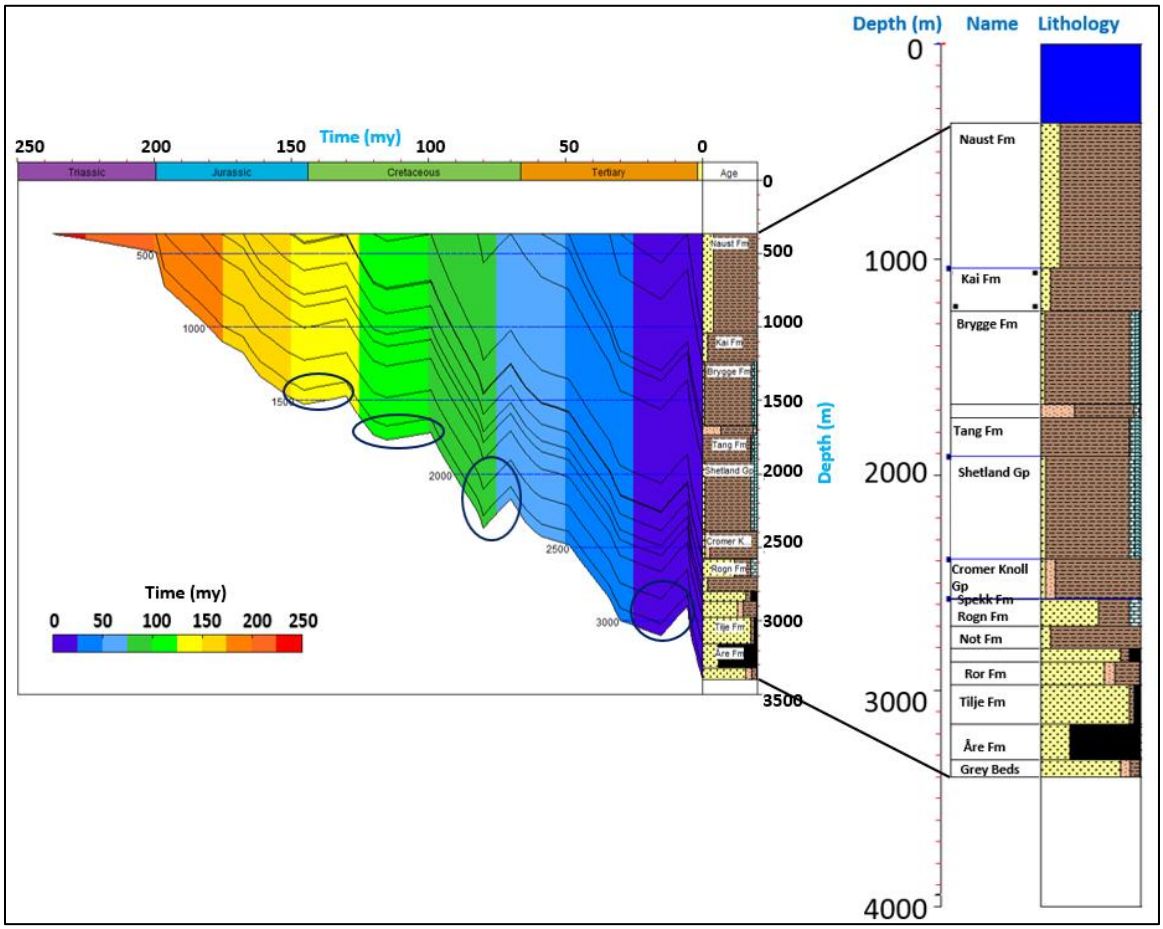

Figure 36: Burial history graph of Well 6407/10-1. Black rings present erosional events.

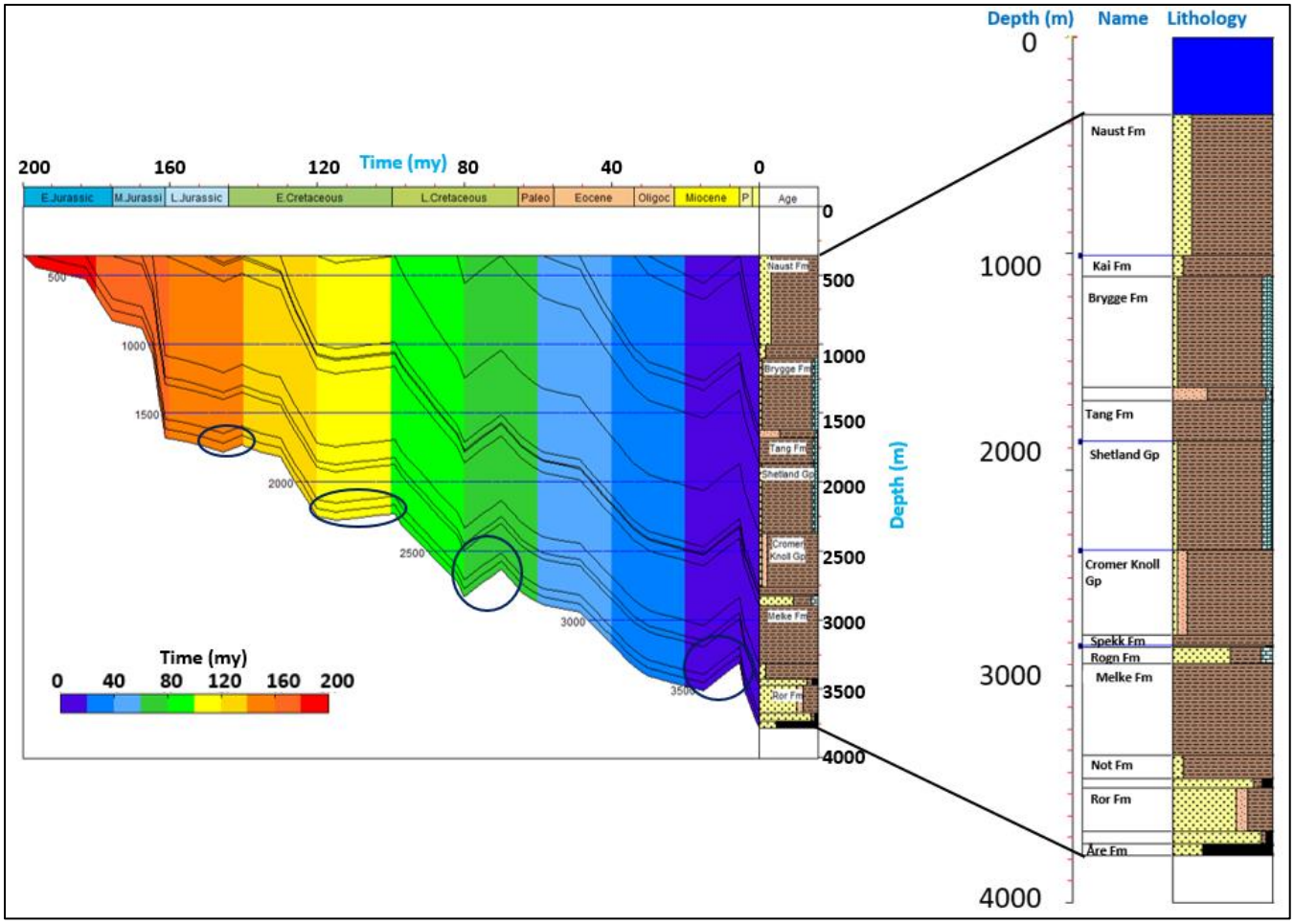

Figure 37: Burial history graph of Well 6407/10-2. Black rings present erosional events.

Evolution of Organic Matter

Organic matter in the form of kerogen in the source rock is transformed when certain specific conditions are fulfilled. This transformation is divided into diagenesis, catagenesis and metagenesis (Figure 38).

Diagenesis is the immature zone where only CH_4 and CO_2 are released.

For catagenesis, burial of the source rock should be more than 1 km and less than 3 km in order to crack heavier and lighter hydrocarbons. At this depth and between the temperature of 65 – 120 °C, most hydrocarbon is generated. This is called the 'oil window'.

Dry hydrocarbon gas is generated during metagenesis when the rock is buried under 4 km of overburden and the temperature is more than 120 °C. The gas window starts from this temperature.

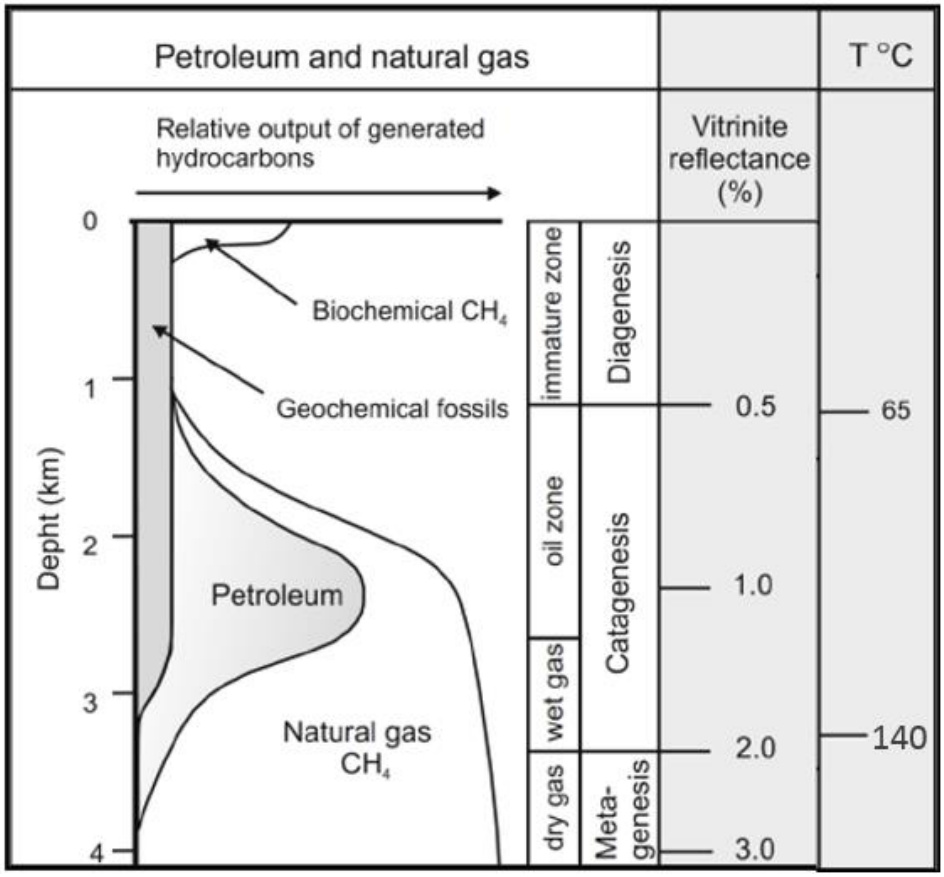

Figure 38: Phases of kerogen evolution.

Temperature Graphs

The temperature distribution can be plotted on the burial history graph (Figures 39 and 40). It provides information about the transition of temperatures as a function of the geological time. The right side of the two Figures also show the present-day temperature as a function of depth.

The temperature distribution on the left side of Figure 39 and 40 illustrate that the Åre Formation entered the oil window during Middle Cretaceous. It remained in the oil window until the Eocene. It entered the gas window quite recently. The Spekk Formation on the other hand entered the oil window in late Cretaceous and is still in the oil window today. The curve on the right side of Figure 39 shows that the temperature for the Spekk Formation is 100 °C. The temperature of the Åre Formation shows a transition from the oil to the gas window as it is in a range of 110 °C-130 °C.

The same curve for well 6407/10-2 in Figure 40 depicts a temperature of 100 °C for the Spekk Formation. The Åre Formation is clearly in the gas window as it shows a temperature of almost 140 °C. The Spekk Formation is highlighted as a red line on both Figures as it is too thin to be visualized efficiently.

6407/10-1

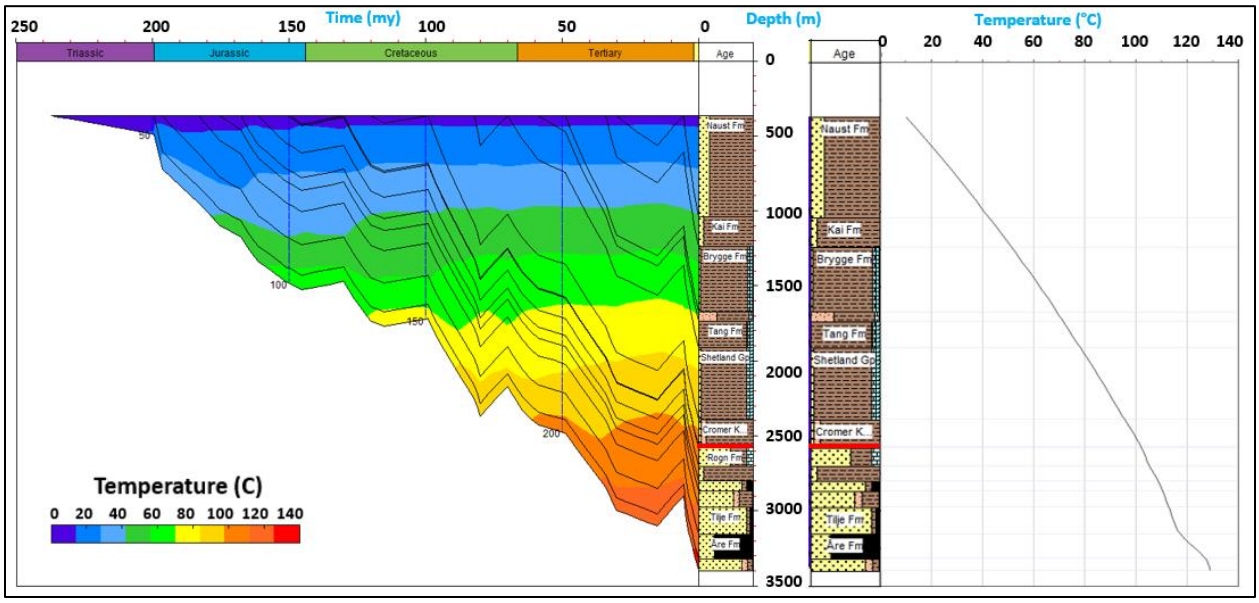

Figure 39: Graph of formation's Temperature as a function of depth for Well 6407/10-1.

6407/10-2

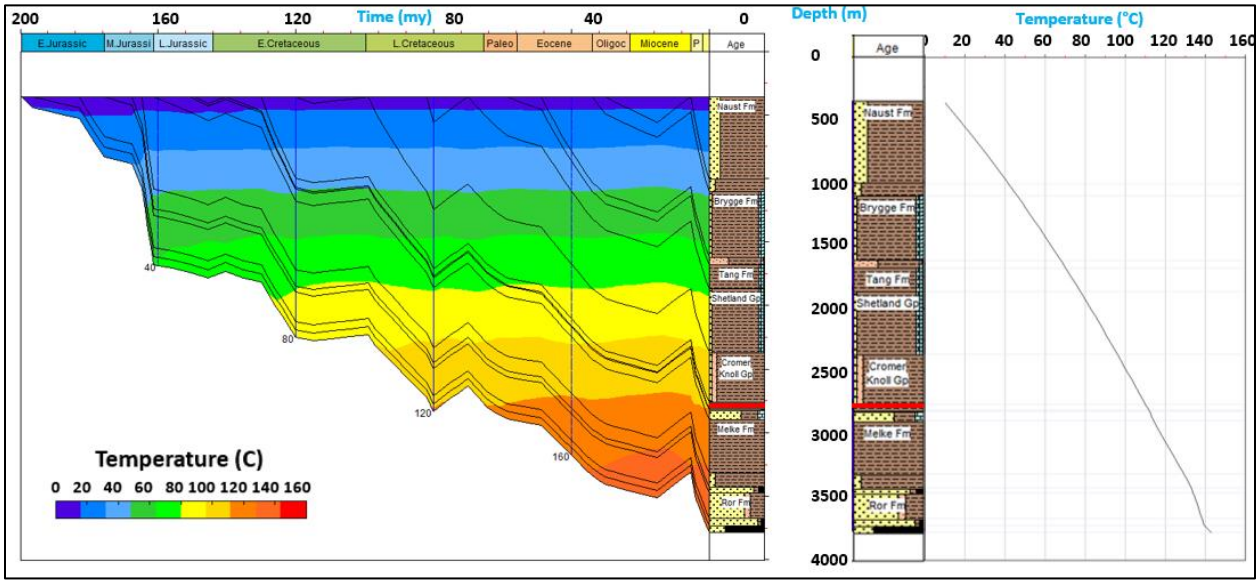

Figure 40: Graph of formation's Temperature as a function of depth for Well 6407/10-2.

Transformation Ratio Graphs

Geochemical data used as input for this modelling demonstrates good TOC and suitable temperature conditions. To check whether transformation of kerogen into hydrocarbon has taken

place or not, the graphs for transformation ratio were generated as a function of time. 15 % transformation ratio is presented by blue color and it holds no importance. Different shades of green color represent the ratio corresponding to transformation of kerogen into valuable hydrocarbons.

6407/10-1

The transformation ratio graph for Well 6407/10-1 (Figure 41) shows that up to 30% of kerogen was transformed. For the Spekk Formation (indicated by red line on the Figure) this transformation started in Pliocene and for the Åre Formation, the age of transformation is Miocene.

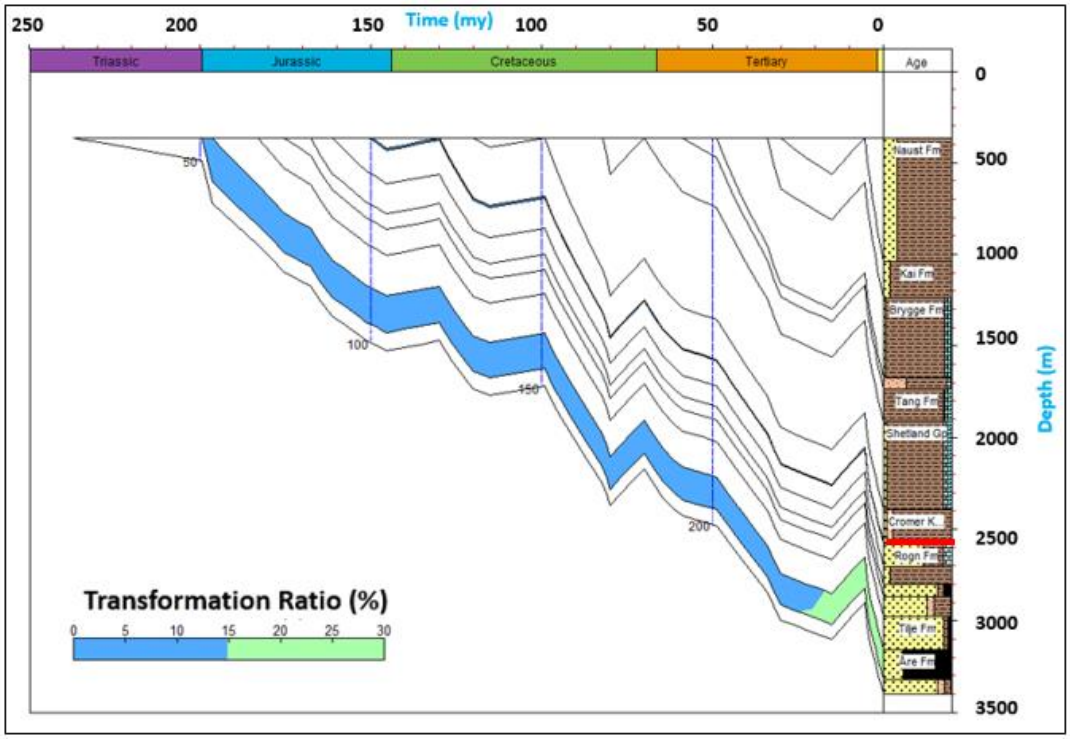

Figure 41: Graph depicting Transformation ratio of hydrocarbons for Well 6407/10-1.

6407/10-2

Well 6407/10-2 has formations at greater depths than Well 6407/10-1. This is visible in the transformation ratio graph (Figure 42). Almost 60% of kerogen is transformed in the Åre formation and the transformation started during Paleocene. For the Spekk Formation, this ratio is between 20–40% and it started during Oligocene.

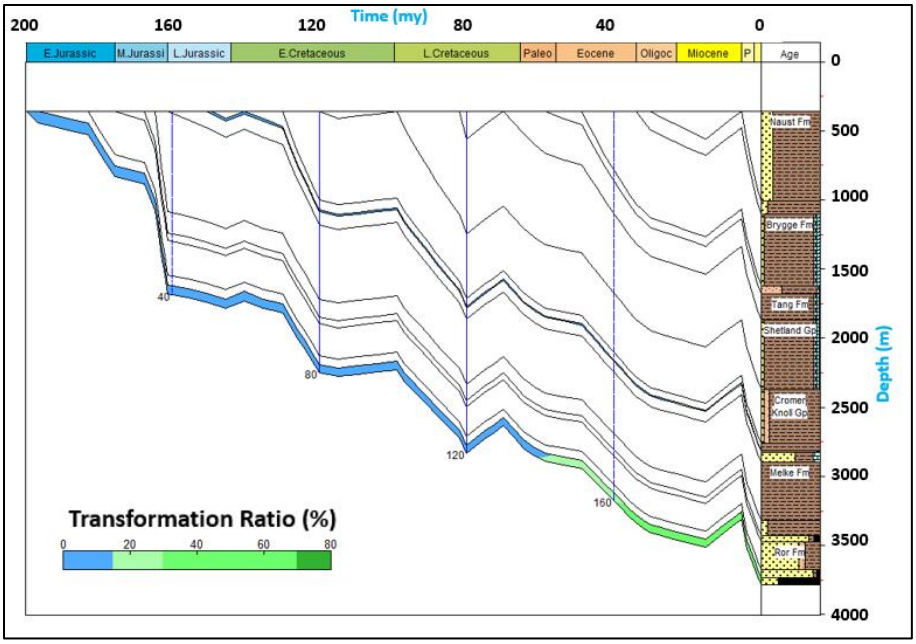

Figure 42: Graph depicting Transformation ratio of hydrocarbons for well 6407/10-2.

Oil & Gas generation curves

To check whether any hydrocarbon was generated and expelled or not, curves for these properties were produced. Oil generation in the Spekk Formation was at peak during Oligocene (Figure 43) and gas was generated in the Åre Formation during Eocene and Oligocene (Figure 44).

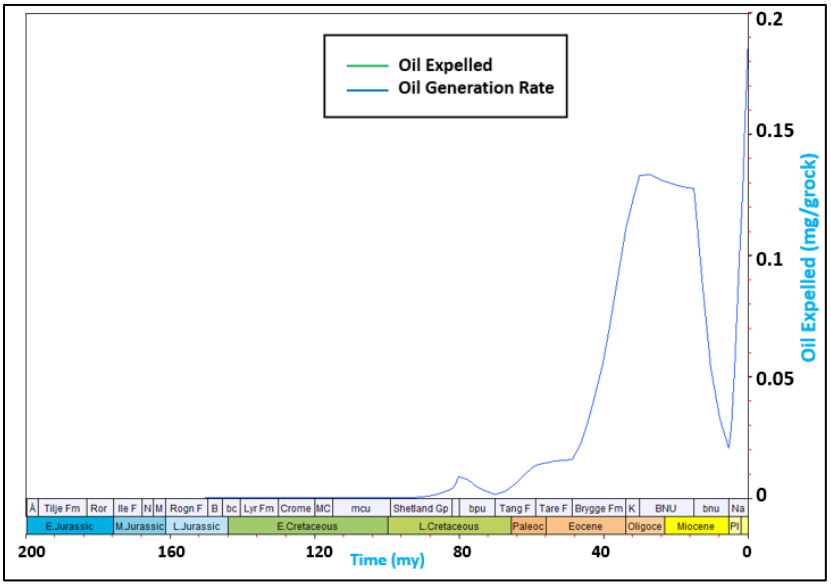

Figure 43: Curve showing oil generation of Spekk Fm in well 6407/10-1. There is no oil expelled.

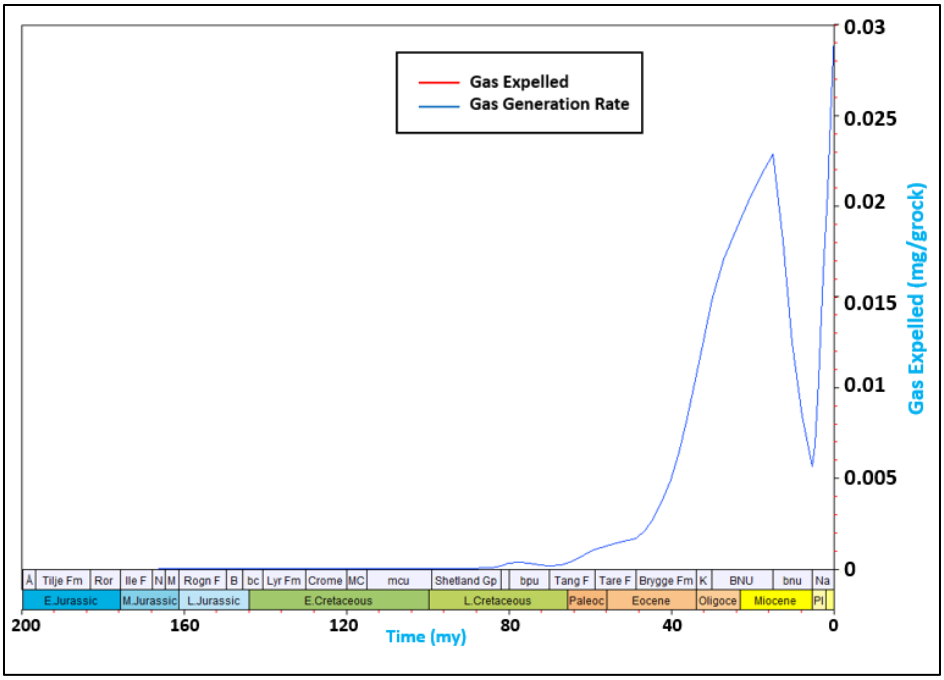

Figure 44: Curve showing gas generation of Åre Fm in Well 6407/10-1 with no gas expelled.

The generated graphs show that in both formations, generation of hydrocarbon took place but there was no hydrocarbon expulsion.

The Åre Formation is more likely to be the source rock for the dry well. There can be three reasons for no hydrocarbon expulsion:

- Less overburden as the same source rock is producing in the deeper parts i.e. in the basins. There was not sufficient time for the source rocks to be buried enough to produce hydrocarbons.
- Probably the source rocks have not reached the certain pressure where hydrocarbons can break out of the source rock.
- The thicknesses of Spekk Fm are just 6 and 9 m in both wells. It is much thicker in the wells who are producing.

The results of basin modeling indicate that local source rocks are not functional in this area. Hence, there must be some long migration of hydrocarbons from the hydrocarbon kitchen to the trap.

The graphs from basin modelling show two depths of source rocks in the area. In Well 6407/10-1, the Åre Formation is present at a depth of 3155 m and the transformation started during Miocene. In Well 6407/10-2, the Åre Formation is encountered at a depth of 3737 m and the hydrocarbon transformation starts during Paleocene. The deeper the rock is buried, the earlier the transformation starts.

The immediate overburden i.e. the Spekk Formation started to deposit on top of the reservoir in Late Jurassic. This means that the hydrocarbon created at this time and later should be captured by the reservoir. Table 10 summarizes the age of elements and processes of the petroleum system in the study area. All the characteristics needed to make a petroleum system functional are present except there is no expulsion observed from the source rocks, either due to less overburden or insufficient pressure exerted on source rocks.

Table 10) Petroleum system chart of the area depicting all the elements and processes functional.

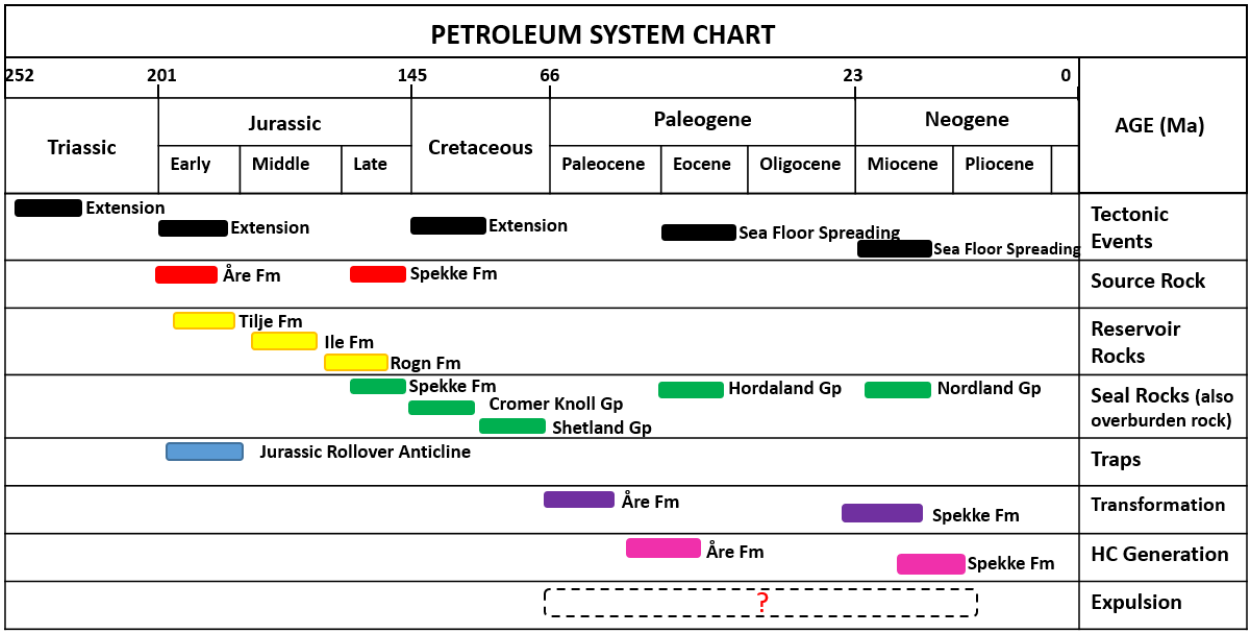

5.4 Top Seal Analysis

The workflow defined in the methodology for seismic attribute analysis was followed for both small cropped cubes: the fault cube and the noise cube (Figure 45). The fault cube covers a volume within the top seal. The noise cube mainly is comprised of seismic noise which is present at greater depths. The patterns after the ant tracking were observed.

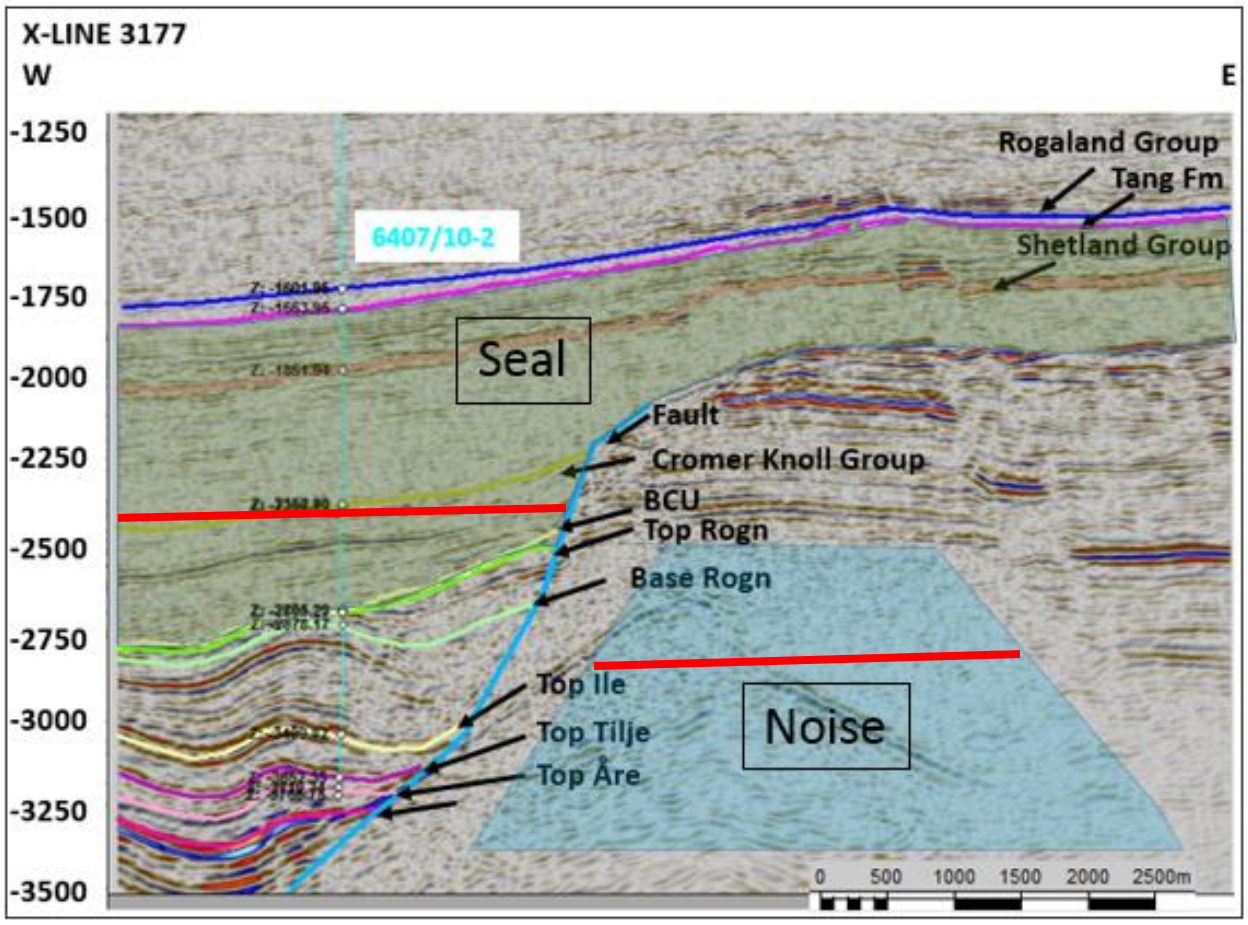

Figure 45: Seismic section showing the reservoir with top seal and area with low S/N. Red lines indicate the location of time slices in Figures 46 and 47.

Time slice across top seal of fault cube shows polygonal fault pattern (Figure 46). Whereas the time slice across the noise area showed somewhat similar polygonal pattern as of fault cube (Figure 47).

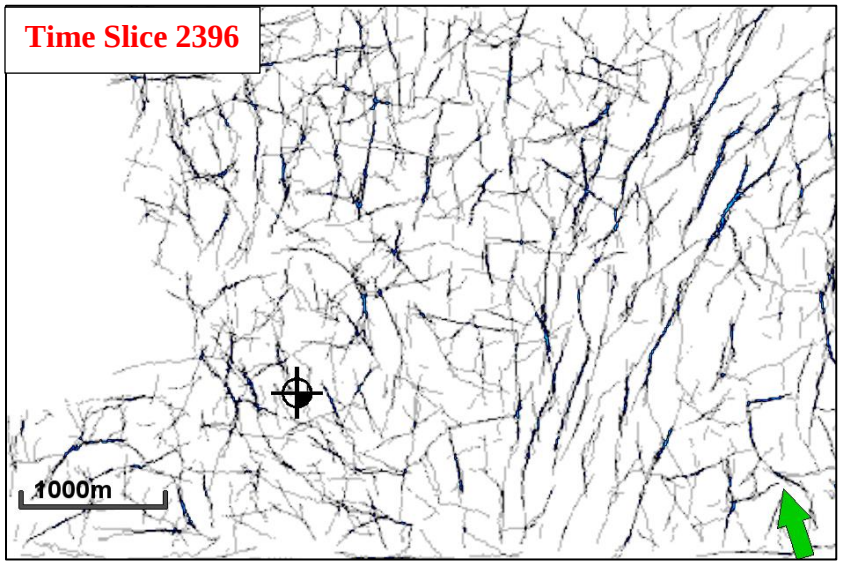

Figure 46: Time slice of fault cube across the top seal.

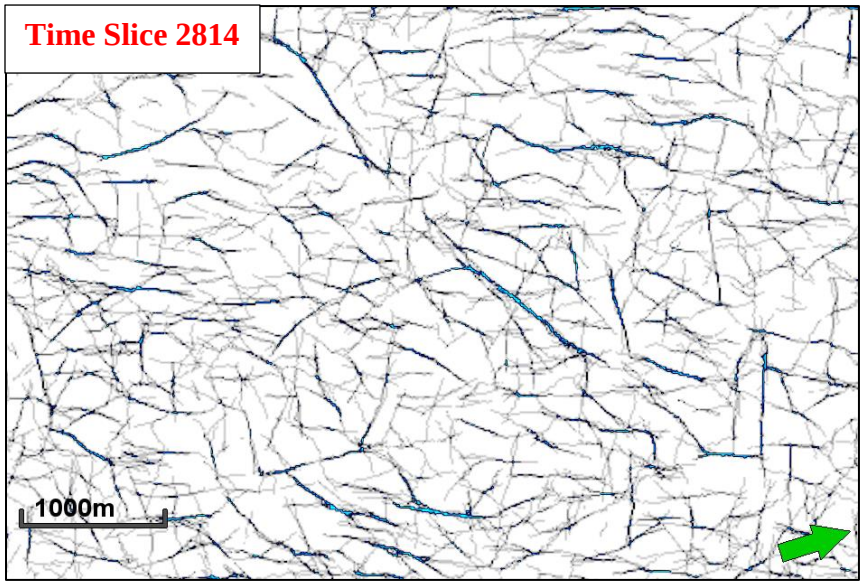

Figure 47: Time slice of fault cube across the area of low S/N.

These cross sections of fault and noise cubes show a clear difference of patterns between top seal and noise. Top seal shows several V shaped lineaments (Figure 48). These types of features can be observed in formations of the Cretaceous and the Paleogene on several lines and are identified as faults (Schulte, personal communication). The fact that the seismic noise shows a display of vertical lineaments (Figure 49) supports the assumption that the fault cube of the sealing formation shows a fault pattern as there is a clear difference between these two.

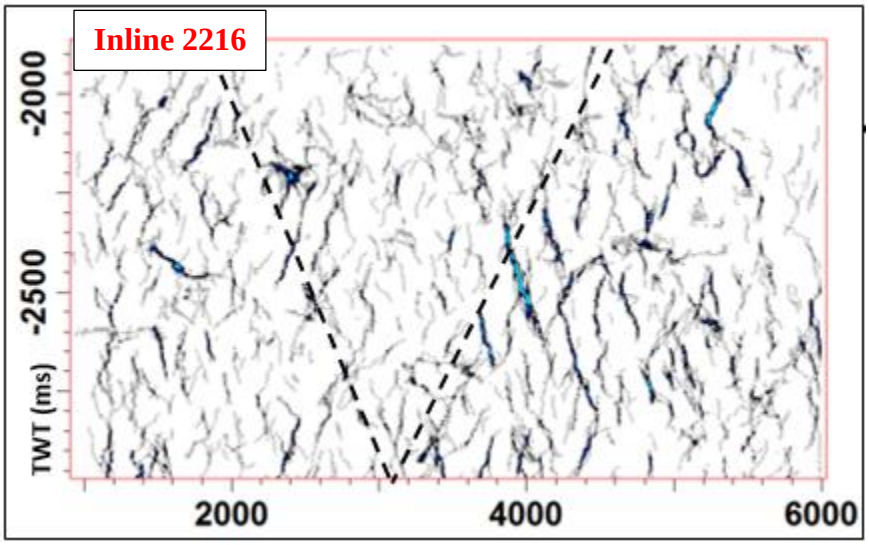

Figure 48: Cross section of top seal shows V-shape pattern - faults.

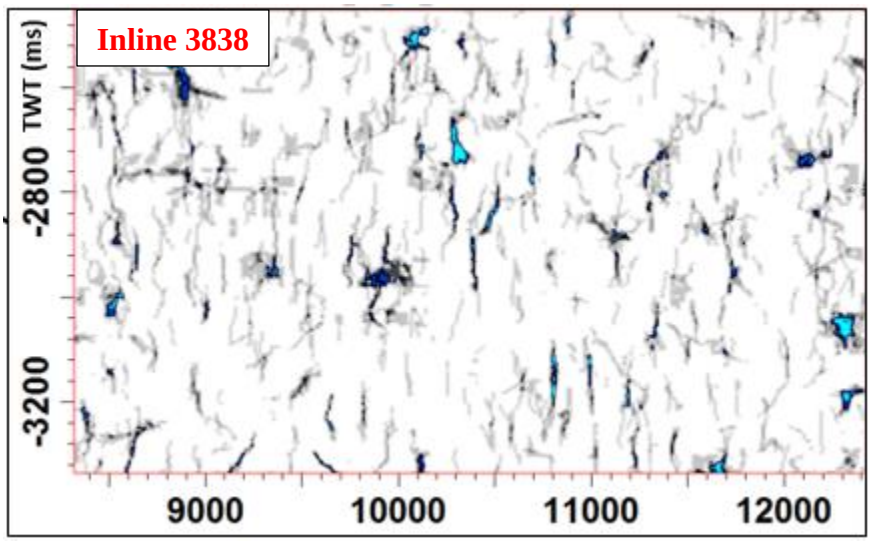

Figure 49: Cross section of noise area shows mainly vertical features - noise.

Ingram et al., (1999) discussed leakage of top seal. Their failed reservoir shows a similar lithology and fault pattern as the study area. The stratigraphy of top seal in their study area

consists of shale with thin layers of siltstones and sandstones. If the porous lithology i.e. sandstones and siltstones juxtapose against each other and fault clay smear is missing, then these faults may act as passages for flow (Figure 50) (Ingram et al., 1999). Leakage can be possible if the detected fault pattern conducts hydrocarbons. This network of juxtaposed leaky beds makes the risk of leakage higher.

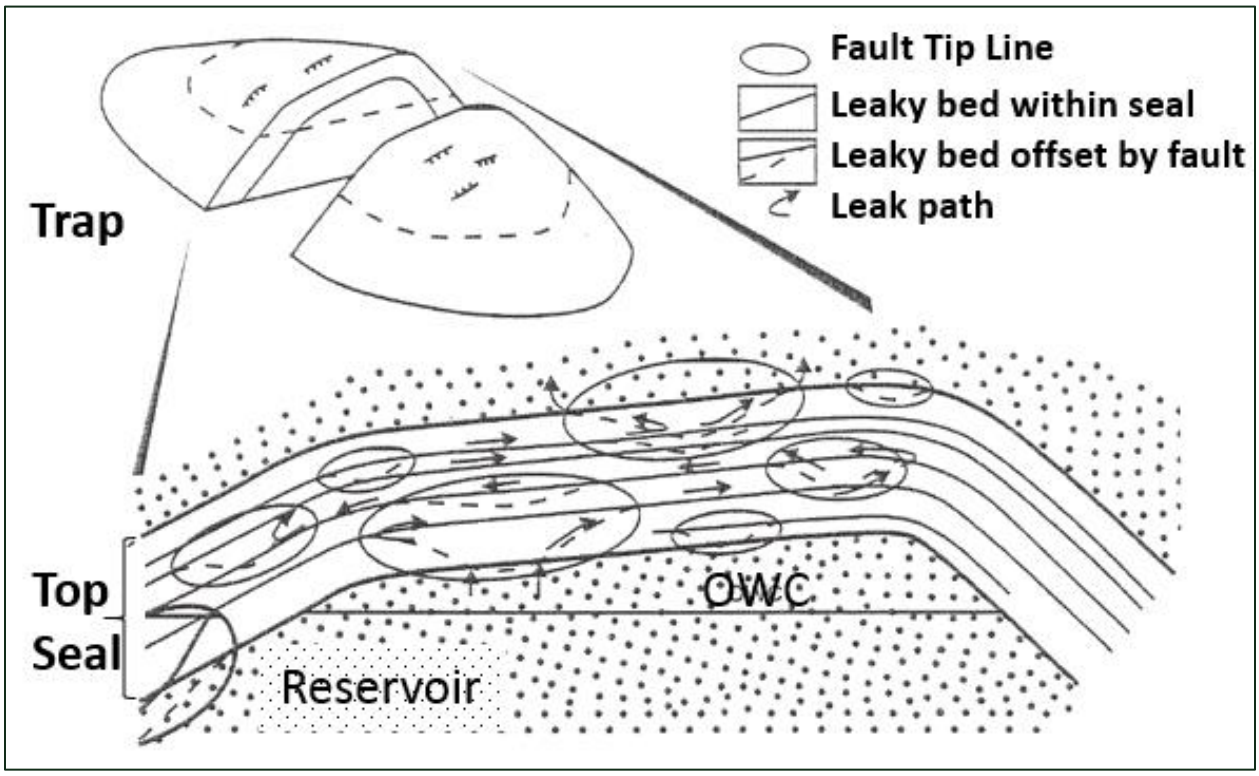

Figure 50: Leak Path linked by faults of top seal due to absence of clay smear. (Modified from Ingram et al., 1999).

5.5 Fault Seal Analysis

Seismic Interpretation

The seismic analysis shows that in the footwall of the fault, only the Spekk Formation is overlying the Åre Formation of Late Jurassic. The whole Jurassic package within these two formations is missing. Some interpreted seismic lines show a juxtaposition of Rogn Formation in the hanging wall against the Åre Formation in the footwall (Figure 51).

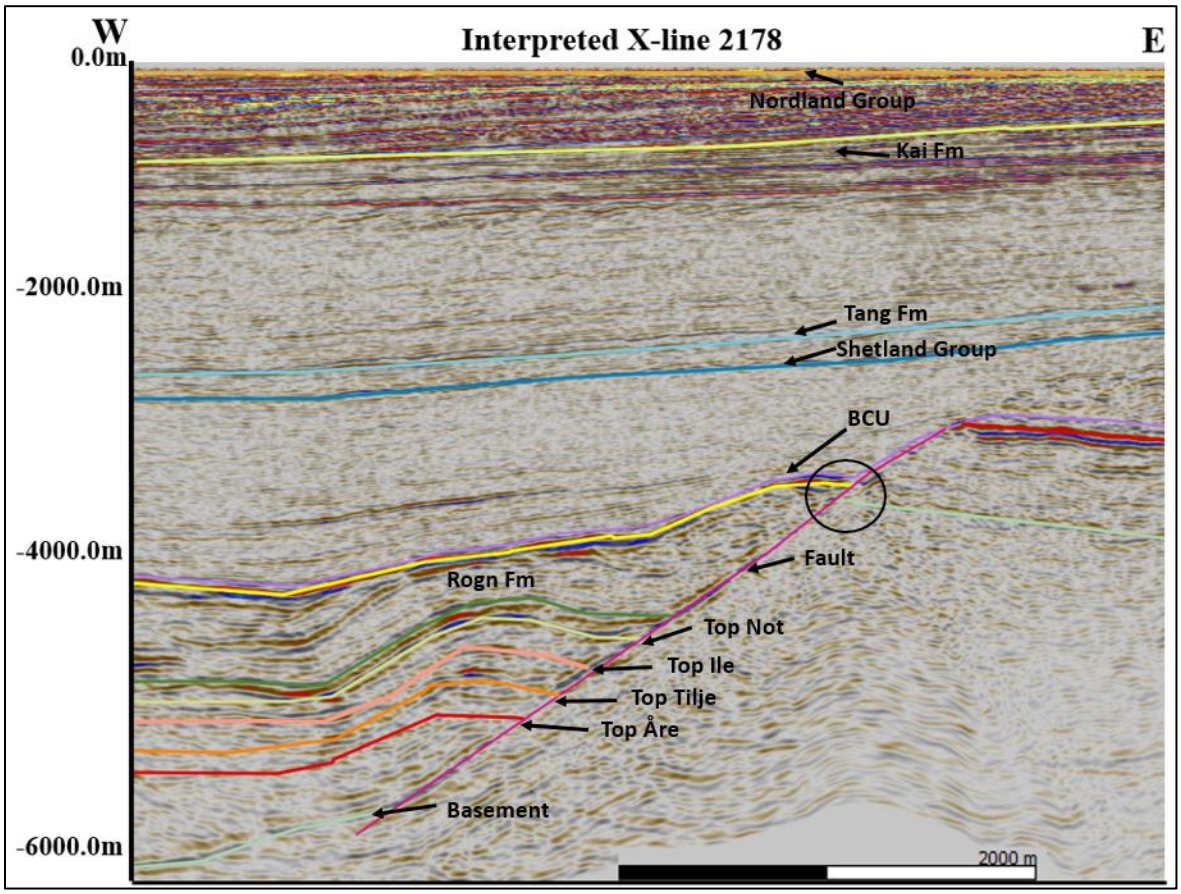

Figure 51: Interpreted seismic line. Black circle indicates fault juxtaposition.

2D Restoration

The results of the 2D restoration also shows juxtaposition of the Rogn Formation with the Åre formation (Figure 52). Both formations consist of sandstones. The results also depict that this present-day juxtaposition also existed at the time of the deposition of the Rogn Formation (Figure 53), which means the sand-sand juxtaposition was there since the Late Jurassic.

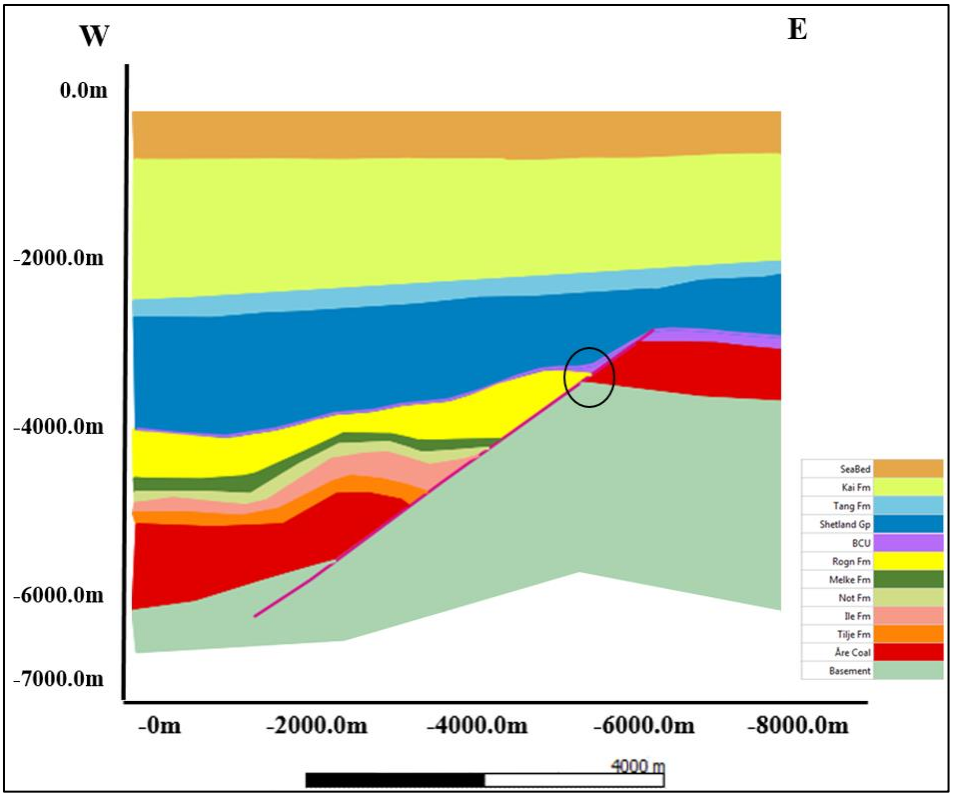

Figure 52: Present day sand-sand juxtaposition.

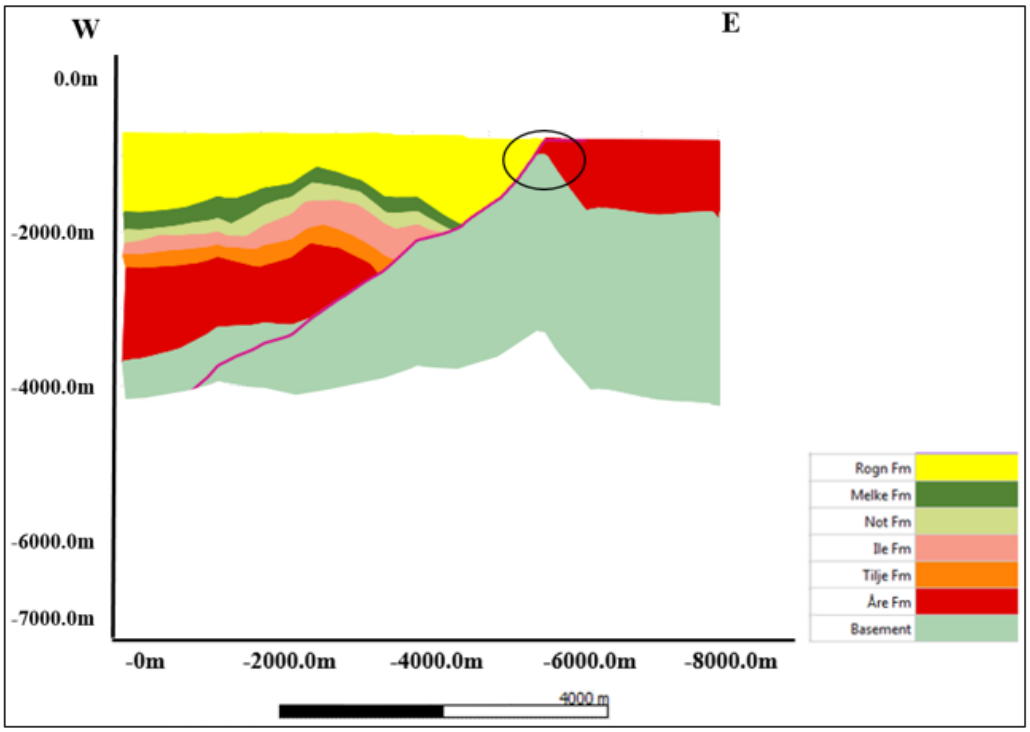

Figure 53: Sand-sand juxtaposition at the time of deposition of the Rogn Formation.

Shale Gouge Ratio

Figure 54 shows fault juxtaposition of the sand-shale facies performed before evaluating shale gouge ratio. The juxtaposition of shale against shale is color-coded as blue. Sand-sand juxtaposition is colored red, and sand-shale is green. This color schemes allows to quickly identify the fault throws that deliver sand-sand or sand-shale juxtaposition for the formation of interest. Figure 54 shows that the juxtaposition of the Rogn Formation with the Åre Formation delivers windows of sand-sand juxtaposition and thus a potential leakage of the fault.

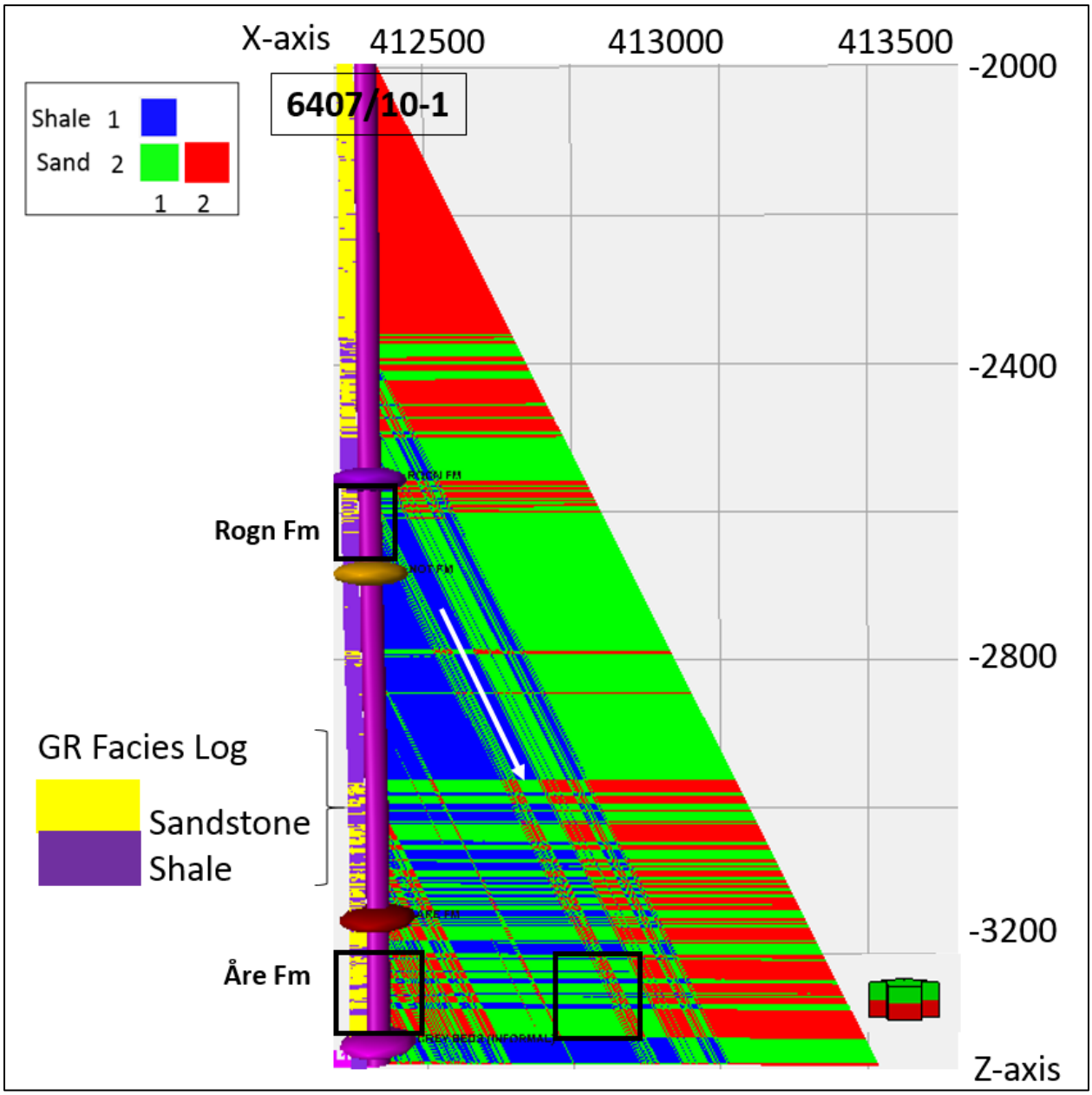

Figure 54: Fault juxtaposition triangle showing sand-shale and sand-sand juxtaposition.

The SGR was assessed for the fault zone (Figure 55). VSH (volume of shale) value of 10 % was assigned to sand and that of 50 % to shale. Figure 54 shows that the value of SGR is around 40 % at the crossover of the reservoir with Åre Formation.

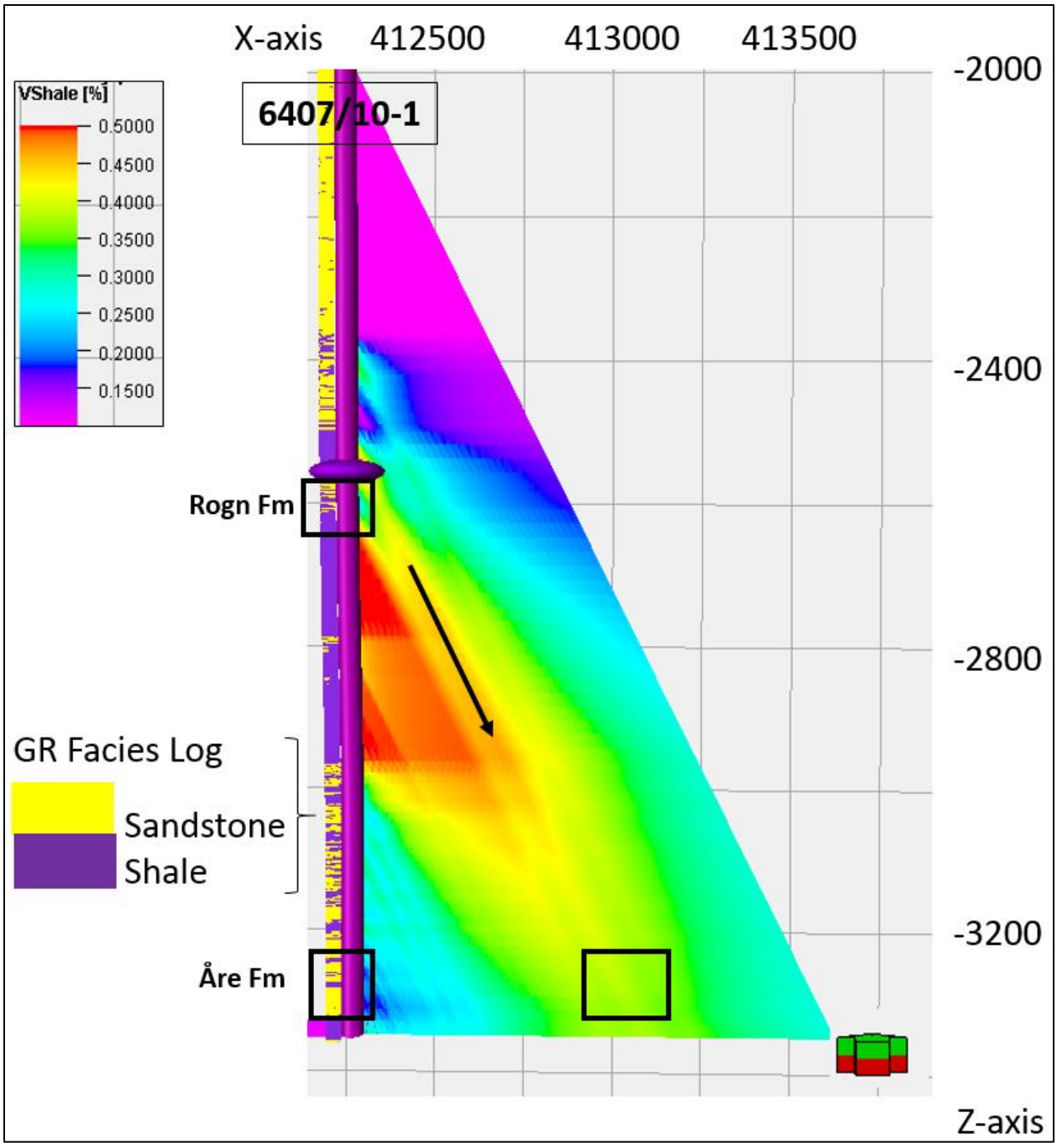

Figure 55: Shale gouge ratio across the fault zone.

Yielding (2002), compiled a histogram of leaking/sealing faults from the Northern North Sea. Figure 56 shows vertical bars that depict SGR (y-axis) of individual faults (x-axis). Red bars are

sealing faults and green bars show leaking faults. Yellow bars show small pressure difference at oil water contact (OWC). According to this Figure, faults can be regarded as leaking when the SGR is below 20-30 %.

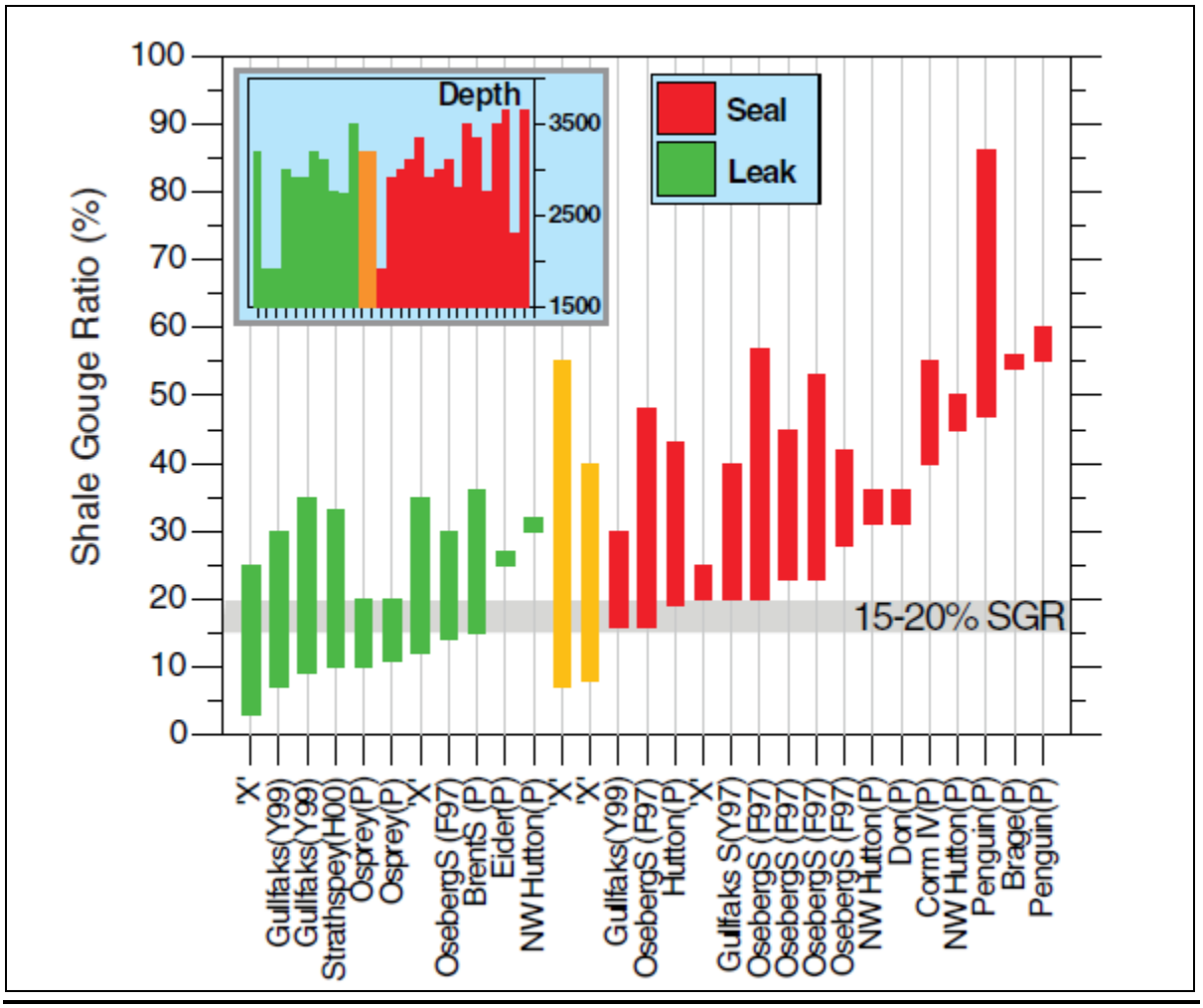

Figure 56: Analysis of leaking and sealing faults according to their SGR ratio. (Modified from Yielding, 2002).

The SGR for the dry well of this project is around 40%. That means the fault is sealing according to the study conducted by Yielding, 2002 in present-day. However, considering the span of geological time, the fault could still be leaking. Yielding's result describes the present-day situation of the analyzed faults based on production data. However, he does not say anything about the sealing behavior of the faults over geological time: then a small leakage that cannot be observed during a small range of time consisting of some years may be vary significantly over millions of years. If that's the case, trap for this reservoir has failed because fault is not holding hydrocarbons and is a leak.

6. Discussion

6.1 Wavelet Selection

The choice of a suitable wavelet is a crucial task because inaccuracies result in a mismatch between the synthetic trace and the seismic trace close to the well. A deterministic wavelet was used for the synthetic trace calculation because it delivers a good estimation of the seismic amplitude and phase spectrum. Therefore, it reduces the effect of time inaccuracy and no the danger to address phase inaccuracy between the synthetic and the seismic by a time shift is reduced. The part above the reservoir was not matched accurately due to time varying changes in the seismic amplitude spectrum. Since that part does not hold much significance, so no further action was done. But to enhance the match between synthetic trace frequencies and seismic frequencies and make it perfect throughout the well, time varying wavelet can be applied.

6.2 Time Depth Conversion

The velocity model is used for depth converting all data used for the 2D restoration. It is important to know that the total vertical depth has a great influence on the structure. In this project's case, if the conversion is not performed correctly, it may push the anticline downwards, which effects the whole result. A great deal of care is required to run time depth conversion accurately and there is always a room for improvement. For this study the well 6407/10-2 is close to the 2D restoration line which increases the chance that the error of the depth conversion is small.

6.3 2D Restoration

In Move software, there are three types of decompaction methods and six types of un-faulting un-faulting techniques available. A common used method, airy isostasy was used for decompaction and simple shear module was applied for un-faulting the footwall and hanging wall. The result showed a sand-sand juxtaposition for the reservoir and a large extension during Jurassic normal faulting period. However, due to the limited research period, the other methods were not applied and thus there was no possibility to compare the results to see if the zone of juxtaposition is bigger or smaller as that is one of the key messages.

Only one interpreted seismic section was used in the 2D restoration. More interpreted seismic sections can be restored in 2D Move and their results can be compared to see if the results are consistent or there lies a variation.

Lithology information is another important input parameter for 2D restoration. The current input is based on a rough estimation. Whereas, a statistical approach based on the available wells in the surrounding area should be a more reliable way.

6.4 The role of seismic attributes in identifying fractures

The application of seismic attributes enhances features that were difficult to observe on the seismic sections. The top seal is characterized by a net of V-shaped faults, that are present in the whole strata. The observation that seismic sections of very high noise show a very different pattern in the ant tracking cube supports the assumption that the V-shape pattern is indeed caused by faults. It indicates that the top seal is heavily faulted but the same formations are acting as a seal in producing wells of the neighboring field. This may indicate that the faulted top seal is not a candidate for the petroleum leakage, probably because the faults do not have enough continuity to transmit hydrocarbons.

6.5 Fault sealing viability

The underlying model for fault seal analysis is oversimplified. For instance, the distribution of shale smear within a fault zone may be very heterogeneous. The fault is eventually not a simple plane but a 3D feature with a complex smear building. The smears may be interrupted and with the passage of time, this interruption might create multiple gaps reducing the sealing ability of the fault. Faults with small throw also aid in breaching the fault smears (Cerveny et al., 2004).

Færseth, 2006 discussed the smear along small and large scale faults. For large scale faults, it is hard to differentiate between the fault zone architecture, mechanism and continuity of smears. The shale smear factor is calculated by using the following formula (Figure 57):

$$Shale\ Smear\ Factor = \frac{\text{Fault Throw}}{Source\ Bed\ Thickness}$$

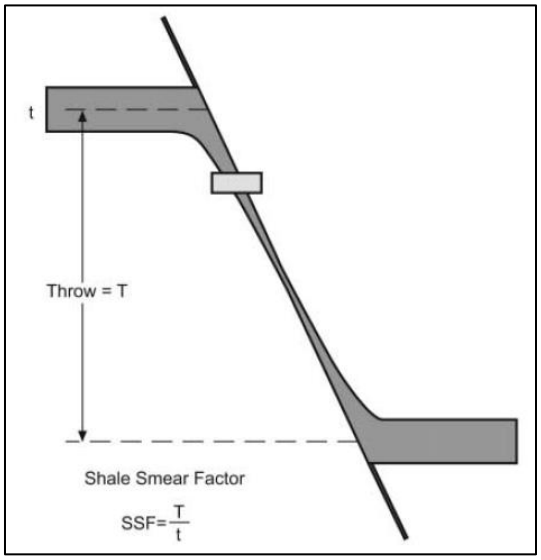

Figure 57: Calculation of SSF-Shale Smear Factor (Færseth, 2006).

The study conducted by Færseth, 2006 states that the smear is continuous when the values of the SSF factor is below 4. When the SSF reaches above 4, the smear in large-scale faults becomes discontinuous.

Cerveny et al. (2004) discuss the study of a normal fault, the Calabacillas fault in New Mexico, USA. The clay smear in this fault zone is continuous up to a distance of two to six times the thickness of the source clay bed. After this distance, it starts thinning away from the source bed in the footwall. The clay smear thickness increases as the source bed becomes thicker but decreases with an increase in the distance from source bed.

Fagerland (1990) postulated that the main risk for hydrocarbon accumulation in the Frøya high is the Vingleia fault, which is acting as a leak. This fault zone is highly likeable to act as a migration path because it has visible offsets into the Tertiary strata. Hydrocarbons have probably migrated into these younger layers to the sea bottom and biodegraded.

Fault seal potential is overestimated by using smear estimation and seal calibration techniques only. Fault juxtaposition and shale gouge ratio underestimate the fault rock properties as clay smears are likely to be discontinuous and many a times breached. To be more precise about these properties and pressure, core studies are suggested as cores offers high resolution. A core study provides significant knowledge about the minor faults, types of lithologies in the fault zone and the effects of geological history. It also gives an insight on pressure and permeability across small faults. This helps in predicting the flow characteristics in those typical fault rocks, as well as the sealing ability of the fault. (Cerveny et al., 2004).

Seismic interpretation shows that the source rock thickness is around 180 m. The fault has a throw of almost 1000 m. Given the above-mentioned facts, the Vingleia fault becomes the most likely factor for the removal of hydrocarbons and the reason for the dry well. Its sealing ability is highly questionable and one cannot rely on SGR only. The juxtaposition against the fault formed millions of years ago, hence the discontinuity in smear is likeable with time. Also, the SSF factor is more than 5 because of the large throw of the fault, which may result in discontinuity. Fagerland 1990 declared this fault as the leaking in the area. To test his theory, a detailed analysis of the fault based on core studies is recommended. This would allow estimating the rock properties across the fault.

7. Conclusions

Different techniques developed to analyze the petroleum system of the study area improve the understanding of all the petroleum system elements in the Halten Terrace and Frøya High, Norwegian Sea. Seismic interpretation performed to gain knowledge of the structure, lateral and vertical extent of key formations provides insight of the subsurface. As the rollover anticline is a product of faulting, performing 2D restoration helps in observing the lithologies across the fault at a certain age and the amount of area growth. The more the growth is, the more it is likely to be compacted in a shorter time. It also gives information about thickness of formations before and after decompaction. The workflow designed for seismic attribute analysis develops a clear distinction between faults in top seal and noise pattern. The hydrocarbon generation and burial history study performed under basin modelling conclude that the local source rock did not expel generated hydrocarbons. Fault seal analysis carried out by juxtaposition diagrams and shale gouge ratio enhances the understanding of the potential sealing of the fault.

The conclusions from all these observations are as follows:

- The hanging wall of the Vingleia fault has a Jurassic succession but most of this succession is missing in the footwall where the Lower Jurassic Åre Formation underlies the Upper Jurassic Spekk Formation. Between these two, the entire Jurassic succession has either been eroded or not deposited.
- Reservoir rock: the Rogn Formation is juxtaposed against the Åre Formation that consists of sandstone and coal. There is a fair chance that sandstone of both formations is juxtaposed against each other and can act as a conducting medium for hydrocarbon.
- There is a gain in thickness in sedimentary layers pre-decompaction, especially in shale layers. It increases when a layer is decompacted, hence a gain in thickness. Shales tend to compact faster and this effects the burial (subsidence) history. Shales compact rapidly as they lose their porosity and this can be seen as steep down going curves in burial history graphs.
- The area has experienced an extension of 2948.9 m, which started in Early Jurassic and prevailed until Middle to Late Jurassic.
- Hydrocarbon shows in the studied wells are not from local source rocks, as basin modelling shows local source rocks did not expel any hydrocarbons.
- The top seal is heavily faulted but these faults have minor throw and they are not connected.
- The shale gouge ratio analysis suggests a sealing fault; however, the ratio is so close to the borderline that the fault could also have leaking potential.

Failure of trap is the main reason for the dry well 6407/10-5. The Vingleia fault present against the rollover anticline has high chances of leaking which implies that hydrocarbons have migrated

from the trap into to the Cretaceous strata lying above the Jurassic reservoir rock, the Rogn Formation.

8. References

AAPG Database. (2017). URL: http://wiki.aapg.org/Shale_gouge_ratio

Blystad, P., Brekke, H., & Faerseth, R. B. (1995). *Structural Elements of the Norwegian Continental Shelf. Pt. 2. The Norwegian Sea Region*: Norwegian Petroleum Directorate.

Bukovics, C., & Ziegler, P. A. (1985). Tectonic development of the Mid-Norway continental margin. *Marine and Petroleum Geology, 2*(1), 2-22.

Bøe, R., Fossen, H., & Smelror, M. (2010). Mesozoic sediments and structures onshore Norway and in the coastal zone. *Norges geologiske undersøkelse Bulletin, 450*, 15-32.

Cerveny, K., Davies, R., Dudley, G., Kaufman, P., Knipe, R., & Krantz, B. (2004). Reducing uncertainty with fault-seal analysis. *Oilfield Review, 16*(4), 2005.

Doré, A., Lundin, E., Kusznir, N., & Pascal, C. (2008). Potential mechanisms for the genesis of Cenozoic domal structures on the NE Atlantic margin: pros, cons and some new ideas. *Geological Society, London, Special Publications, 306*(1), 1-26.

Fagerland, N. (1990). Mid-Norway shelf-hydrocarbon habitat in relation to tectonic elements. *Norsk Geologisk Tidsskrift, 70*, 65-79.

Færseth, R. B., Johnsen, E., & Sperrevik, S. (2007). Methodology for risking fault seal capacity: Implications of fault zone architecture. *AAPG bulletin, 91*(9), 1231-1246.

Færseth, R. B. (2006). Shale smear along large faults: continuity of smear and the fault seal capacity. *Journal of the Geological Society, 163*(5), 741-751.

Gowers, M. (1995). The Norwegian Central Graben—potential and pitfalls. *Norwegian Petroleum Society Special Publications, 4*, 41-52.

Koch, J.-O., & Heum, O. (1995). Exploration trends of the Halten Terrace. *Norwegian Petroleum Society Special Publications, 4*, 235-251.

Larsen, R., Brekke, H., Larsen, B., & Talleraas, E. (2013). *Structural and Tectonic Modelling and Its Application to Petroleum Geology: Proceedings of Norwegian Petroleum Society Workshop, 18-20 October 1989, Stavanger, Norway* (Vol. 1): Elsevier.

Lien, T. (2005). From rifting to drifting: effects on the development of deep-water hydrocarbon reservoirs in a passive margin setting, Norwegian Sea. *Norsk Geologisk Tidsskrift, 85*(4), 319.

Lingrey, S., & Vidal-Royo, O. (2015). Evaluating the quality of bed length and area balance in 2D structural restorations. *Interpretation, 3*(4), SAA133-SAA160.

Martinius, A., Ringrose, P. S., Brostrøm, C., Elfenbein, C., Næss, A., & Ringås, J. (2005). Reservoir challenges of heterolithic tidal sandstone reservoirs in the Halten Terrace, mid-Norway. *Petroleum Geoscience, 11*(1), 3-16.

McKerrow, W., Mac Niocaill, C., & Dewey, J. (2000). The Caledonian orogeny redefined. *Journal of the Geological Society, 157*(6), 1149-1154.

Moretti, I. (2008). Working in complex areas: New restoration workflow based on quality control, 2D and 3D restorations. *Marine and Petroleum Geology, 25*(3), 205-218.

Ngeri, A., Tamunobereton-ari, I., & Amakiri, A. (2015). Ant-tracker attributes: an effective approach to enhancing fault identification and interpretation. *Journal of VLSI and Signal Processing, 5*, 67-73.

Norwegian Petroleum Directorate (NPD). 2017. URL: http://factpages.npd.no

Norwegian Petroleum Directorate (NPD). 2017. Factpages. URL: http://factpages.npd.no/factpages

Schlumberger. 2017. URL: http://Schlumberger.com

Sclater, J. G.,and P. A. F. Christie. (1980,). Continental Stretching - an explanation of the Post-Mid-Cretaceous subsidence of the central North-Sea Basin: *Journal of Geophysical Research*, 85, 3711-3739.

UK Governemnt. (2017). URL: https://www.gov.uk/government/uploads/system/uploads/attachment_data/file/472100/2CXRM_Post_Well_Analysis_Christian_Mathieu_talk.pdf

Volcan, M. H., Chahine, C., & TrueLove, L. (2015). Enhanced delineation of reservoir compartmentalization from advanced Pre and Post-stack seismic attribute analysis. *ASEG Extended Abstracts, 2015*(1), 1-9.

Wilson, P., Elliot, M, G., Gawthorpe, R, L., Jackson, C, AL., Michelsen, L., & Sharp, I. R. (2015). Lateral variation in structural style along an evaporite-influenced rift fault system in the Halten Terrace, Norway: Influence of basement structure and evaporite facies. *Journal of Structural Geology, 2015*(79), 110-123.

Xiao, H., & Suppe, J. (1992). Origin of Rollover (1). *AAPG bulletin, 76*(4), 509-529.

Yamada, Y., & McClay, K. (2003). Application of geometric models to inverted listric fault systems in sandbox experiments. Paper 1: 2D hanging wall deformation and section restoration. *Journal of structural geology, 25*(9), 1551-1560.

Yielding, G. (2002). Shale gouge ratio—Calibration by geohistory. *Norwegian Petroleum Society Special Publications, 11*, 1-15.